Supporting Information

A tetrazine-driven photocatalytic system suitable for the synthesis of unstable 2,3-dihydroisoxazoles

Tiantian Chen, Zijian Yuan, Shuo Wang, Jianchun Wang*

Department of Chemistry, Capital Normal University, Beijing 100048, P. R. China.E-mail: cnuwjc@cnu.edu.cn

Contents

Index of Figures

Experimental Section

Most materials and reagents were purchased from commercial suppliers and used without further purification. ^{1}H and ^{13}C NMR spectra were mainly recorded on 600 MHz Varian VNMRS Spectrometer using D_2O, DMSO-d_6, or $CDCl_3$ as solvent at 25°C. High-resolution mass spectroscopy (HRMS) was performed on a Bruker APEXIIFT-ICR mass spectrometer. Melting points were measured on a WRS-1B micro-melting point apparatus (YiCe, Shanghai).

1. Optimization of reaction conditions

1.1 Screning of catalysis

Several studies have reported the use of metal complexes as catalysts for 1,3-dipolar cycloaddition reactions; [1,2,3] however, to date, no catalytic application of tetrazine in this transformation has been documented. In our study, the reaction between substrates **1a** and **1b** was conducted with a molar ratio of **1a:1b** = 1:10, employing 0.1 equivalents of catalyst. The reaction was performed at 40 °C for 3 hours in dichloromethane as the solvent. The results are summarized in Table S1. In the absence of any catalyst, the yield was low, amounting to only 24% (Entry 1). As shown in the table, the incorporation of tetrazine derivatives significantly enhances the reaction yield. Notably, 3,6-di(pyridin-2-yl)-1,2,4,5-tetrazine **(pytz)** proved particularly effective, increasing the yield to 88% while suppressing by-product formation (Entry 4). Based on these results, **pytz** was selected as the catalyst of choice for subsequent investigations.

Table S1 Range of Catalysis

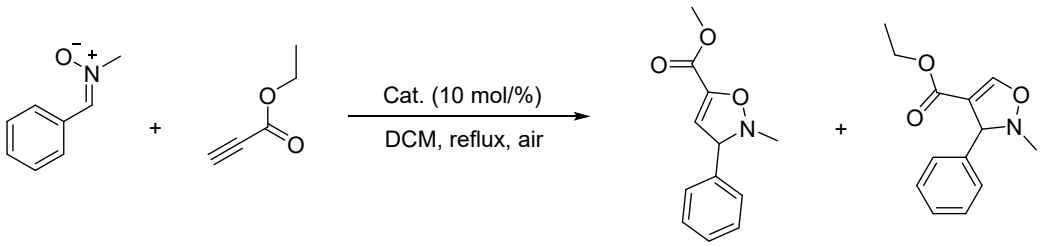

1a **1b** **1c** **1c'**

Catalysis: **4aa:** Z = Cl; **4ab:** Z = Br; **4ac (Pytz):** Z = ; **4ad:** Z =

Entry	Cat.	1c:1c'	$Yield_{1c+1c'}$ (%)

[1] G. Desimoni, G. Faita, A. Mortoni and P. Righetti, 1,3-Dipolar cycloadditions catalyzed by bis(oxazoline)-magnesium-based chiral complexes. The importance of a Mg(II) counterion, *Tetrahedron Lett.*, 1999, **40**, 2001-2004.

[2] M. Kawamura and S. Kobayashi, A switch of enantiofacial selectivity in chiral ytterbium-catalyzed 1,3-dipolar cycloaddition reactions, *Tetrahedron Lett.*, 1999, **40**, 3213-3216.

[3] S. Kanemasa, N. Ueno and M. Shirahase, Nitrone cycloaddition reactions to α,β-unsaturated carbonyl acceptors catalyzed by a pinhole Lewis acid catalyst. Dramatic rate acceleration and improvement of regioselectivity and diastereoselectivity, *Tetrahedron Lett.*, 2002, **43**, 657-660.

1	None	1:2	24
2	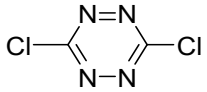	1:2	38
3	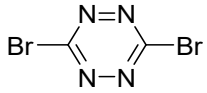	5:9	57
4	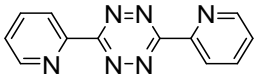	4:9	88
5	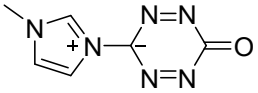	5:9	73
6	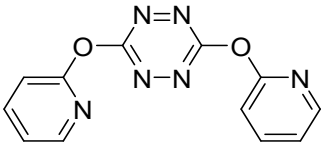	6:7	75

1.2 Selection of catalyst dosage

Pytz was employed as the catalyst, with a substrate molar ratio of **1a** to **1b** of 1:10, using dichloromethane as the solvent. The reaction was conducted at 40 °C for 3 hours. The influence of varying catalyst loading on the reaction yield was systematically investigated, and the results are summarized in Table S2. As the catalyst loading increased, the formation of by-product decreased significantly; however, the overall yield also declined markedly. Based on this trade-off, a catalyst loading of 10 mol% was determined to be optimal for **pytz**.

Table S2 Selection of catalyst dosage

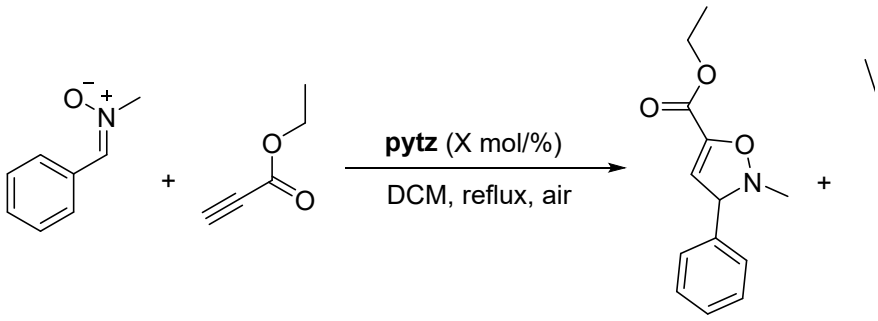

1a **1b** **1c**

Entry	Cat.(mol%)	1c:1c′	$Yield_{1c+1c'}$ (%)
1	5	1:2	59
2	10	1:2	88
3	15	1:2	55

1.3 Screening of feed ratio

To further enhance the reaction yield, a systematic investigation of the feeding ratios of substrates **1a** and **1b** was conducted. The reactions were carried out using **pytz** (10 mol%) as the catalyst, with varying molar ratios of **1a** and **1b** under an air atmosphere at 40 °C with reflux for 3 hours. The results are summarized in Table S3. As indicated in the table, increasing the molar proportion of **1b** relative to **1a** leads to a marked improvement in reaction yield. The maximum yield of 88% was achieved when the molar ratio of **1a** to **1b** was set at 1:10. A slight decrease in yield was observed when the ratio was increased to 1:15. Based on these findings, a 1:10 molar ratio of **1a** to **1b** was determined to be optimal for this transformation.

Table S3 Screening of feed ratio

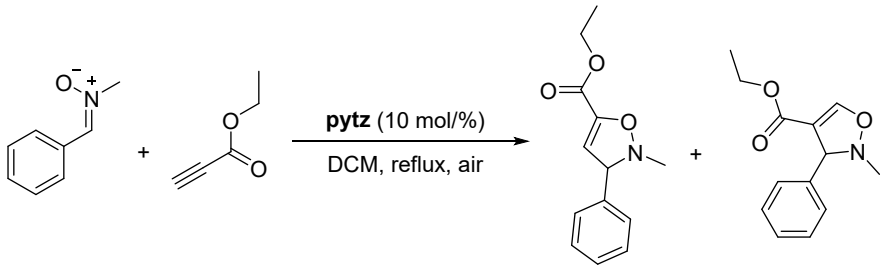

1a **1b** **1c** **1c'**

Entry	Ratio(1a:1b)	1c:1c′	Yield$_{1c+1c'}$ (%)
1	1:1	1:2	56
2	1:3	2:5	68
3	1:5	1:2	77
4	1:10	4:9	88
5	1:15	1:2	87

1.4 Selection of solvents

In organic reactions, the choice of an appropriate solvent is often critical to the success or failure of the transformation. Accordingly, several commonly used laboratory solvents were selected for evaluation. The reactions were conducted using **pytz** (10 mol%) as the catalyst, with a 1:10 molar ratio of substrates **1a** to **1b**, under ambient atmospheric conditions at a controlled temperature of 40 °C for 3 hours. The results are summarized in Table S4. Protic solvents such as methanol and HFIP yielded no detectable amounts of the desired product or by-products, indicating a pronounced inhibitory effect of protic solvents on this reaction. This observation is consistent with previously reported literature. Among the aprotic solvents tested, toluene and acetonitrile afforded no by-products; however, the highest product yield was achieved when dichloromethane was employed as the solvent. Based on a comprehensive assessment of these results, dichloromethane was identified as the optimal solvent for this transformation.

Table S4 Selection of solvents

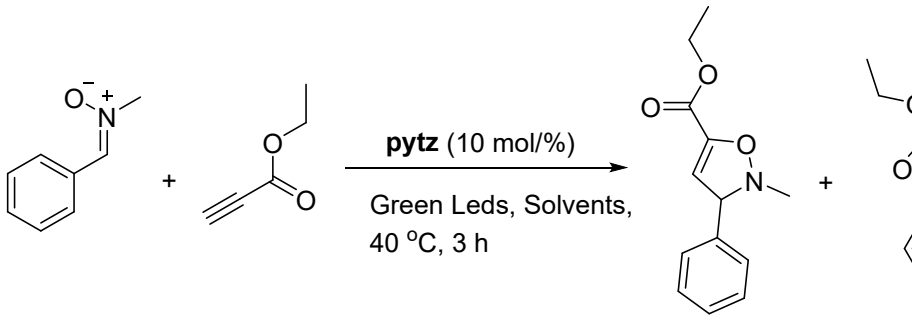

1a **1b** **1c**

Entry	Solvent	1c:1c′	Yield$_{1c+1c'}$ (%)
1	Toluene	1:2	80
2	CH_3CN	7:9	45
3	DMF	6:7	67
4	THF	4:9	50
5	$CHCl_3$	3:7	57
6	DCM	1:2	88
7	MeOH	0	0
8	HFIP	0	0

1.5 Selection of temperature

Given that dichloromethane was selected as the solvent and most photocatalytic reactions are conducted under ambient temperature conditions, a temperature range of 5 to 40 °C was chosen for evaluation. The catalyst employed was **pytz** (10 mol%), with a molar ratio of substrates **1a** to **1b** set at 1:10. The reaction was carried out in dichloromethane under an air atmosphere for 3 hours, and the results are summarized in Table S5. The data indicate that lower temperatures are unfavorable for the reaction. As the temperature increases, the yield improves significantly; however, the formation of by-product also gradually increases. Subsequent experiments demonstrated that extending the reaction time to 6 hours at 25 °C afforded a yield of 84%. Taking into account the trade-off between reaction time and yield, 40 °C was determined to be the optimal reaction temperature.

Table S5 Selection of temperature

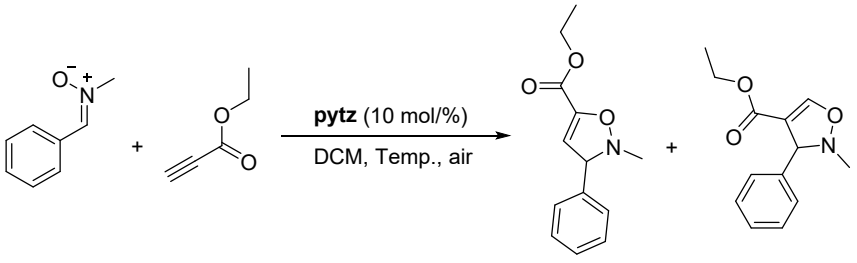

1a **1b** **1c** **1c'**

Entry	Temp.(°C)	1c:1c′	Yield$_{1c+1c'}$ (%)
1	40	1:2	88

2	25	1:2	80 (84[a])
3	5	2:3	32

[a] The reaction time was extended to 6 h at 25 °C.

1.6 Selection of oxidant

Chemical reactions mediated by tetrazines necessitate the presence of an oxidant. In this study, **pytz** was employed as the catalyst, with a reactant molar ratio of 1:10 and dichloromethane serving as the solvent. The reaction was conducted at 40 °C for 3 hours under various oxidative conditions. As summarized in Table S6, the influence of different oxidants on reaction efficiency was systematically evaluated. Under a nitrogen atmosphere, the reaction yield was found to be minimal. In contrast, the use of either pure oxygen or ambient air significantly enhanced the yield. Notably, no substantial improvement was observed when oxygen was used instead of air. Therefore, air was considered the most effective and practical oxidant for this transformation.

Table S6 Selection of oxidant

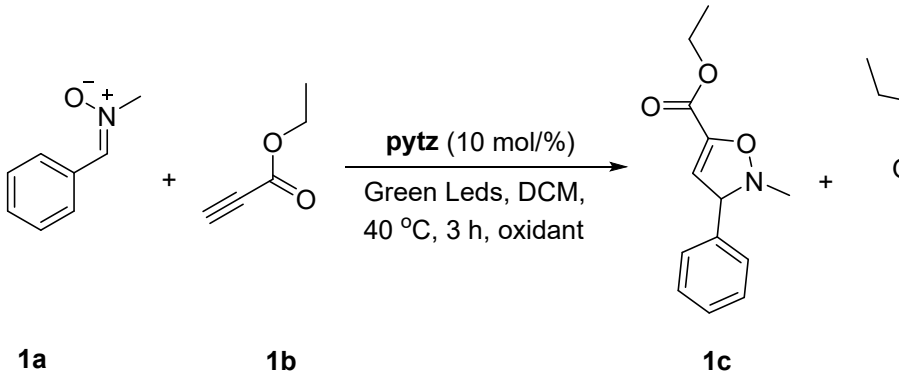

Entry	Solvent	1c:1c′	Yield$_{1c+1c'}$ (%)
1	O_2	5:9	91
2	air	1:2	88
3	N_2	3:5	21

1.7 Selection of light source

Ultraviolet-visible spectrophotometric analysis revealed that a dichloromethane solution of **pytz** (7.5×10^{-3} M) exhibits a distinct maximum absorption peak in the visible region at approximately 545 nm. Based on this finding, the light source screening was conducted under three conditions: dark environment, ambient light, and green light illumination. As shown in Table S7 and Figure S1, the reaction yield decreased significantly under complete darkness, reaching only 37.9%. In contrast, the yield improved markedly under ambient light and reached 97.3% when green light was applied. These results indicate that green light is the optimal illumination source, with an effective illumination distance recommended between 2 and 5 cm.

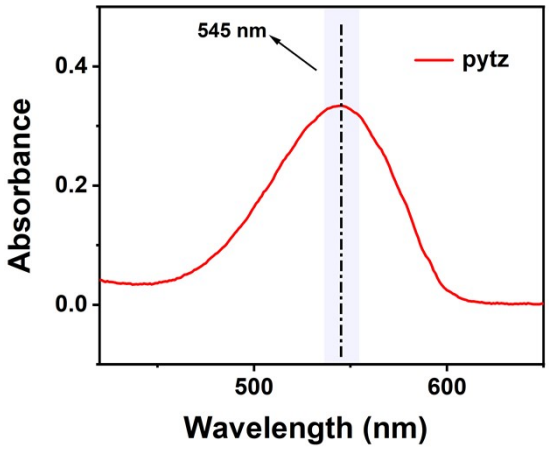

Figure S1 UV-Vis absorption spectrum of 3,6-(2-pyridyl)-1,2,4,5-tetrazine [**pytz**, 7.5 × 10^{-3} M] in dichloromethane

Table S7 Selection of light source

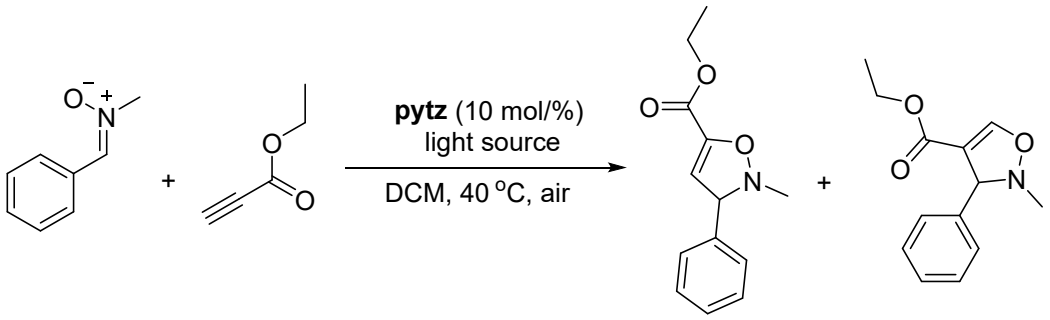

1a **1b** **1c** **1c'**

Entry	Light	1c:1c′	$Yield_{1c+1c'}$ (%)
1	12W Green LEDs	5:9	97
2	Dark	4:9	38
3	Ambient light	1:2	88

The optimal conditions for this reaction are as follows: 0.1 equivalents of 3,6-bis(2-pyridinyl)-1,2,4,5-tetrazine (**pytz**) as the catalyst, irradiation with 12 W green LEDs, a molar ratio of substrates **1a** to **1b** of 1:10, dichloromethane as the solvent, air as the oxidant, and a reaction temperature of 40 °C for a duration of 3 hours.

2. Control experiments

2.1 LC-MS analysis of reaction mixture and isolation of H_2pytz

To elucidate the reaction mechanism, liquid chromatography – mass spectrometry (LC – MS) analysis was performed on the mixture obtained from the standard reaction, as follows. In addition to reactant **1a**, catalyst **pytz**, and products **1c** and **1c'** signals corresponding to **H_2pytz** and by-product **1f** were detected. **H_2pytz** was successfully isolated from the reaction mixture, and its structure was confirmed by ^{1}H NMR and high-resolution mass spectrometry (HRMS), with data consistent with previously reported literature values. [4] Although **1f** could not be fully characterized due to low yield and instability, its high-resolution mass spectrum was obtained (Figure S96). The experimental molecular ion peak agrees well with the theoretical value, and the isotopic distribution pattern matches the simulated isotope profile.

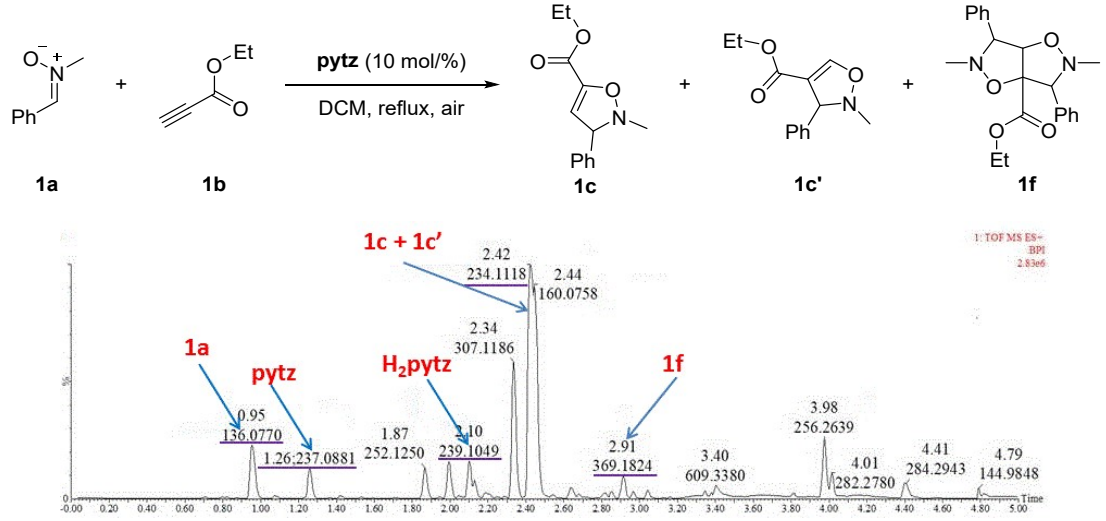

Figure S2 LC-MS of reaction mixture of **1a** with **1b** catalyzed by **pytz**

2.2 Add TEMPO to the standard reaction mixture under controlled conditions.

A radical trap (TEMPO) was introduced at a 1:1 molar ratio relative to **pytz** under optimized reaction conditions. ^{1}H NMR analysis revealed a significant decrease in product yield, dropping from 97% to 41%, with no detectable peaks corresponding to **H_2pytz**. This result indicates that TEMPO effectively suppressed the catalytic reduction mediated by **pytz**, thereby supporting the involvement of a radical-based mechanism.

[4] S. Ray, R. Biswas, R. Banerjee, A. B. Ghosh and P. Biswas, Non-Aggregation-Induced Colorimetric Detection of Ag^+ by Tetrazine-Capped Gold Nanoparticles Based on the Formation of Au-Ag Core-Shell Nanoparticles, *ChemistrySelect*, 2019, **4**, 12409-12417.

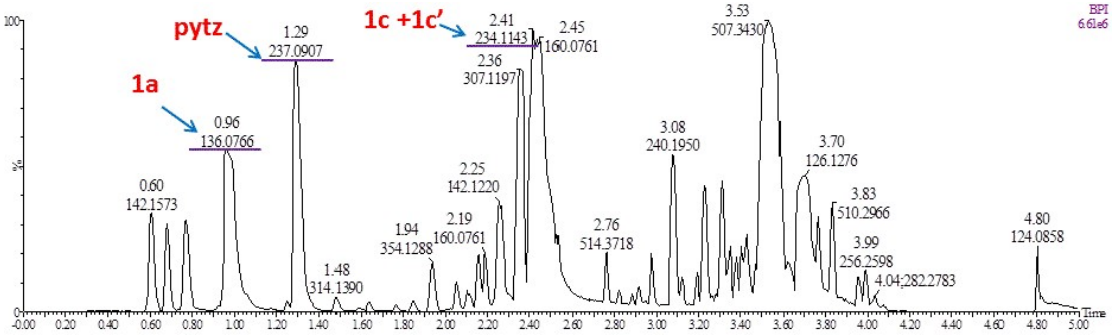

Figure S3 LC-MS of the reaction mixture with TEMPO added under standard reaction conditions

2.3 Cyclic voltammetry analysis

To elucidate the catalytic mechanism of the catalyst **pytz** in this reaction and to determine whether a single-electron transfer process (SET) occurs between **pytz** and the substrate, cyclic voltammetry experiments were conducted. Dichloromethane (HPLC grade) was used as the solvent, and tetrabutylammonium hexafluorophosphate (10 mM) served as the supporting electrolyte. A standard three-electrode system was employed, consisting of a glassy carbon working electrode, an Ag/AgCl reference electrode, and a platinum counter electrode. Ferrocene was added as an internal standard for potential calibration. Prior to each measurement, all solutions were degassed by purging with high-purity argon gas for at least 2 minutes to minimize interference from dissolved oxygen.

First, a dichloromethane solution of ferrocene (10 mM) was employed for electrochemical testing, and the results are presented in Figure S4. Ferrocene exhibits reversible redox behavior, with an oxidation peak potential at 0.72 V vs. reference and a reduction peak potential at 0.31 V vs. reference, indicating effective performance of the three-electrode system.

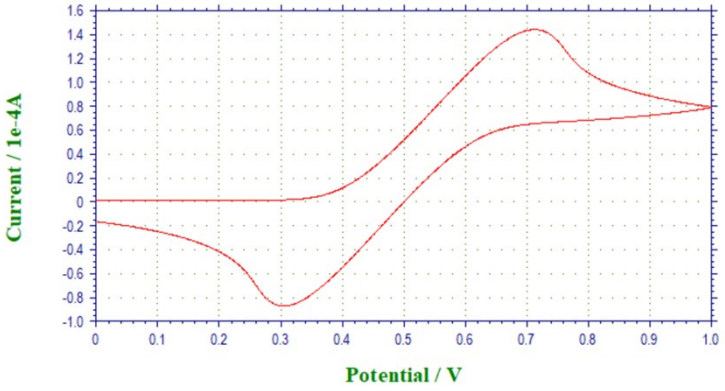

Figure S4 Cyclic voltammetry of ferrocene in dichloromethane: voltage range from 0 to 1 V; scan rate of 50 mV/s

Subsequently, the electrochemical response of pure dichloromethane solvent was measured (Figure S5), which displays an irreversible reduction wave with an inflection potential of approximately –0.80 V.

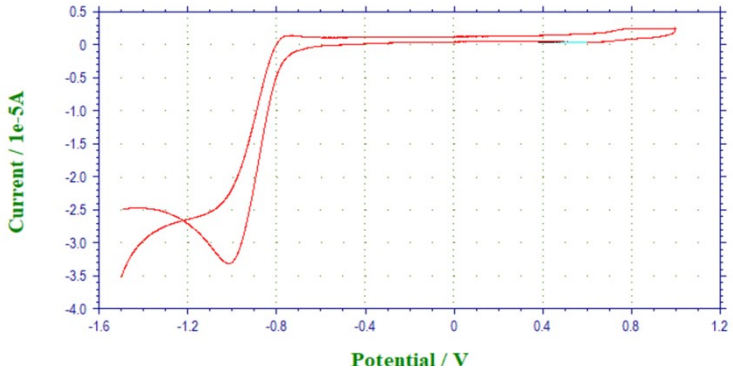

Figure S5 Cyclic voltammetry of the pure solvent DCM was conducted over a voltage range of 1.0 to -1.5 V at a scan rate of 50 mV/s

Next, cyclic voltammetry of **pytz** (10 mM) was conducted, and the resulting data are shown in Figure S6. **Pytz** demonstrates a reversible redox process, characterized by an oxidation peak potential of approximately –0.70 V (with a current of 0.038 mA) and a reduction peak potential of –1.00 V (with a current of 0.121 mA). The redox peak potential separation for **pytz** is 0.30 V, which is in good agreement with literature values. [5]

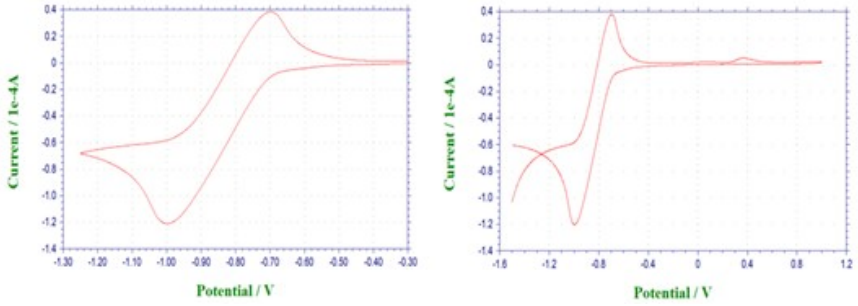

(A) (B)

Figure S6 Cyclic voltammetry of **pytz** in dichloromethane: (A) voltage range from −0.30 to −1.25 V; (B) voltage range from 1.5 to −1.5 V; scan rate: 50 mV/s

Finally, cyclic voltammetry measurements were carried out for the two substrates involved in the standard reaction: nitrone (**1a**) and ethyl propiolate (**1b**), with results displayed in Figures S7 and S8, respectively. The concentrations of both substrates were maintained at 10 mM. As illustrated in the figure S5, S7 and S8, their cyclic voltammetry (CV) profiles exhibit nearly complete overlap with those of the pure solvent (dichloromethane, DCM), indicating that the applied electrode potential lacks significant catalytic activity toward the two substrates—specifically, the potential is insufficient to induce oxidation of either compound.

[5] G. Clavier and P. Audebert, s-Tetrazines as Building Blocks for New Functional Molecules and Molecular Materials, *Chem. Rev.*, 2010, **110**, 3299-3314.

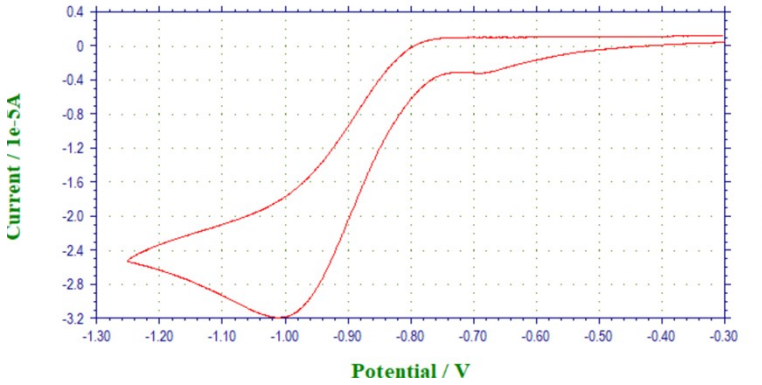

Figure S7 Cyclic voltammetry of nitrone **1a** was conducted in dichloromethane (DCM) over a potential range of -0.30 to -1.25 V versus the reference electrode, with a scan rate of 50 mV/s

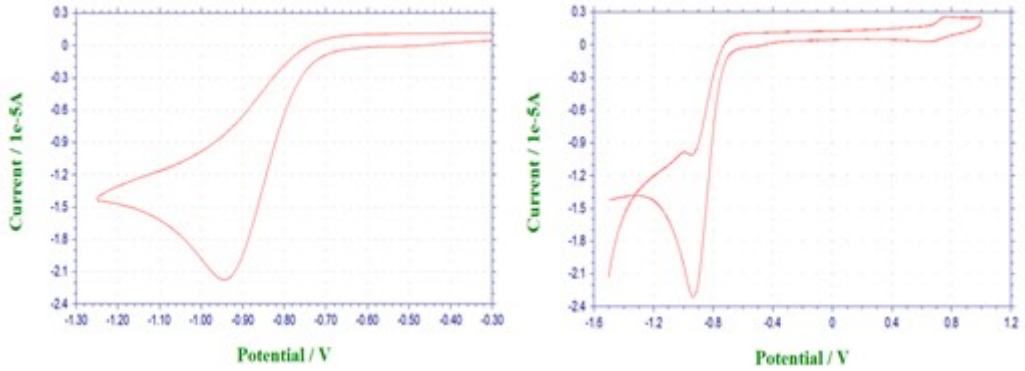

(C) (D)

Figure S8 Cyclic voltammetry of ethyl propiolate (**1b**) in dichloromethane: (C) voltage range from -0.30 to -1.25 V; (D) voltage range from 1.5 to -1.5 V, with a scan rate of 50 mV/s

Subsequently, **pytz** was mixed with **1b** in a 1:1 molar ratio. The resulting solution, prepared in dichloromethane, was subjected to cyclic voltammetry analysis (Figure S9). The CV curve reveals a weak oxidation peak at −0.8 V and a corresponding reduction peak at −0.75 V, with a reduction peak current of 58 mA. Concurrently, a decrease in the oxidation peak intensity of **pytz** is observed, suggesting that **pytz** exhibits catalytic activity toward **1b**. This behavior implies the occurrence of a single-electron transfer (SET) process between **pytz** and **1b**.

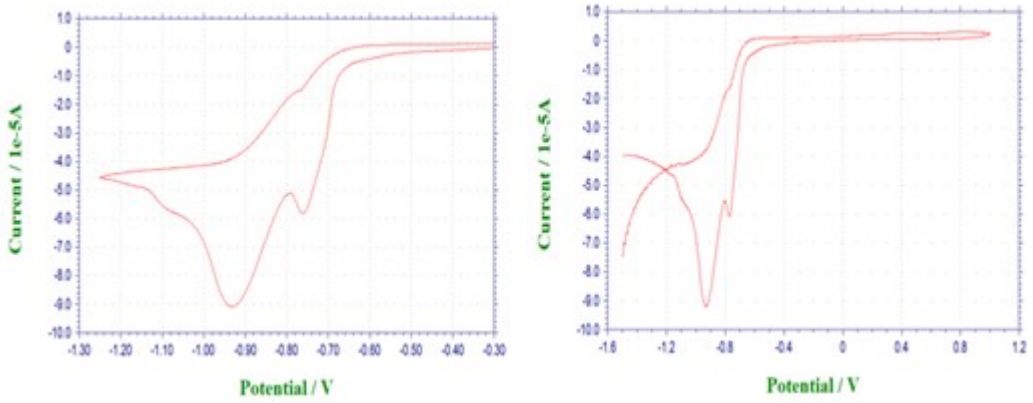

(E) (F)

Figure S9 Cyclic voltammetry of ethyl propargyl and **pytz** in dichloromethane at a molar ratio of 2:1 was performed over two voltage ranges: (E) −0.30 to −1.25 V and (F) −1.50 to +1.50 V, with a scan rate of 50 mV/s

In contrast, when a dichloromethane solution containing **pytz** and **1a** in a 1:2 molar ratio was tested, the resulting voltammogram closely matched that of **pytz** alone, with no additional reduction peaks detected, indicating the absence of a SET interaction between **pytz** and **1a** (Figure S10).

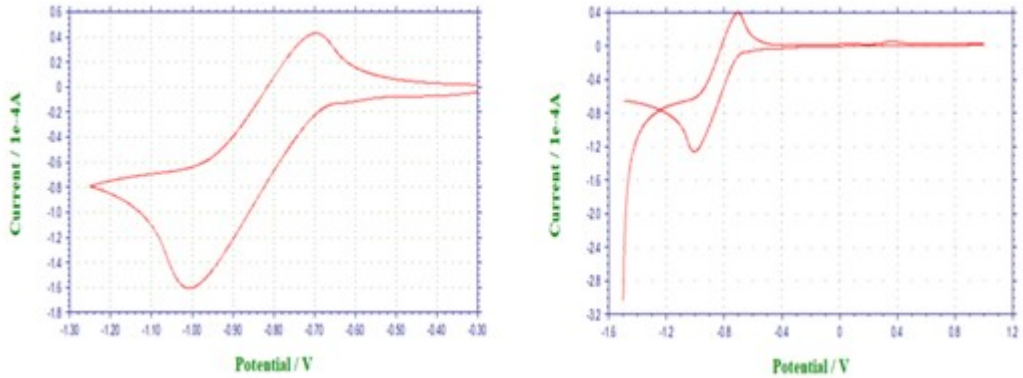

(G) (H)

Figure S10 Cyclic voltammetry of nitrone **1a** and **pytz** in dichloromethane at a molar ratio of 2:1 was performed over two voltage ranges: (G) −0.30 to −1.25 V and (H) 1.5 to −1.5 V, with a scan rate of 50 mV/s

These findings collectively demonstrate that **pytz** undergoes a specific single-electron transfer reaction with **1b**, but not with **1a**.

3. Synthesis of nitrones

General method：

Method A：

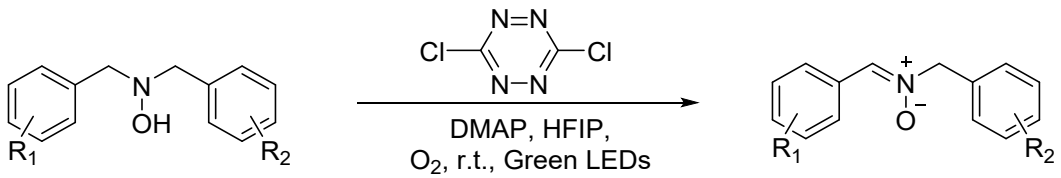

According to the previously reported procedure, [6] N,N-dibenzylhydroxylamine, 3,6-dichloro-tetrazine (10 mol%), DMAP (2.1 equiv.), and HFIP were sequentially introduced into a Schlenk tube. Following the bubbing O_2 for one minute, the reaction was stirred under an oxygen atmosphere and irradiated with green light for 16 hours. Upon completion, the organic solvent was

[6] Lyu, J.; Le, T.; Claraz, A.; Allain, C.; Audebert, P.; Masson, G. s-Tetrazine: robust and green photoorganocatalyst for aerobic oxidation of N, N-disubstituted hydroxylamines to nitrones. *Synlett* 2022, **33 (02)**, 177-181.

removed *via* rotary evaporation, and the target product was obtained through column chromatography.

Method B:

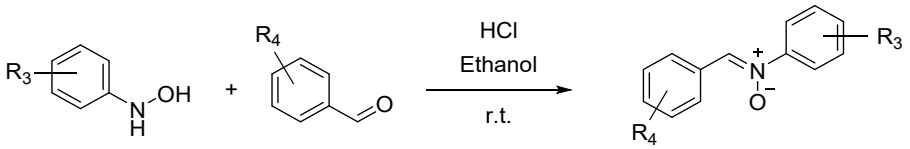

According to the reported literature, [7] N-phenylhydroxylamine was introduced into a 100 mL three-necked flask, followed by the addition of one equivalent of aromatic aldehyde and a few drops of hydrochloric acid. The reaction mixture was then stirred at room temperature for approximately two hours, with the progress monitored by thin-layer chromatography (TLC) until the reaction reached completion. Upon completion, the organic solvents were removed under reduced pressure, and the target compound was further purified by column chromatography followed by recrystallization.

Method C:

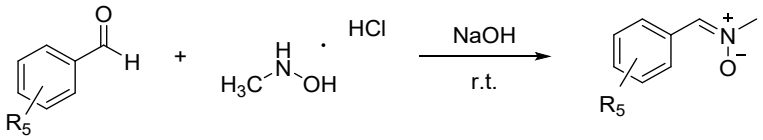

According to the literature, [8] an aqueous sodium hydroxide solution of N-methyl-hydroxylamine hydrochloride was introduced into a 100 mL three-necked flask, followed by the addition of one equivalent of aromatic aldehyde. The reaction mixture was stirred at room temperature for one hour. Subsequently, the mixture was extracted multiple times with chloroform. The organic layer was collected, dried over anhydrous magnesium sulfate, filtered, and concentrated under vacuum. The resulting crude product was further purified by column chromatography to yield the pure compound.

Table S8 Summary of synthetic nitrones (**1a-15a**)

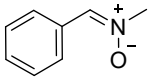	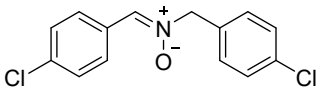	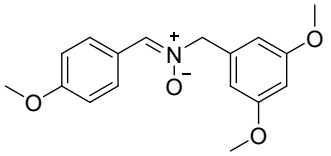
1a[c], 71%, [6]	**2a**[a], 67%, [6]	**3a**[b,d], 38%
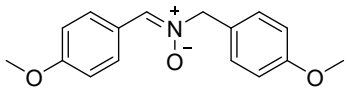	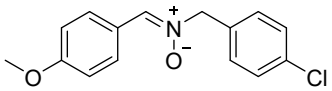	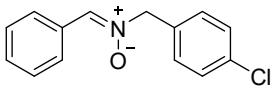

[7] Martínez-Pardo, P.; Blay, G.; Escrivá-Palomo, A.; Sanz-Marco, A.; Vila, C.; Pedro, J. R. Catalytic Diastereo- and Enantioselective Synthesis of 2-Imidazolinones. *Org. Lett.* 2019, **21 (11)**, 4063-4066.
[8] Tyrrell, E.; Allen, J.; Jones, K.; Beauchet, R. Asymmetric 1,3-Dipolar Cycloaddition Reactions of Nitrones with (S)-(-)-4-Benzyl-N-methacryloyl-2-oxazolidinone. *Synthesis* 2005, **14**, 2393-2399.

4a[b], 65%, [6]	**5a**[b], 68%, [6]	**6a**[b], 54%, [6]
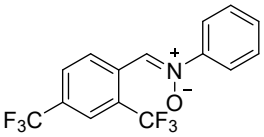	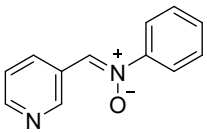	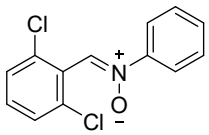
7a[b], 15%, [9]	**8a**[b,d], 45%	**9a**[b,d], 89%
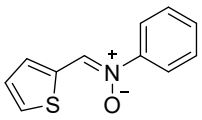	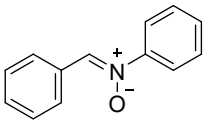	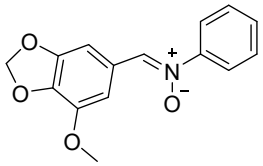
10a[b,d], 63%	**11a**[b], 61%, [9]	**12a**[b,d], 15%
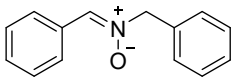	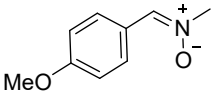	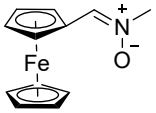
13a[a], 89%, [6]	**14a**[c,d], 60%	**15a**[c,d], 78%

[a] It was prepared by Method A; [b] It was prepared by Method B; [c] It was prepared by Method C; [d] new compound

All the synthesized nitrones are presented in Table S8. Among these, seven nitrones are novel compounds, and their ^{1}H NMR, ^{13}C NMR, and HRMS data are provided below.

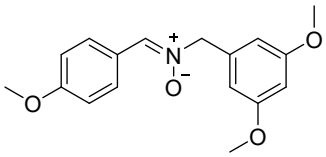

(Z)-N-(3,5-dimethoxybenzyl)-1-(4-methoxyphenyl)methanimine oxide (**3a**)

White solid, Yield: 38%, mp: 112-113 °C, ^{1}H NMR (600 MHz, DMSO-d_6) δ 7.99 (s, 1H), 7.48 – 7.40 (m, 4H), 6.98 – 6.92 (m, 2H), 6.56 (t, J = 2.3 Hz, 1H), 4.96 (s, 2H), 3.75 (s, 3H), 3.74 (s, 6H). ^{13}C NMR (151 MHz, DMSO-d_6) δ 160.08 , 159.39 , 132.79 , 130.60 , 126.61 , 113.75 , 105.68 , 102.38 , 69.74 , 55.19 , 55.13 , 39.52 .$C_{17}H_{19}NO_4$ $[M+H]^+$m/z: Calc. 302.1387, Found 302.1386.

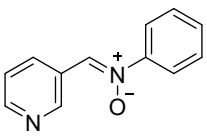

(Z)-N-phenyl-1-(pyridin-3-yl)methanimine oxide (**8a**)

Yellowish solid, Yield: 45%, mp: 92-93 °C,^{1}H NMR (600 MHz, DMSO-d_6) δ 9.26 – 9.21 (m, 1H), 8.71 (dt, *J* = 4.3, 1.9 Hz, 1H), 8.46 (d, *J* = 1.6 Hz, 1H), 7.97 – 7.91 (m, 3H), 7.53 (dt, *J* = 5.0, 2.2 Hz, 3H), 7.44 (ddt, *J* = 6.3, 4.6, 1.4 Hz, 1H). ^{13}C NMR (151 MHz, DMSO-d_6) δ 149.89 , 149.56 , 148.23 , 136.85 , 134.38 , 130.30 , 129.15 , 124.65 , 122.98 , 121.54 . $C_{12}H_{10}N_2O$ $[M+H]^+$m/z: Calc. 199.0866, Found 199.0866.

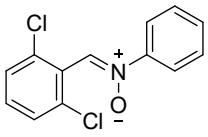

(Z)-1-(2,6-dichlorophenyl)-N-phenylmethanimine oxide (**9a**)

White solid, Yield: 89%, mp: 95-96 °C, ^{1}H NMR (600 MHz, Chloroform-*d*) δ 8.06 (s, 1H), 7.86 – 7.80 (m, 2H), 7.55 – 7.48 (m, 3H), 7.43 – 7.38 (m, 2H), 7.33 (dd, *J* = 8.7, 7.4 Hz, 1H). ^{13}C NMR (151 MHz, DMSO-d_6) δ 147.10 , 134.65 , 131.69 , 130.67 , 129.41 , 129.26 , 128.90 , 128.22 , 121.56. $C_{13}H_9Cl_2NO$ $[M+H]^+$m/z: Calc. 266.0134, Found 266.0136.

(Z)-N-phenyl-1-(thiophen-2-yl)methanimine oxide (**10a**)

[9] Prakash, P.; Gravel, E.; Nguyen, D. V.; et al. Direct and Co-catalytic Oxidation of Hydroxylamines to Nitrones Promoted by Rhodium Nanoparticles Supported on Carbon Nanotubes. *ChemCatChem* 2017, **9(12)**, 2091-2094.

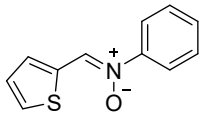

Brown solid, Yield: 63%, mp: 96-97 °C, ^{1}H NMR (600 MHz, Chloroform-*d*) δ 8.49 (d, *J* = 0.7 Hz, 1H), 7.87 – 7.81 (m, 2H), 7.62 (dt, *J* = 3.9, 0.8 Hz, 1H), 7.57 (dt, *J* = 5.1, 0.9 Hz, 1H), 7.52 – 7.42 (m, 3H), 7.22 (dd, *J* = 5.1, 3.9 Hz, 1H). ^{13}C NMR (151 MHz, DMSO-d_6) δ 145.98 , 132.86 , 131.70 , 129.75 , 129.66 , 129.12 , 128.75 , 127.22 , 120.68. $C_{11}H_9NOS$ [M+H]$^+$m/z: Calc. 204.0478, Found 204.0476.

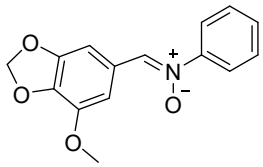

(Z)-1-(7-methoxybenzo[d][1,3]dioxol-5-yl)-N-phenylmethanimine oxide (**12a**)

Colourless liquid, Yield: 15%, ^{1}H NMR (600 MHz, DMSO-d_6) δ 8.43 (s, 1H), 7.97 (d, *J* = 1.3 Hz, 1H), 7.90 – 7.85 (m, 3H), 7.57 – 7.51 (m, 2H), 7.51 – 7.47 (m, 1H), 6.10 (s, 2H), 3.87 (s, 3H). ^{13}C NMR (151 MHz, DMSO-d_6) δ 148.35 , 148.07 , 142.82 , 136.91 , 133.15 , 129.64 , 129.05 , 125.64 , 121.25 , 109.61 , 102.60 , 101.90 , 56.19 , 39.52 . $C_{15}H_{13}NO_4$ [M+H]$^+$m/z: Calc. 272.0918, Found 272.0919.

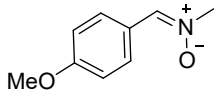

(Z)-1-(4-methoxyphenyl)-N-methylmethanimine oxide (**14a**)

Yellowish solid, Yield: 60%, mp: 91-92 °C, ^{1}H NMR (600 MHz, Chloroform-*d*) δ 8.24 – 8.16 (m, 2H), 7.30 (s, 1H), 6.96 – 6.90 (m, 2H), 3.84 (s, 6H). ^{13}C NMR (151 MHz, DMSO-d_6) δ 160.13 , 133.33 , 129.67 , 124.08 , 113.68 , 55.17 , 53.59 , .$C_9H_{11}NO_2$ [M+H]$^+$m/z: Calc 166.0863, Found 166.0863.

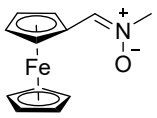

(Z)-N-methyl-1-ferroceneylmethanimine oxide (**15a**)

Reddish brown solid, Yield: 78%, mp: 118-119 °C, ^{1}H NMR (600 MHz, DMSO-d_6) δ 7.44 (s, 1H), 4.98 (s, 2H), 4.37 (s, 2H), 4.17 (s, 5H), 3.58 (s, 3H). ^{13}C NMR (151 MHz, DMSO-d_6) δ 133.58 , 74.78 , 69.43 , 69.08 , 68.79 , 52.78. $C_{12}H_{13}FeNO$ [M+H]$^+$m/z：Calc. 244.0420, Found 244.0421.

4. Alkynyl ester

Four alkynes, including both symmetrical and asymmetrical ones, were employed in the paper and are presented in Table S9.

Table S9 Range of alkynyl ester (**1b-4b**) [a]

Entry	No.	R_3	R_4	Structure
1	**1b**	H	CO_2Et	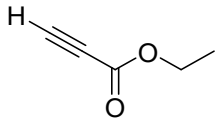
2	**2b**	Ph	CO_2Me	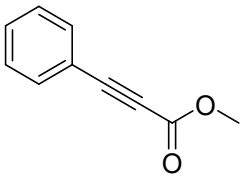
3	**3b**	CO_2Et	CO_2Et	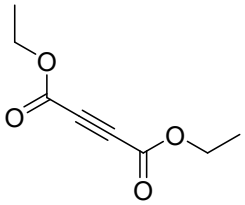
4	**4b**	CF_3	CO_2Et	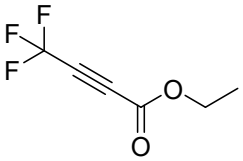

[a] All of alkynyl esters were purchased from commercial suppliers and used without further purification.

5. Synthesis of 2,3-dihydroisoxazoles

The general method for the synthesis of 2,3-dihydroisoxazole is as follows. In a 50 mL three-neck round-bottom flask, 0.5 mmol of nitrone, 0.1 eq. of **pytz**, and 3 mL of dichloromethane were sequentially introduced, followed by the addition of 5 mmol of ethyl propiolate using a pipette. The reaction mixture was irradiated with green light, with the flask positioned 2–5 cm from the light source, and stirred at 40 °C for at least 3 hours. TLC was used to monitor the reaction progress, with reaction time varying depending on the substrate. Once TLC confirmed complete conversion of nitrone, the reaction was cooled to room temperature, and the organic solvent and residual ethyl propiolate were removed by vacuum. The target product was then purified by column chromatography (For those separable *cis-trans* isomers, multiple PTLC purifications could be used.)

Ethyl 2-methyl-3-phenyl-2,3-dihydroisoxazole-5-carboxylate (**1c**), **Ethyl 2-methyl-3-phenyl-2,3-dihydroisoxazole-4-carboxylate (1c')**

Colorless oily liquid, Yield: 97% (**1c:1c′**=5:9) ^{1}H NMR (600 MHz, DMSO-d^{6}) δ 7.94 – 7.92 (m, 1H), 7.39 – 7.24 (m, 21H), 6.11 (d, J = 3.0 Hz, 3H), 4.98 (dd, J = 35.2, 2.4 Hz, 4H), 4.21 (qd, J = 7.1, 2.8 Hz, 6H), 4.09 – 3.96 (m, 3H), 2.85 (d, J = 20.0 Hz, 14H), 1.24 (t, J = 7.1 Hz, 12H), 1.12 (t, J = 7.1 Hz, 4H). ^{13}C NMR (151 MHz, DMSO-d^{6}) δ 153.03 , 143.83 , 128.44 , 128.16 , 127.63 , 127.56 , 127.09 , 126.71 , 110.75 , 74.82 , 72.69 , 61.19 , 59.49 , 47.17 , 46.66 , 39.52 , 14.06 , 13.89 . HRMS(ESI) $C_{13}H_{15}NO_3$ $[M+H]^{+}$m/z: Calc 234.1125, Found 234.1126.

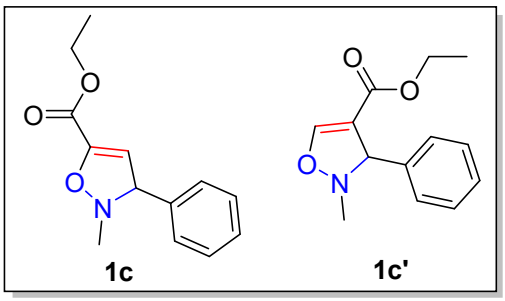

Ethyl 2-(4-chlorobenzyl)-3-(4-chlorophenyl)-2,3-dihydroisoxazole-5-carboxylate (2c), ethyl 2-(4-chlorobenzyl)-3-(4-chlorophenyl)-2,3-dihydroisoxazole-4-carboxylate (2c')

Colorless oily liquid, Yield: 42% (**2c:2c′**=2:3) ^{1}H NMR (600 MHz, DMSO-d_6) δ 7.96 (d, J = 1.5 Hz, 1H), 7.44 – 7.35 (m, 13H), 7.35 – 7.31 (m, 2H), 7.29 (d, J = 8.5 Hz, 3H), 6.18 (d, J = 3.1 Hz, 1H), 5.24 (dd, J = 15.1, 2.3 Hz, 2H), 4.28 – 4.15 (m, 6H), 4.15 – 4.04 (m, 2H), 4.04 – 3.97 (m, 2H), 1.22 (t, J = 7.1 Hz, 3H), 1.12 (t, J = 7.1 Hz, 4H).^{13}C NMR (151 MHz, DMSO-d^{6}) δ 192.06 , 160.08 , 158.34 , 144.26 , 139.56 , 135.46 , 134.48 , 132.26 , 132.06 , 131.14 , 130.90 , 130.03 , 129.33 , 128.93 , 128.84 , 128.50 , 128.48 , 128.42 , 128.15 , 110.85 , 90.13 , 71.69 , 61.64 , 61.26 , 39.52 , 13.91 . HRMS(ESI) $C_{19}H_{17}Cl_2NO_3$ $[M+H]^{+}$ *m/z*: Calc 378.0659, Found 378.0657

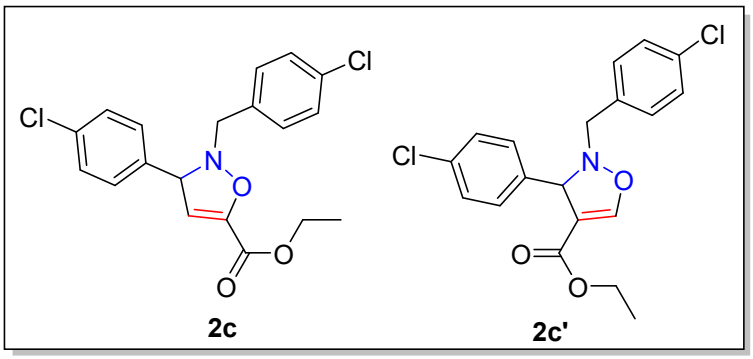

Ethyl 2-(4-chlorobenzyl)-3-phenyl-2,3-dihydroisoxazole-5-carboxylate (3c), ethyl 2-(4-chlorobenzyl)-3-phenyl-2,3-dihydroisoxazole-4-carboxylate (3c')

Colorless oily liquid, Yield: 78% (**3c:3c′**=3:4) ^{1}H NMR (600 MHz, DMSO-d_6) δ 7.97 (s, 1H), 7.42 – 7.33 (m, 9H), 7.33 – 7.24 (m, 9H), 6.17 (d, J = 3.1 Hz, 1H), 5.23 (dd, J = 11.1, 2.3 Hz, 2H), 4.27 (d, J = 13.7 Hz, 2H), 4.21 (dtd, J = 10.2, 7.0, 3.7 Hz, 3H), 4.11 (s, 1H), 4.09 – 3.97 (m, 3H), 1.23 (t, J = 7.1 Hz, 3H), 1.13 (t, J = 7.1 Hz, 4H).^{13}C NMR (151 MHz, DMSO-d^{6}) δ 193.11 , 192.02 , 158.40 , 153.59 , 144.35 , 139.67 , 136.22 , 132.22 , 131.13 , 129.44 , 129.32 , 129.18 , 129.10 , 129.07 , 128.92 , 128.82 , 128.81 , 128.70 , 128.68 , 128.48 , 128.45 , 128.39 , 128.37 ,

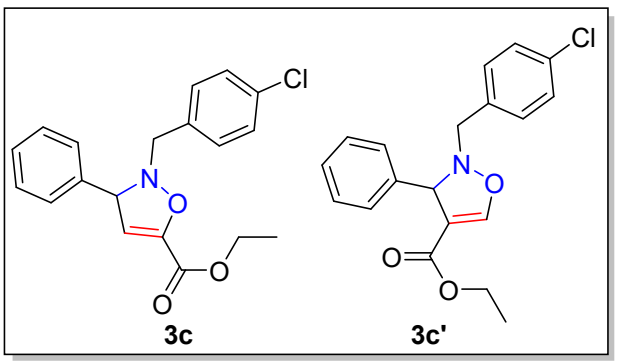

128.36 , 128.23 , 128.20 , 128.18 , 127.50 , 127.43 , 127.07 , 110.70 , 71.57 , 62.47 , 61.24 , 59.62 , 39.52 , 14.09 , 13.91 . HRMS(ESI) $C_{19}H_{18}ClNO_3$ $[M+H]^+$ *m/z*: Calc. 344.1048, Found 344.1044.

Ethyl 2-(4-chlorobenzyl)-3-(4-methoxyphenyl)-2,3-dihydroisoxazole-5-carboxylate (4c), ethyl 2-(4-chlorobenzyl)-3-(4-methoxyphenyl)-2,3-dihydroisoxazole-4-carboxylate (4c')

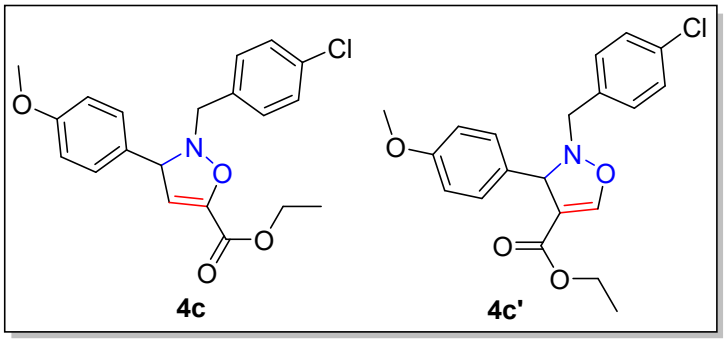

Colorless oily liquid, Yield: 80% (**4c**:**4c′**=2:3) ^{1}H NMR (600 MHz, DMSO-d_6) δ 7.96 (s, 1H), 7.37 (td, *J* = 9.1, 2.4 Hz, 3H), 7.33 – 7.21 (m, 7H), 6.88 (dq, *J* = 7.9, 2.6 Hz, 3H), 6.14 (t, *J* = 2.7 Hz, 1H), 5.19 (dt, *J* = 8.7, 2.4 Hz, 2H), 4.23 – 4.17 (m, 3H), 4.15 – 3.97 (m, 4H), 3.73 (d, *J* = 2.4 Hz, 5H), 1.23 (td, *J* = 7.1, 2.5 Hz, 2H), 1.12 (td, *J* = 7.1, 2.5 Hz, 3H).^{13}C NMR (151 MHz, DMSO-d_6) δ 191.19 , 158.70 , 158.42 , 153.67 , 144.42 , 139.75 , 132.28 , 132.18 , 131.77 , 130.61 , 130.53 , 130.03 , 129.97 , 129.32 , 128.90 , 128.87 , 128.46 , 128.43 , 128.21 , 127.86 , 114.79 , 114.46 , 114.10 , 113.60 , 110.58 , 71.18 , 61.81 , 61.23 , 59.60 , 54.98 , 39.52 , 14.08 , 13.91 . HRMS(ESI) $C_{20}H_{20}ClNO_4$ $[M+H]^+$ *m/z*: Calc 374.1154, Found 374.1153.

Ethyl 2-(3,5-dimethoxybenzyl)-3-(4-methoxyphenyl)-2,3-dihydroisoxazole-5-carboxylate (5c), ethyl 2-(3,5-dimethoxy-benzyl)-3-(4-methoxyphenyl)-2,3-dihydroisoxazole-4-carboxylate (5c')

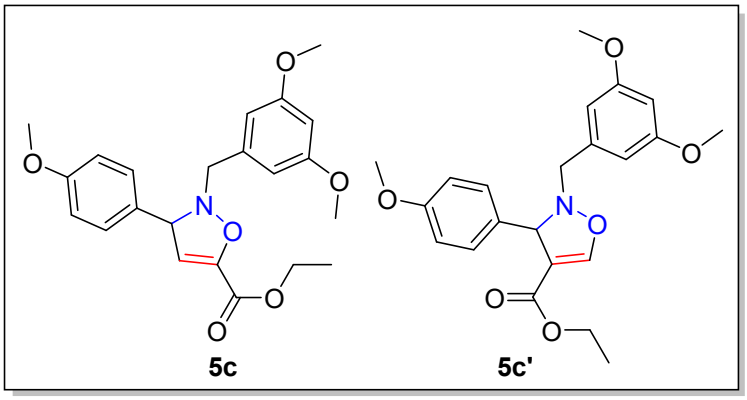

Yellow oily liquid, Yield: 64% (**5c**:**5c′**=1:1); ^{1}H NMR (600 MHz, DMSO-d_6) δ 7.95 (d, *J* = 1.4 Hz, 1H), 7.34 – 7.27 (m, 4H), 6.93 – 6.88 (m, 4H), 6.44 – 6.37 (m, 4H), 6.30 (d, *J* = 2.3 Hz, 2H), 5.10 (dd, *J* = 19.2, 2.4 Hz, 2H), 4.24 – 4.17 (m, 4H), 4.10 – 4.00 (m, 4H), 3.76 – 3.65 (m, 18H), 1.23 (t, *J* = 7.1 Hz, 3H), 1.14 (t, *J* = 7.1 Hz, 3H).^{13}C NMR (151 MHz, DMSO-d_6) δ 162.99 , 160.54 , 160.31 , 158.78 , 153.71 , 143.38 , 130.73 , 130.72 , 127.66 , 113.65 , 113.63 , 110.69 , 108.58 , 105.08 , 104.48 , 99.10 , 99.08 , 71.68 , 69.72 , 62.46 , 61.84 , 61.20 , 59.57 , 55.12 , 55.04 , 55.03 , 55.01 , 39.52 , 14.15 , 13.93 . HRMS(ESI) $C_{22}H_{25}NO_6$ $[M+H]^+$ *m/z*: Calc 400.1755, Found 400.1757

Ethyl 2-benzyl-3-phenyl-2,3-dihydroisoxazole-5-carboxylate (6c), ethyl 2-benzyl-3-phenyl-2,3-dihydroisoxazole-4-carboxylate (6c')

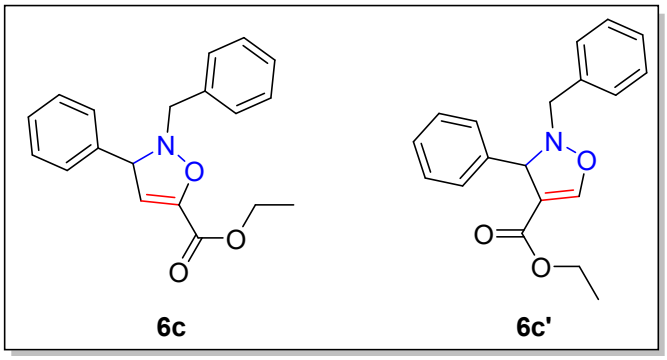

Colorless oily liquid, Yield: 84% (**6c**:**6c′**=3:1) ^{1}H NMR (600 MHz, DMSO-d_6) δ 7.94 – 7.92 (m, 1H), 7.39 – 7.24 (m, 21H), 6.11 (d, J = 3.0 Hz, 3H), 4.98 (dd, J = 35.2, 2.4 Hz, 4H), 4.21 (qd, J = 7.1, 2.8 Hz, 6H), 4.09 – 3.96 (m, 3H), 2.85 (d, J = 20.0 Hz, 14H), 1.24 (t, J = 7.1 Hz, 12H), 1.12 (t, J = 7.1 Hz, 4H). ^{13}C NMR (151 MHz, DMSO-d_6) δ 153.03 , 143.83 , 128.44 , 128.16 , 127.63 , 127.56 , 127.09 , 126.71 , 110.75 , 74.82 , 72.69 , 61.19 , 59.49 , 47.17 , 46.66 , 39.52 , 14.06 , 13.89 . HRMS(ESI) $C_{13}H_{15}NO_3$ [M+H]$^+$*m/z*: Calc. 234.1125, Found 234.1126.

Ethyl 3-(4-methoxyphenyl)-2-methyl-2,3-dihydroisoxazole-5-carboxylate (7c), ethyl 3-(4-methoxyphenyl)-2-methyl-2,3-dihydroisoxazole-4-carboxylate (7c')

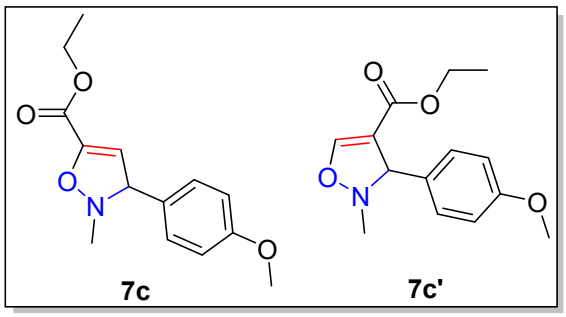

Colorless oily liquid, Yield: 80% (**7c**:**7c′**=1:5); ^{1}H NMR (600 MHz, Chloroform-*d*) δ 7.44 (dd, J = 1.7, 0.8 Hz, 1H), 7.31 – 7.22 (m, 2H), 6.90 – 6.83 (m, 2H), 5.86 (d, J = 2.8 Hz, 0H), 4.85 (d, J = 1.6 Hz, 1H), 4.16 – 4.02 (m, 2H), 3.77 (d, J = 4.7 Hz, 4H), 2.93 (s, 3H), 1.32 (t, J = 7.1 Hz, 1H), 1.18 (t, J = 7.1 Hz, 3H). ^{13}C NMR (151 MHz, $CDCl_3$) δ 162.64, 158.32, 150.93, 127.32, 113.10, 112.83, 109.53, 109.05, 76.32, 76.11, 75.89, 72.62, 60.54, 58.99, 54.26, 54.19, 46.38, 13.17, 13.10, 0.00. HRMS(ESI) $C_{14}H_{17}NO_4$ [M+H]$^+$*m/z*: Calc 264.1231, Found 264.1236

Ethyl 2-(tert-butyl)-3-phenyl-2,3-dihydroisoxazole-5-carboxylate (8c), ethyl 2-(tert-butyl)- 3-phenyl-2,3-dihydroisoxazole-4-carboxylate (8c')

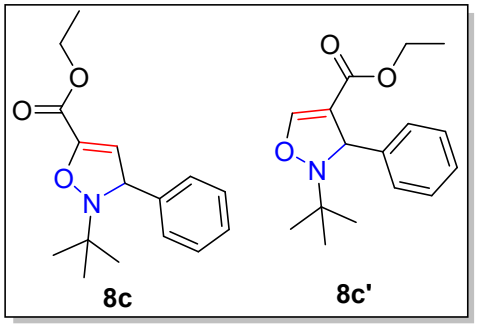

Colorless oily liquid, Yield: 20% **(8c:8c′**=1:6); ^{1}H NMR (600 MHz, DMSO-d_6) δ 7.45 – 7.28 (m, 8H), 7.24 (dt, J = 12.9, 7.3 Hz, 2H), 5.89 (d, J = 3.0 Hz, 1H), 5.45 (d, J = 3.1 Hz, 1H), 4.20 (qd, J = 7.1, 2.0 Hz, 2H), 4.04 – 3.91 (m, 2H), 1.22 (t, J = 7.1 Hz, 3H), 1.16 – 1.02 (m, 21H).^{13}C NMR (151 MHz, DMSO-d_6) δ 158.26 , 153.37 , 144.39 , 128.33 , 127.95 , 127.51 , 127.17 , 127.06 , 126.84 , 111.58 ,

67.06 , 65.06 , 61.00 , 60.75 , 60.47 , 59.23 , 24.45 , 24.34 , 13.95 , 13.83 . HRMS(ESI) $C_{16}H_{21}NO_3$ $[M+H]^+$ *m/z*: Calc 276.1595, Found 276.1590

Ethyl 3a*H*-isoxazolo[2,3-*a*]quinoline-2-carboxylate (9c)

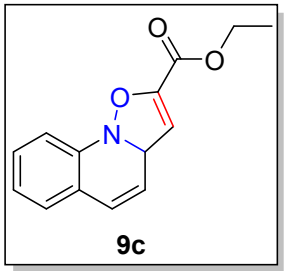

Yellow solid, Yield: 91%, mp: 112-113 °C, ^{1}H NMR (600 MHz, Chloroform-*d*) δ 9.93 (s, 2H), 8.72 – 8.65 (m, 2H), 8.11 – 8.04 (m, 2H), 7.76 – 7.61 (m, 6H), 7.45 (ddd, *J* = 8.1, 6.9, 1.3 Hz, 2H), 4.30 (q, *J* = 7.1 Hz, 4H), 1.37 (t, *J* = 7.1 Hz, 6H).^{13}C NMR (151 MHz, $CDCl_3$) δ 188.83, 167.78, 154.84, 139.15, 135.92, 131.73, 127.74, 125.47, 123.85, 120.35, 118.72, 59.46, 14.52. HRMS(ESI) $C_{14}H_{13}NO_3$ $[M+H]^+$ *m/z*: Calc 244.0969, Found 244.0969

Ethyl 6,6-dimethyl-3a,4,5,6-tetrahydropyrrolo[1,2-*b*]isoxazole-2-carboxylate (10c)

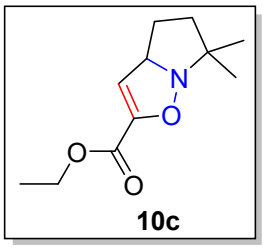

Yellow oily liquid, Yield: 86%; ^{1}H NMR (600 MHz, cdcl$_3$) δ 7.23 (d, *J* = 1.4 Hz, 1H), 4.76 (ddd, *J* = 8.0, 2.9, 1.4 Hz, 1H), 4.20 – 4.09 (m, 2H), 2.14 (ddt, *J* = 13.1, 10.9, 8.0 Hz, 1H), 1.82 (ddt, *J* = 13.2, 7.5, 2.8 Hz, 1H), 1.70 – 1.59 (m, 2H), 1.32 (s, 3H), 1.24 (t, *J* = 7.1 Hz, 3H), 1.08 (s, 3H). ^{13}C NMR (151 MHz, Chloroform-*d*) δ 163.91 , 152.28 , 110.70 , 70.16 , 67.83 , 59.97 , 34.49 , 32.41 , 26.28 , 23.49 , 14.45 . HRMS(ESI) $C_{16}H_{21}NO_3$ $[M+H]^+$ *m/z*: Calc 212.1282, Found 212.1276

Ethyl 3-(2,6-dichlorophenyl)-2-phenyl-2,3-dihydroisoxazole-5-carboxylate (11c)

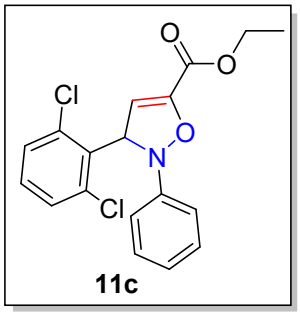

Colorless oily liquid, Yield: 46%; ^{1}H NMR (600 MHz, DMSO-d_6) δ 8.08 (s, 1H), 7.65 (s, 1H), 7.56 (d, *J* = 8.1 Hz, 2H), 7.50 (dd, *J* = 7.9, 1.5 Hz, 1H), 7.24 – 7.18 (m, 2H), 6.91 – 6.81 (m, 3H), 4.19 (q, *J* = 7.1 Hz, 2H), 1.25 (t, *J* = 7.1 Hz, 3H). ^{13}C NMR (151 MHz, $CDCl_3$) δ 160.42, 138.93, 136.65, 132.45, 131.30, 130.04, 129.52, 122.50, 121.76, 115.15, 93.54, 77.20, 76.99, 76.78, 60.57, 29.68, 14.44. HRMS(ESI) $C_{18}H_{15}Cl_2NO_3$ $[M+H]^+$ *m/z*: Calc 364.0502, Found 364.0499

Methyl 2-benzyl-3,5-diphenyl-2,3-dihydroisoxazole-4-carboxylate (12c')

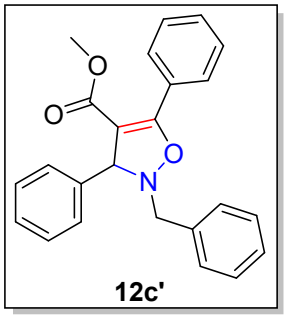

Colorless oily liquid, Yield: 81%; ^{1}H NMR (600 MHz, DMSO-d_6) δ 7.78 – 7.73 (m, 2H), 7.57 – 7.51 (m, 1H), 7.50 – 7.42 (m, 4H), 7.40 – 7.25 (m, 8H), 5.41 (s, 1H), 4.39 (d, *J* = 13.4 Hz, 1H), 4.29 (d, *J* = 13.4 Hz, 1H), 3.52 (s, 3H).^{13}C NMR (151 MHz, DMSO-d_6) δ 163.45 , 161.75 , 141.45 , 136.16 , 131.31 , 129.60 , 129.30 , 128.38 , 128.31 , 128.06 , 127.63 , 127.57 , 127.02 , 126.92 , 103.04 , 72.77 , 65.00 ,

62.77 , 51.05 , 29.99 , 18.64 , 13.52 . HRMS(ESI) $C_{24}H_{21}NO_3$ $[M+H]^+$ *m/z*: Calc 370.1443, Measured 370.1448

Methyl 6,6-dimethyl-2-phenyl-3a,4,5,6-tetrahydropyrrolo[1,2-*b*]isoxazole-3-carboxylate (13c')

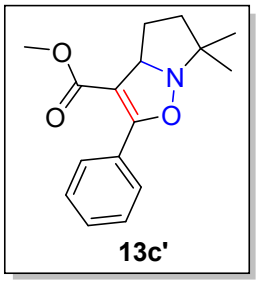

Yellow oily liquid, Yield: 68%; ^{1}H NMR (600 MHz, Chloroform-*d*) δ 7.78 – 7.72 (m, 2H), 7.45 – 7.34 (m, 3H), 5.00 (dd, *J* = 8.1, 3.2 Hz, 1H), 3.66 (s, 3H), 2.27 (ddt, *J* = 13.1, 10.7, 8.0 Hz, 1H), 1.96 (ddt, *J* = 13.2, 8.4, 2.9 Hz, 1H), 1.77 (ddd, *J* = 12.5, 10.8, 8.4 Hz, 1H), 1.70 (ddd, *J* = 12.5, 7.8, 2.6 Hz, 1H), 1.41 (s, 3H), 1.15 (s, 3H).^{13}C NMR (151 MHz, Chloroform-*d*) δ 164.27 , 162.14 , 130.66 , 129.29 , 127.76 , 127.41 , 104.31 , 70.55 , 70.01 , 50.97 , 34.60 , 33.49 , 26.11 , 23.42 . HRMS(ESI) $C_{16}H_{19}NO_3$ $[M+H]^+$ *m/z*: Calc 274.1438, Measured 274.1435

Methyl 2-methyl-3,5-diphenyl-2,3-dihydroisoxazole-4-carboxylate (14c')

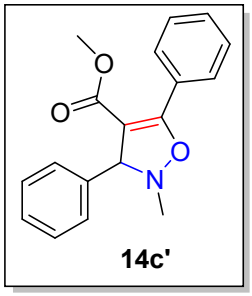

Colorless oily liquid, Yield: 48%; ^{1}H NMR (600 MHz, DMSO-d_6) δ 7.82 – 7.77 (m, 2H), 7.58 – 7.53 (m, 1H), 7.49 (dd, *J* = 8.3, 6.9 Hz, 2H), 7.41 – 7.33 (m, 4H), 7.33 – 7.26 (m, 1H), 5.19 (s, 1H), 3.51 (s, 3H), 2.96 (s, 3H). ^{13}C NMR (151 MHz, DMSO-d_6) δ 163.56 , 161.24 , 131.26 , 129.50 , 128.32 , 128.05 , 127.64 , 127.08 , 102.74 , 75.16 , 50.99 . HRMS(ESI) $C_{18}H_{17}NO_3$ $[M+H]^+$ *m/z*: Calc 296.1282, Measured 296.1282

Diethyl 2-benzyl-3-phenyl-2,3-dihydroisoxazole-4,5-dicarboxylate (15c)

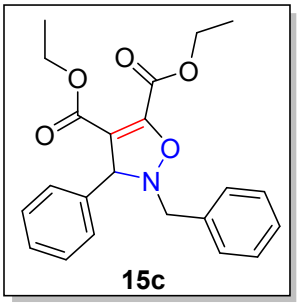

Colorless oily liquid, Yield: 84%; ^{1}H NMR (600 MHz, Chloroform-*d*) δ 7.41 – 7.36 (m, 2H), 7.36 – 7.29 (m, 6H), 7.29 – 7.25 (m, 2H), 5.24 (s, 1H), 4.46 (d, *J* = 13.0 Hz, 1H), 4.38 (q, *J* = 7.2 Hz, 2H), 4.18 – 4.04 (m, 3H), 1.39 (d, *J* = 14.3 Hz, 3H), 1.17 (t, *J* = 7.1 Hz, 3H). ^{13}C NMR (151 MHz, Chloroform-*d*) δ 162.28 , 159.31 , 152.09 , 139.74 , 134.93 , 129.58 , 128.59 , 128.56 , 128.17 , 128.07 , 127.47 , 109.15 , 72.88 , 63.58 , 62.86 , 60.77 , 14.04 , 14.03 . HRMS(ESI) $C_{18}H_{15}Cl_2NO_3$ $[M+H]^+$ *m/z*: Calc 382.1610, Measured 382.1639

Diethyl 6,6-dimethyl-3a,4,5,6-tetrahydropyrrolo[1,2-*b*]isoxazole-2,3-dicarboxylate (16c)

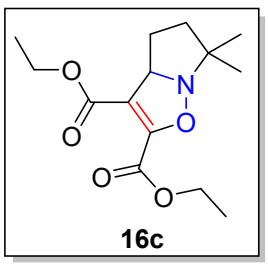

Yellow oily liquid, Yield: 66%; ^{1}H NMR (600 MHz, $CDCl_3$) δ 4.82 (dd, *J* = 8.1, 3.2 Hz, 1H), 4.26 (q, *J* = 7.2 Hz, 2H), 4.16 – 4.05 (m, 2H), 2.13 (ddt, *J* = 13.2, 10.6, 7.9 Hz, 1H), 1.97 – 1.83 (m, 1H), 1.74 – 1.60 (m, 2H), 1.30 (s, 3H), 1.28 (t, *J* = 7.2 Hz, 3H), 1.19 (t, *J* = 7.2 Hz, 3H), 1.04 (s, 3H). ^{13}C NMR (151 MHz, $CDCl_3$) δ 161.37, 158.26, 151.18, 108.14, 69.53,

68.67, 61.51, 59.43, 33.60, 31.21, 25.14, 22.13, 13.13, 12.91.

HRMS(ESI) $C_{14}H_{21}NO_5$ $[M+H]^+$ *m/z*: Calc 284.1493, Measured 284.1489

Diethyl 2-methyl-3-phenyl-2,3-dihydroisoxazole-4,5-dicarboxylate (17c)

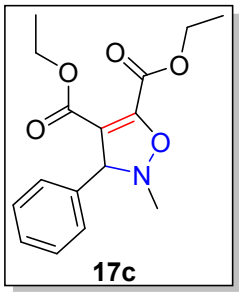

Colorless oily liquid, Yield: 72%; ^{1}H NMR (600 MHz, DMSO-d_6) δ 7.40 – 7.34 (m, 2H), 7.31 (tt, *J* = 6.4, 1.3 Hz, 3H), 5.19 (s, 1H), 4.33 (q, *J* = 7.1 Hz, 2H), 4.09 – 3.96 (m, 2H), 2.93 (s, 3H), 1.29 (t, *J* = 7.1 Hz, 3H), 1.08 (t, *J* = 7.1 Hz, 3H).^{13}C NMR (151 MHz, DMSO-d_6) δ 161.56 , 158.98 , 151.05 , 128.44 , 128.04 , 127.05 , 108.23 , 74.09 , 62.79 , 60.38 , 46.99 , 30.00 , 13.75 , 13.71 . HRMS(ESI) $C_{16}H_{19}NO_5$ $[M+H]^+$ *m/z*: Calc 306.1336, Measured 306.1339

Ethyl 2-methyl-3-phenyl-4-(trifluoromethyl)-2,3-dihydroisoxazole-5-carboxylate (18c)

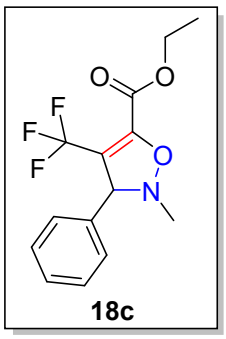

Colorless oily liquid, Yield: 94%; ^{1}H NMR (600 MHz, DMSO-d_6) δ 7.38 (tt, *J* = 7.0, 1.1 Hz, 2H), 7.33 (tt, *J* = 7.9, 1.4 Hz, 3H), 5.34 (q, *J* = 2.1 Hz, 1H), 4.13 – 4.02 (m, 2H), 2.96 (s, 3H), 1.09 (t, *J* = 7.1 Hz, 3H). ^{13}C NMR (151 MHz, DMSO-d_6) δ 160.26 , 128.54 , 128.32 , 127.18 , 118.75 , 116.94 , 110.32 (q, $J_{C\text{-}F}$ = 3.0 Hz) , 75.36 , 65.00 , 60.89 , 46.81 , 30.00 , 18.64 , 13.53 . HRMS(ESI) $C_{14}H_{14}F_3NO_3$ $[M+H]^+$ *m/z*: Calc 302.0999, Measured 302.0998

6. ^{1}H NMR, ^{13}C NMR, HRMS Spectra of New Compounds

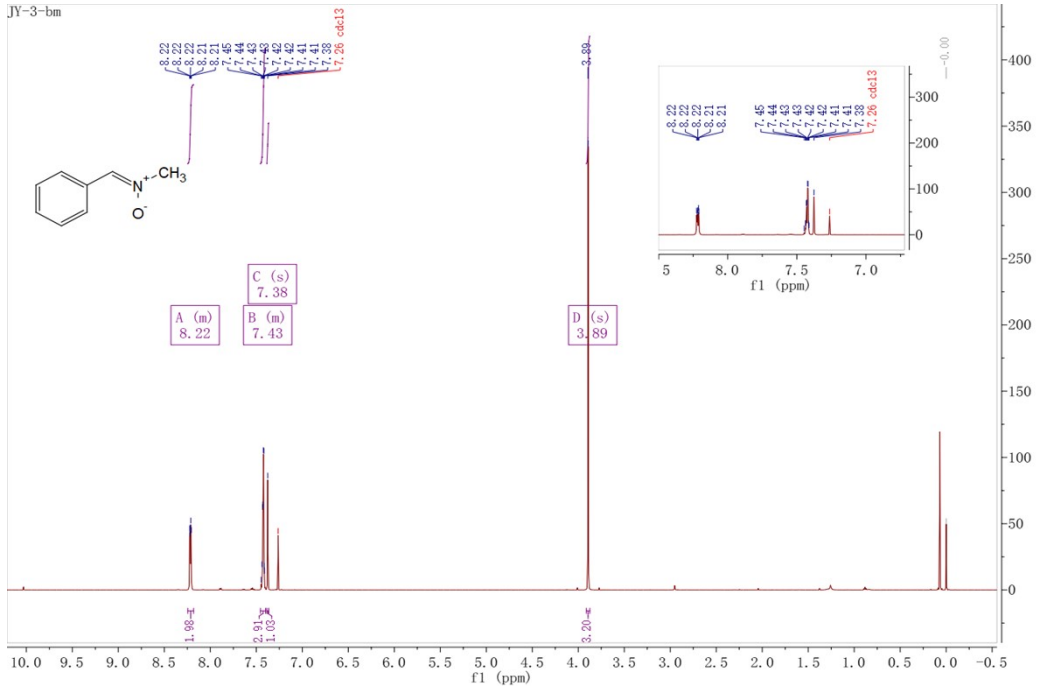

Figure S11 ^{1}H NMR of **1a**

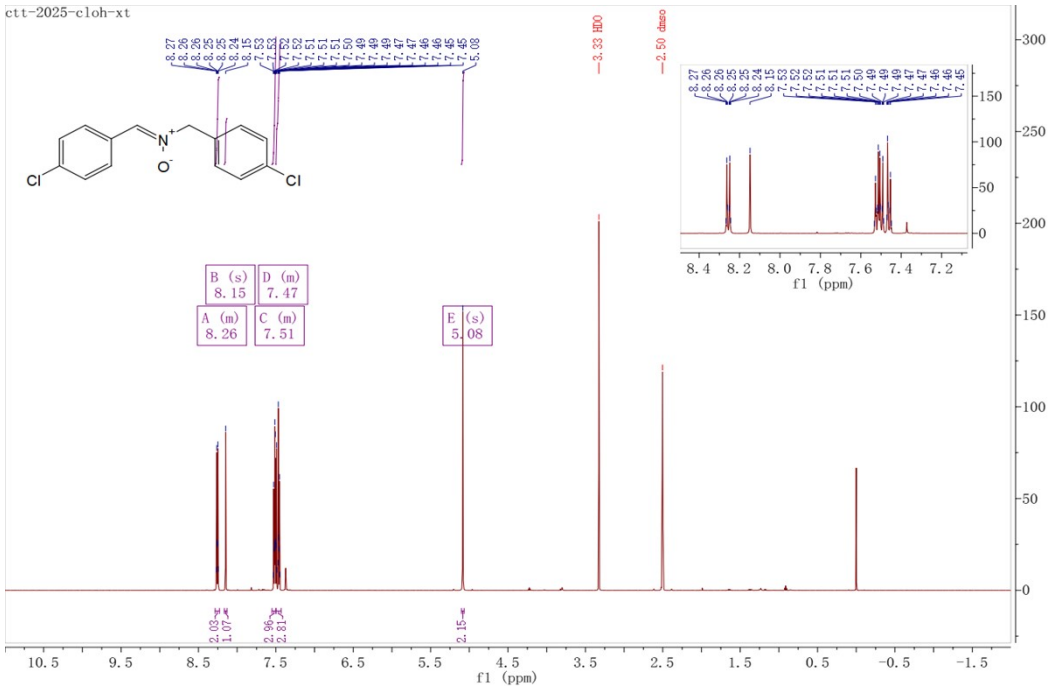

Figure S12 ^{1}H NMR of **2a**

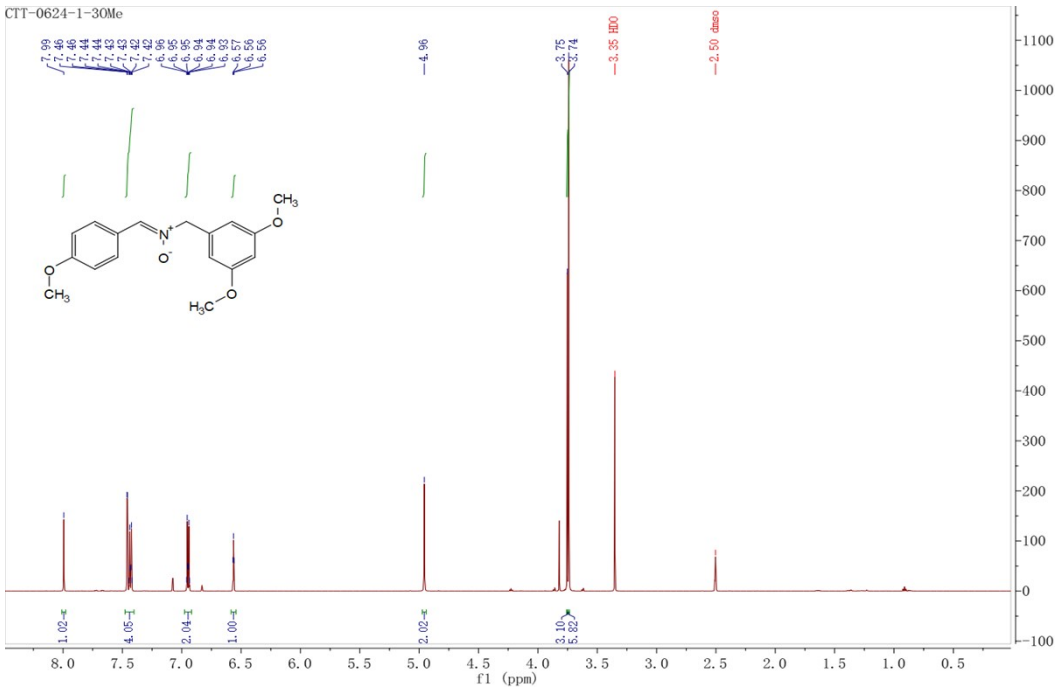

Figure S13 ^{1}H NMR of **3a**

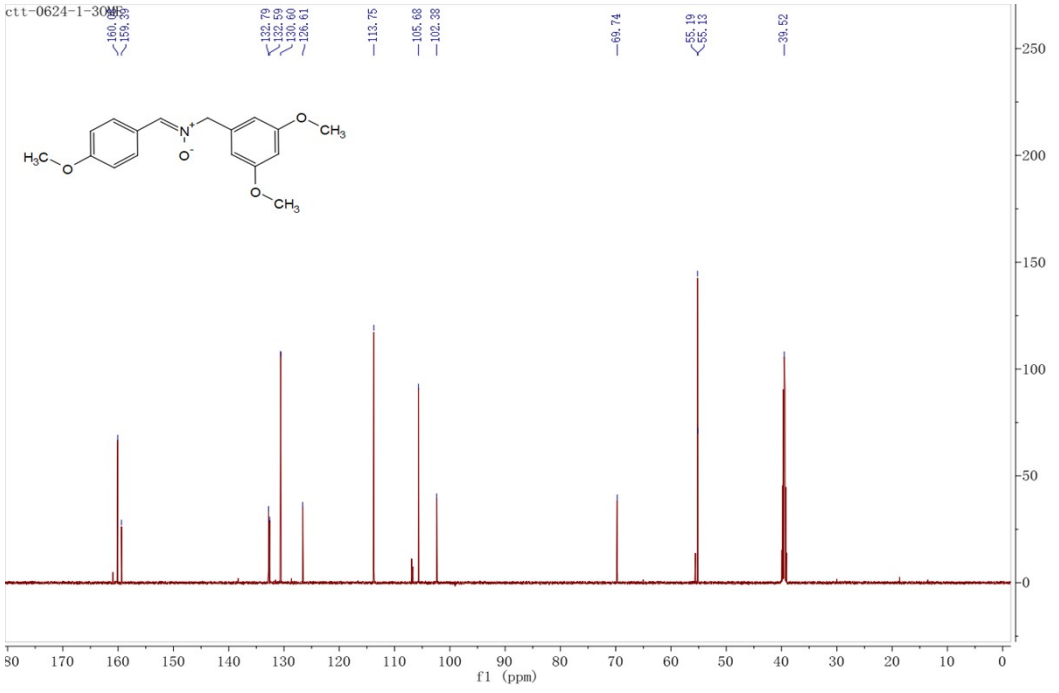

Figure S14 ^{13}C NMR of **3a**

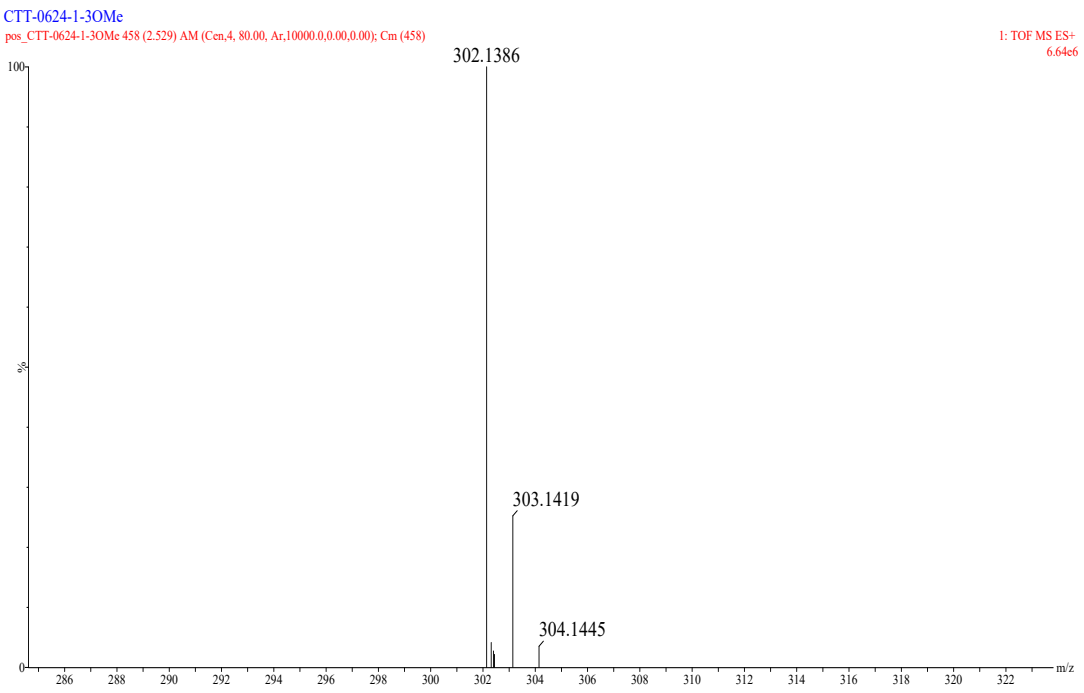

Figure S15 HRMS of **3a**

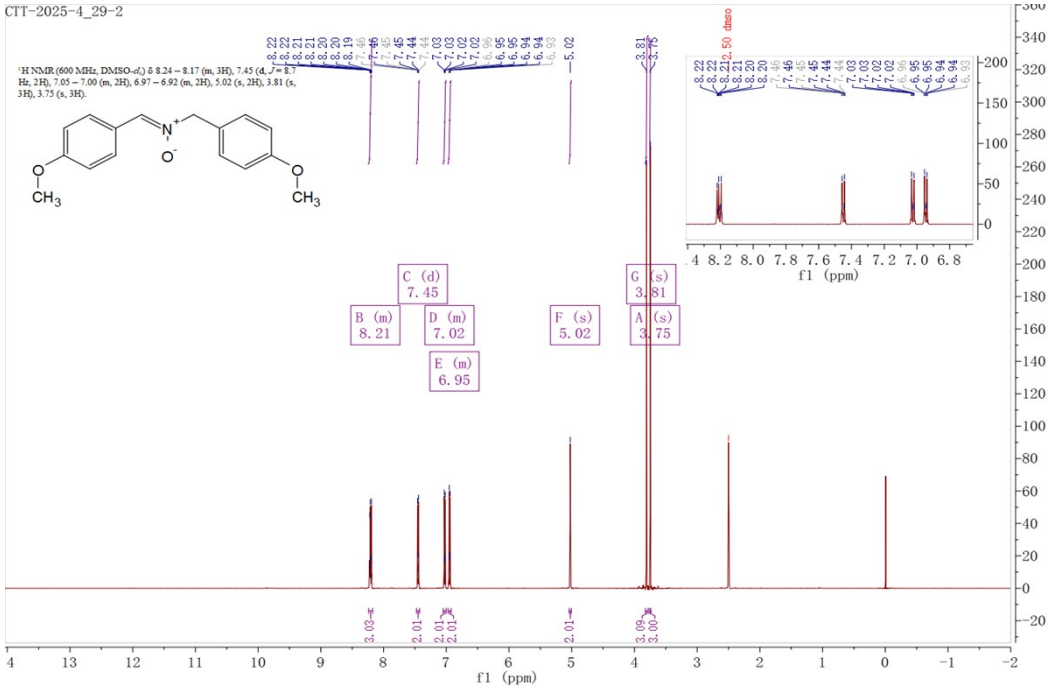

Figure S16 ^{1}H NMR of **4a**

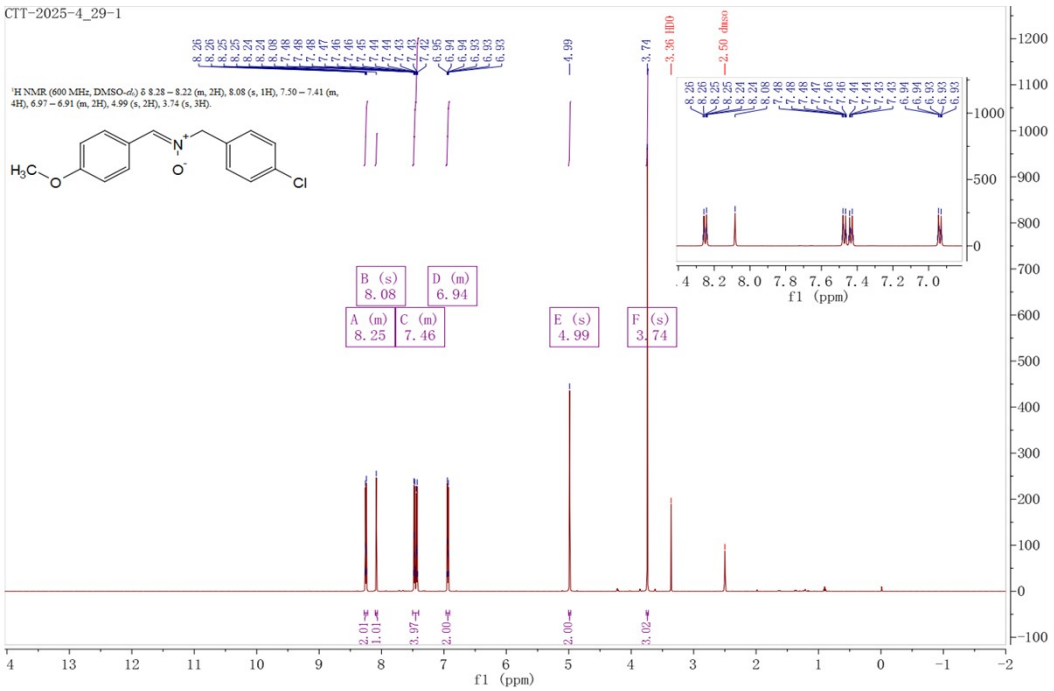

Figure S17 ^{1}H NMR of **5a**

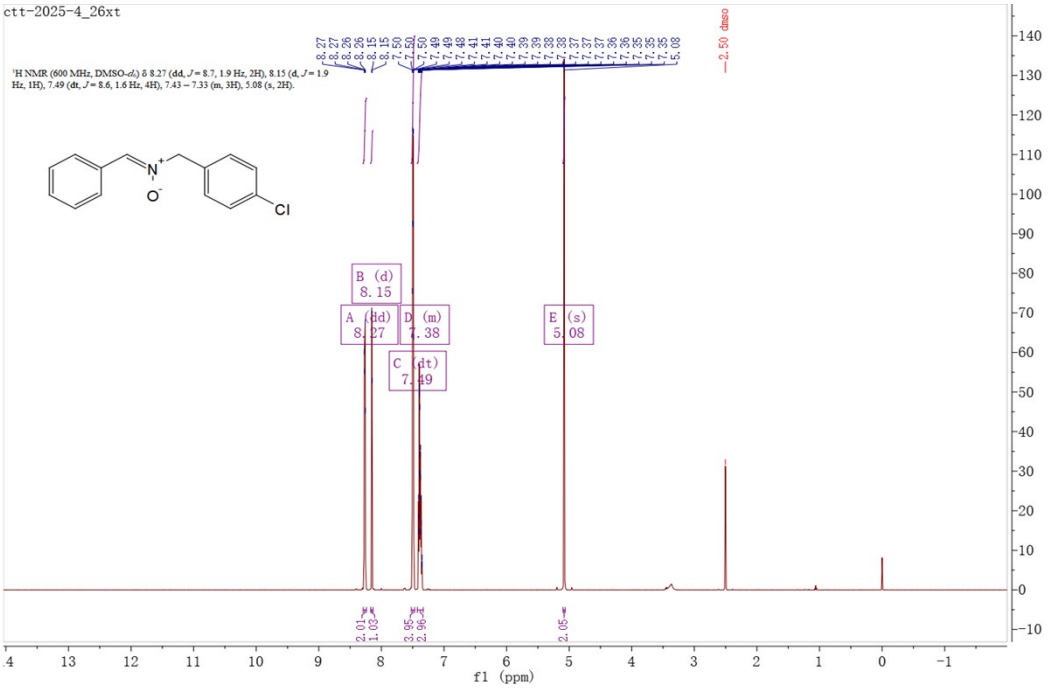

Figure S18 ^{1}H NMR of **6a**

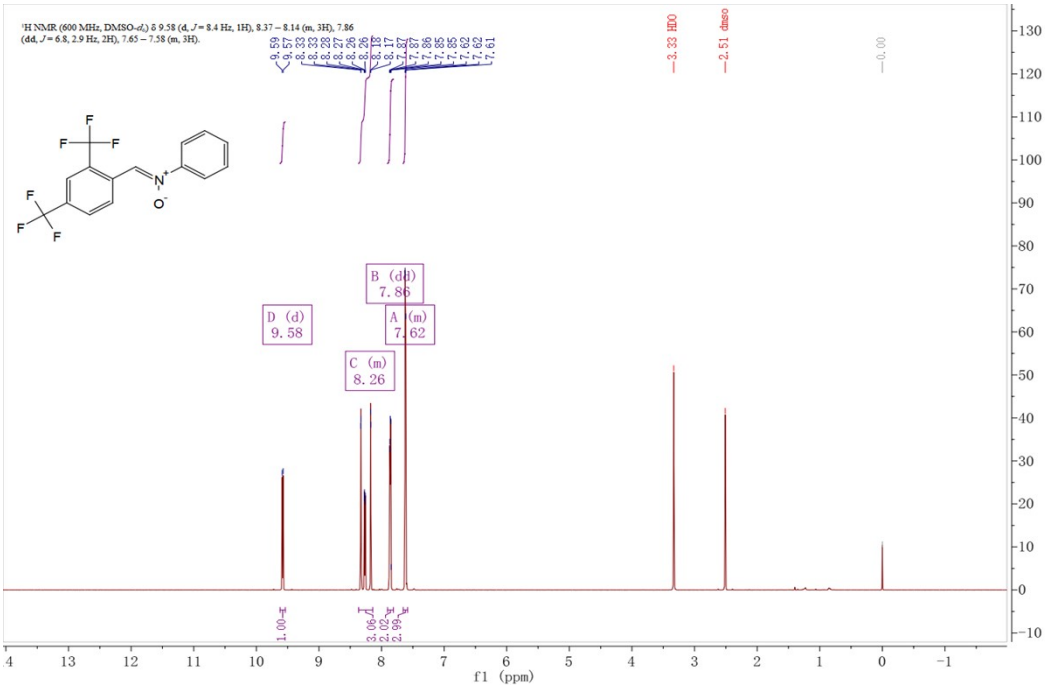

Figure S19 ^{1}H NMR of **7a**

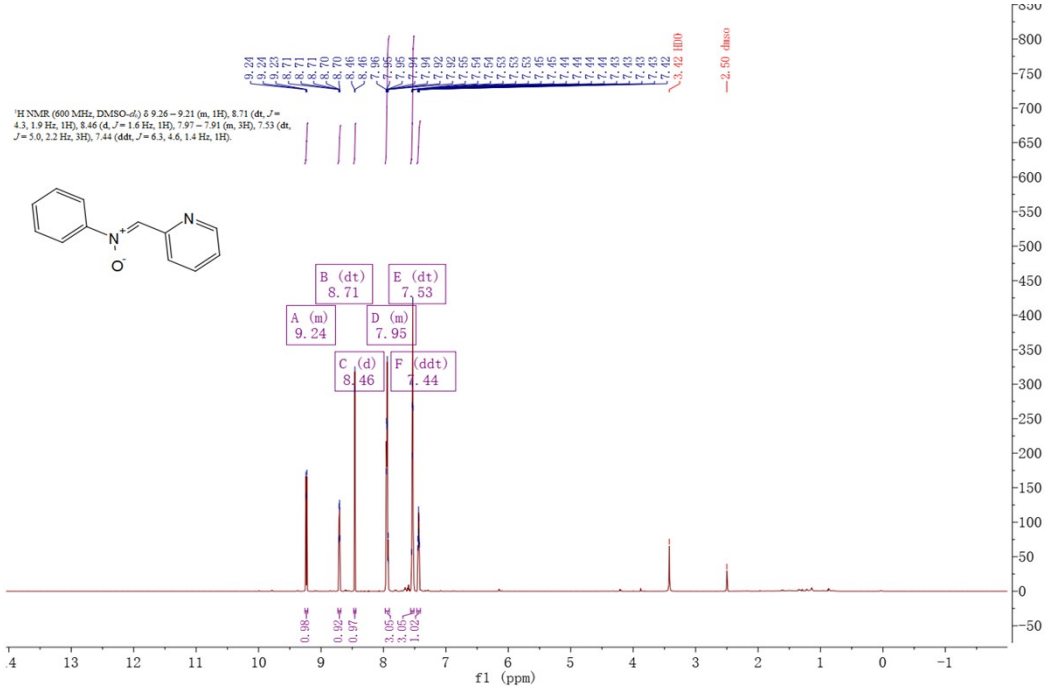

Figure S20 ^{1}H NMR of **8a**

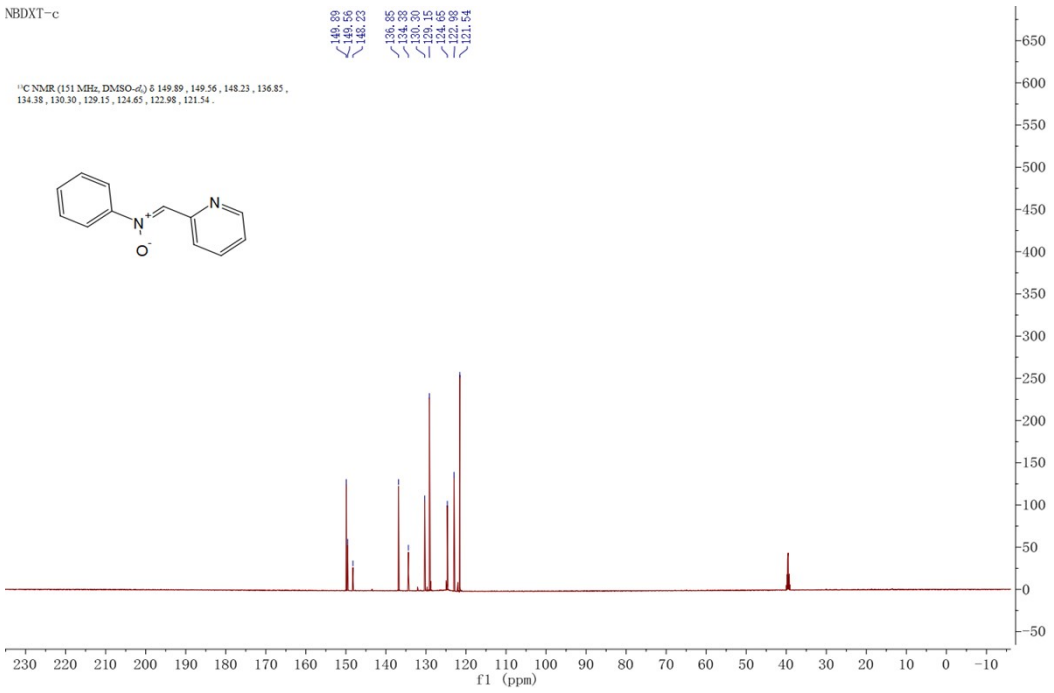

Figure S21 ^{13}C NMR of **8a**

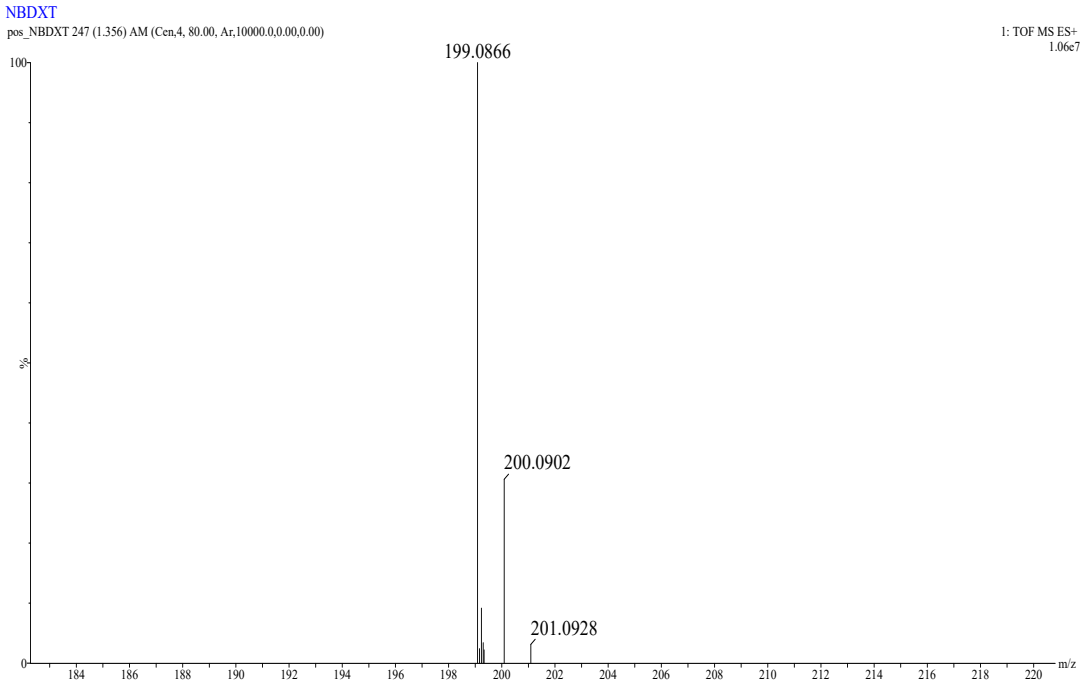

Figure S22 HRMS of **8a**

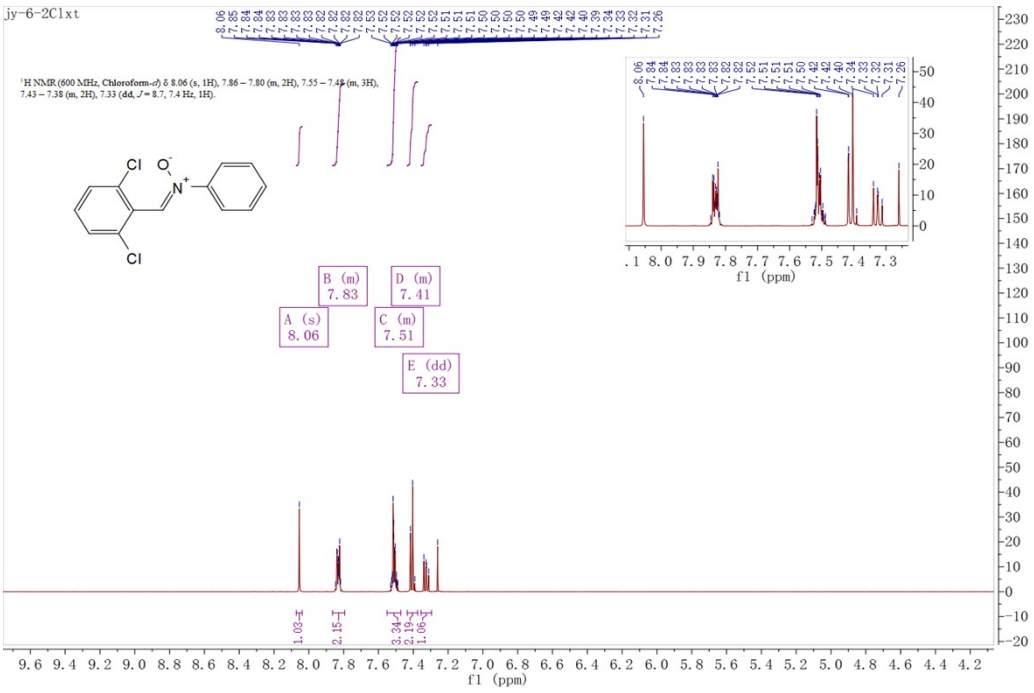

Figure S23 ^{1}H NMR of **9a**

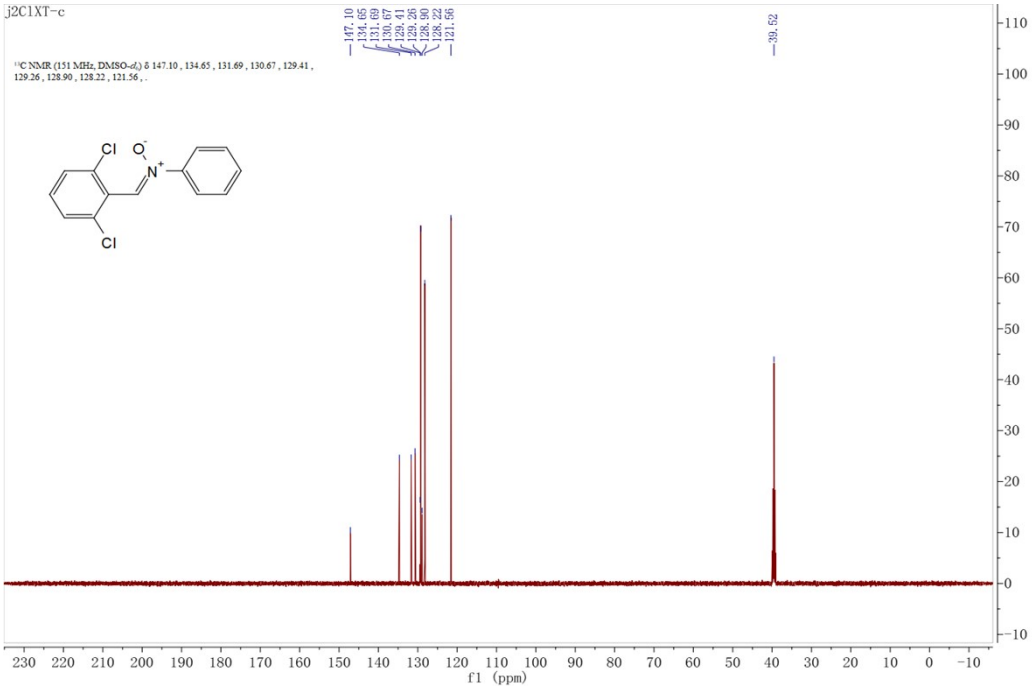

Figure S24 ^{13}C NMR of **9a**

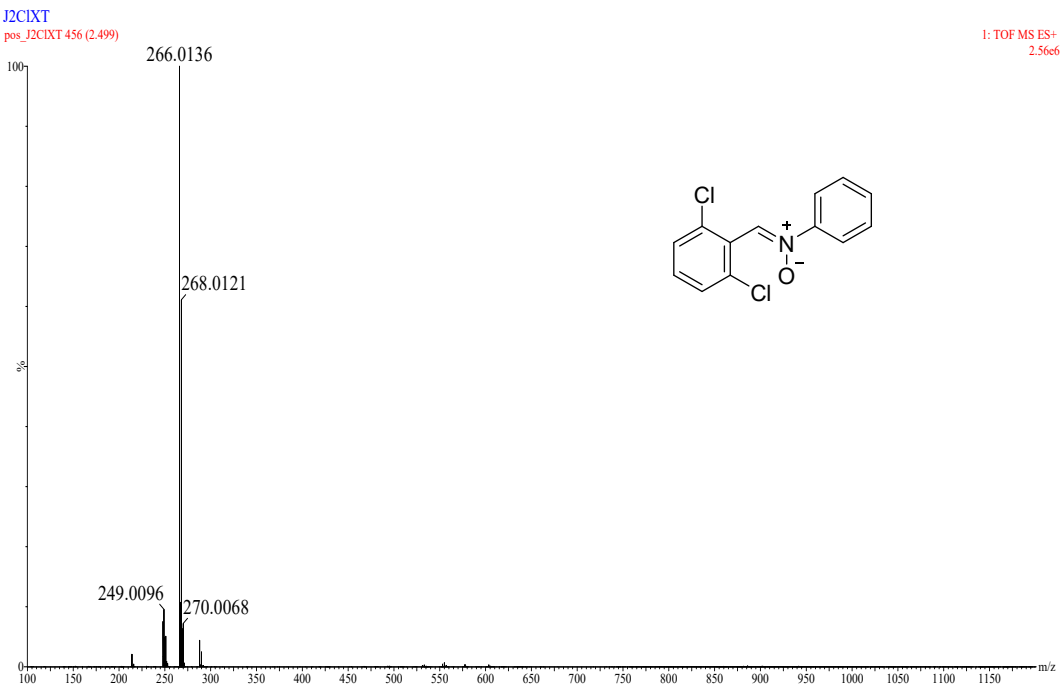

Figure S25 HRMS of **9a**

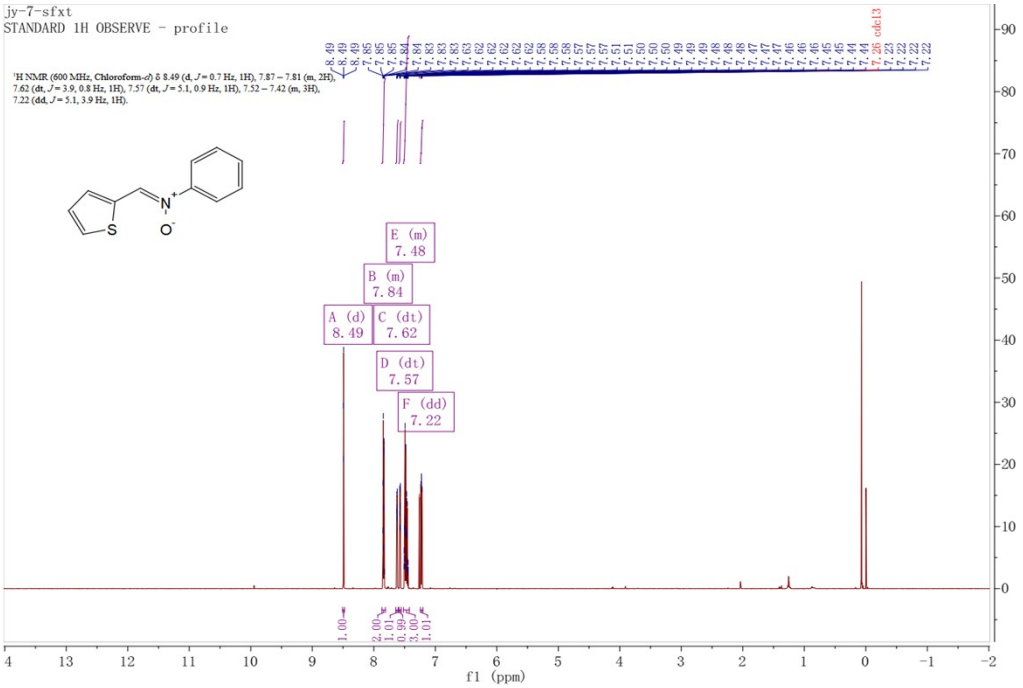

Figure S26 ^{1}H NMR of **10a**

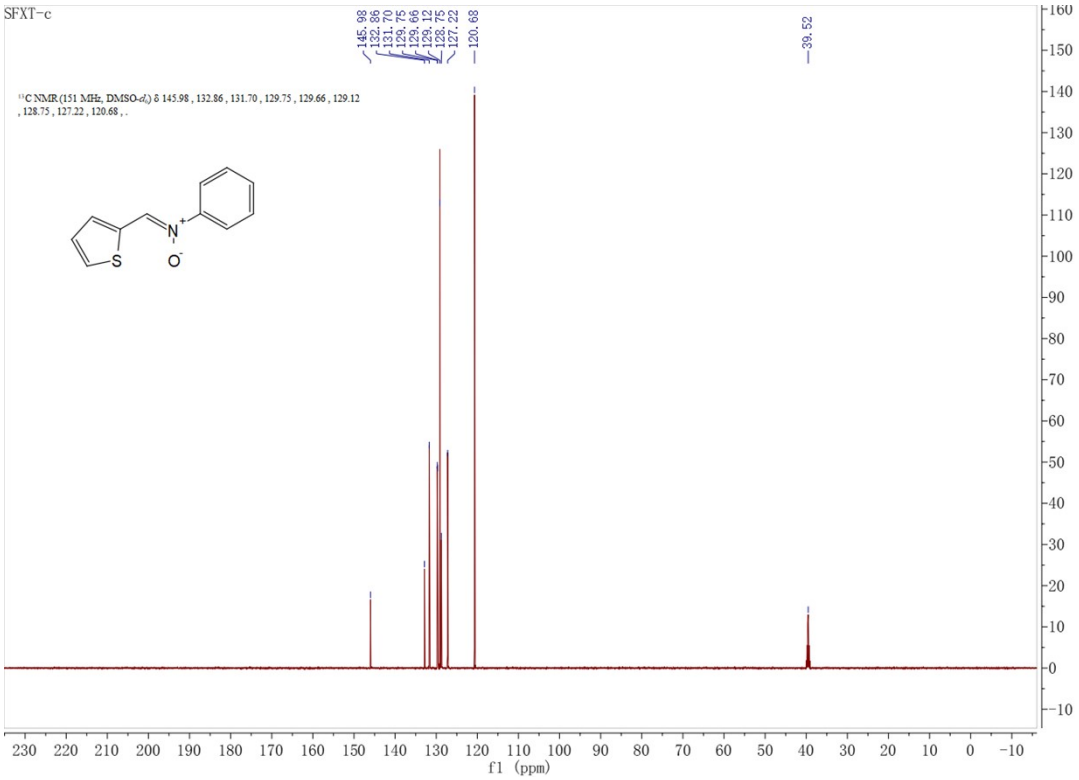

Figure S27 ^{13}C NMR of **10a**

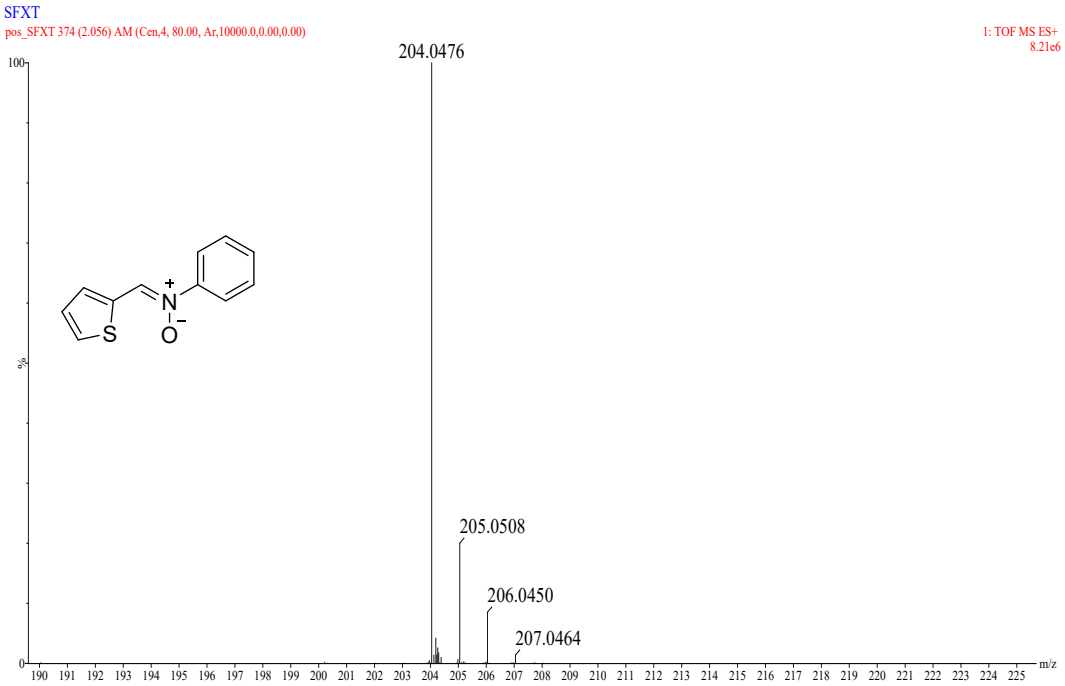

Figure S28 HRMS of **10a**

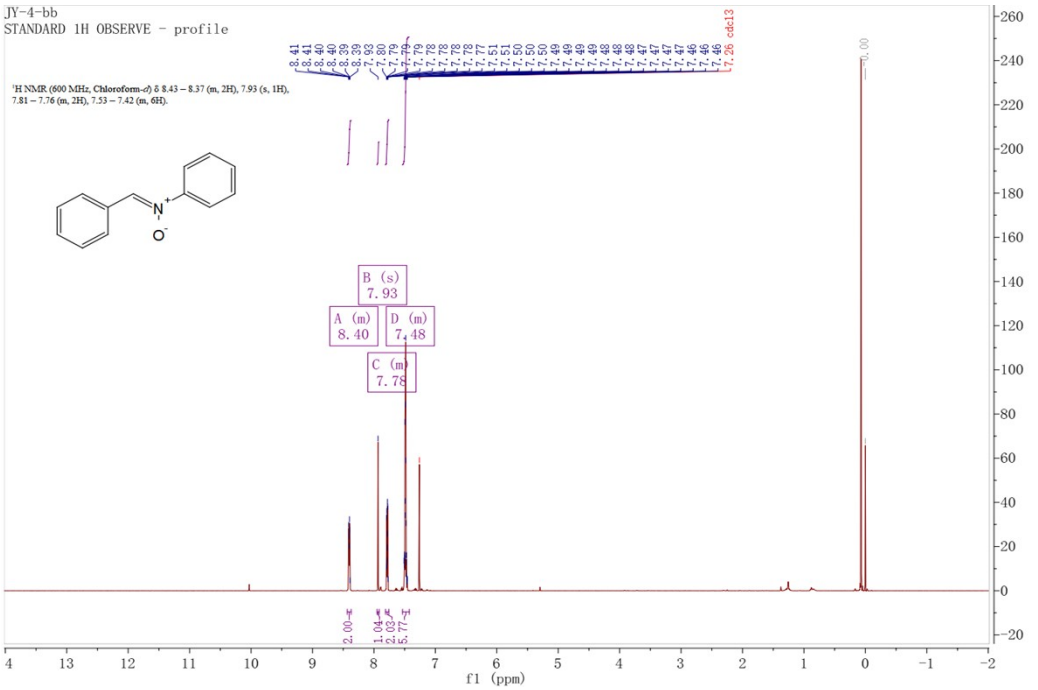

Figure S29 ^{1}H NMR of **11a**

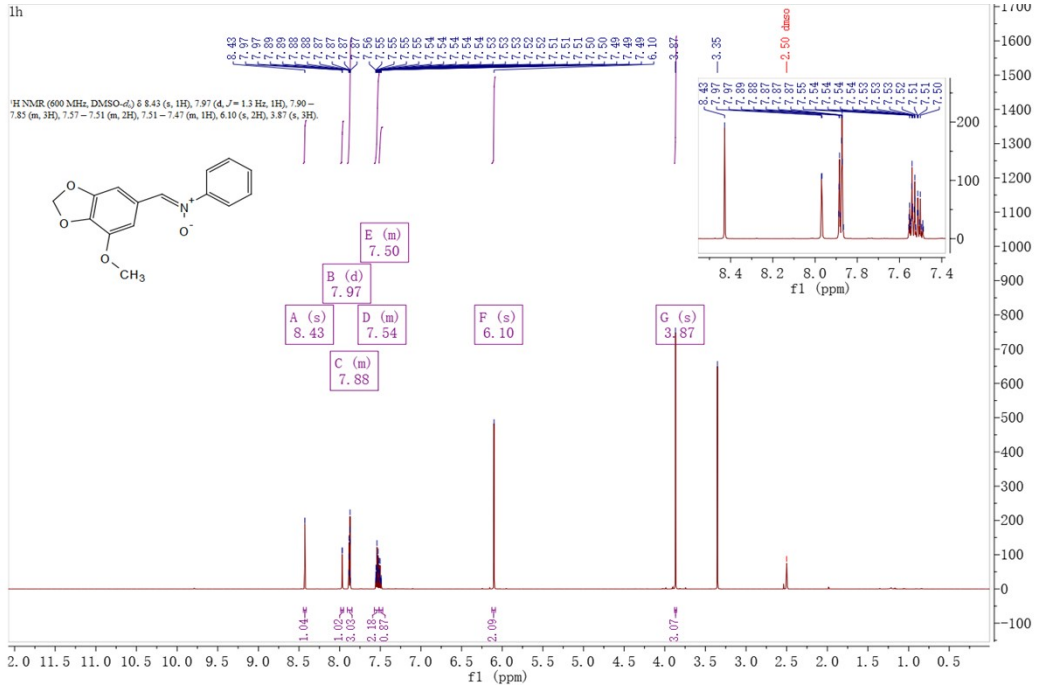

Figure S30 ^{1}H NMR of **12a**

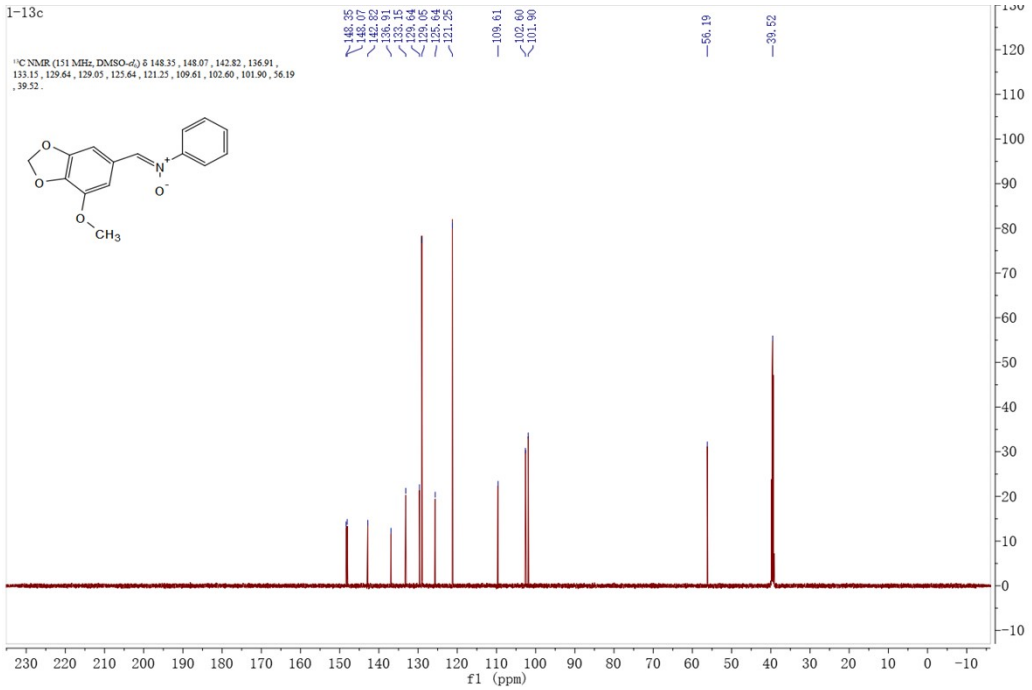

Figure S31 ^{13}C NMR of **12a**

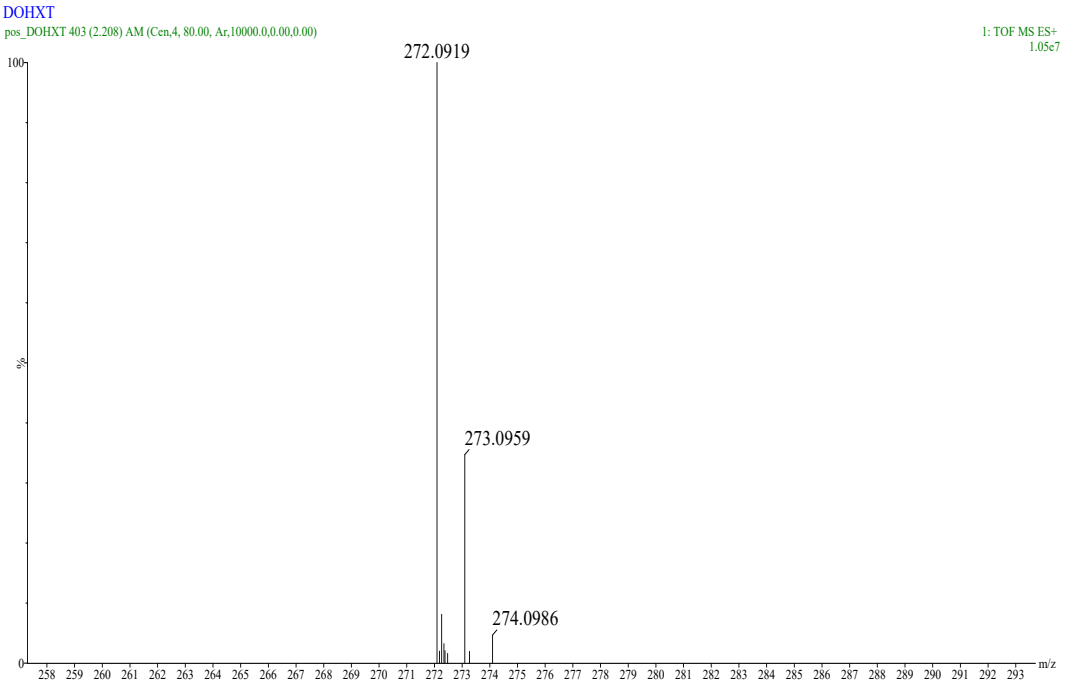

Figure S32 HRMS of **12a**

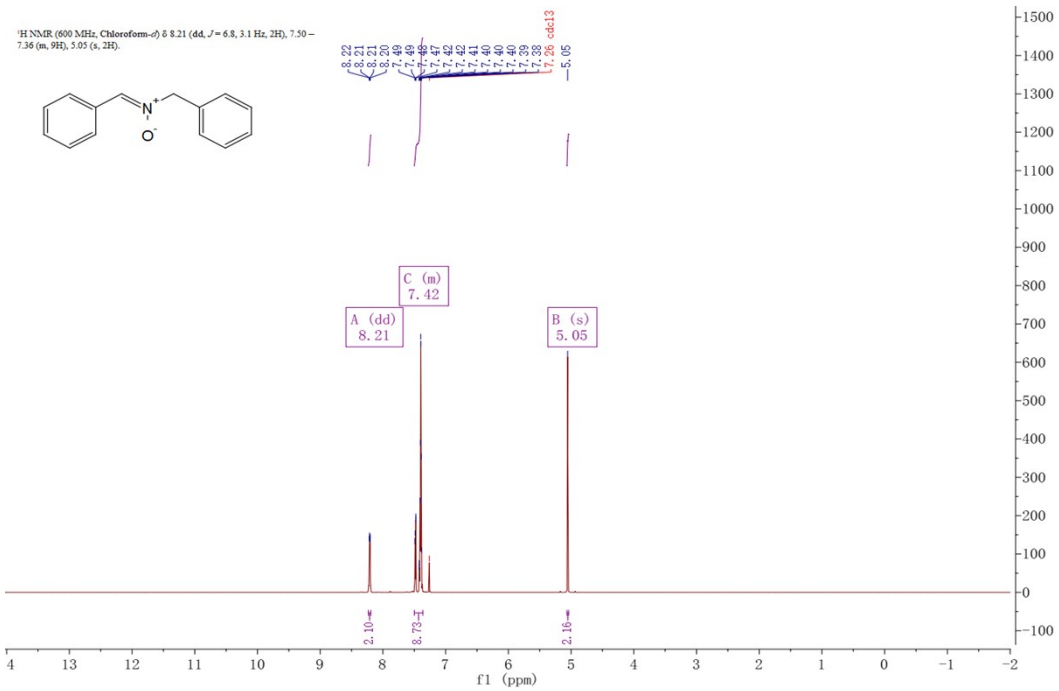

Figure S33 ^{1}H NMR of **13a**

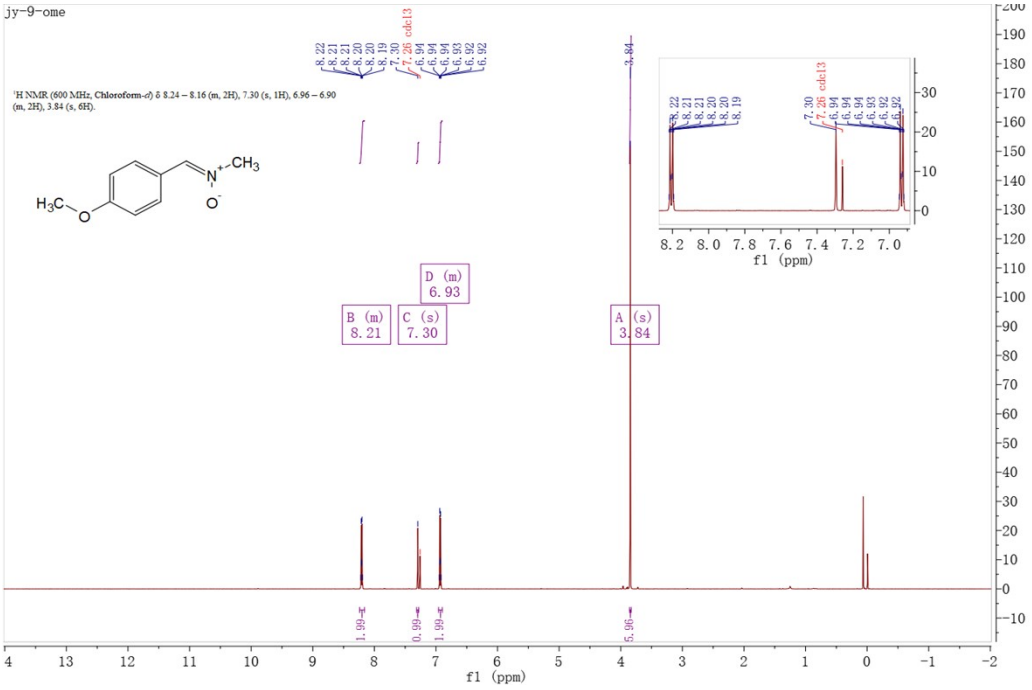

Figure S34 ^{1}H NMR of **14a**

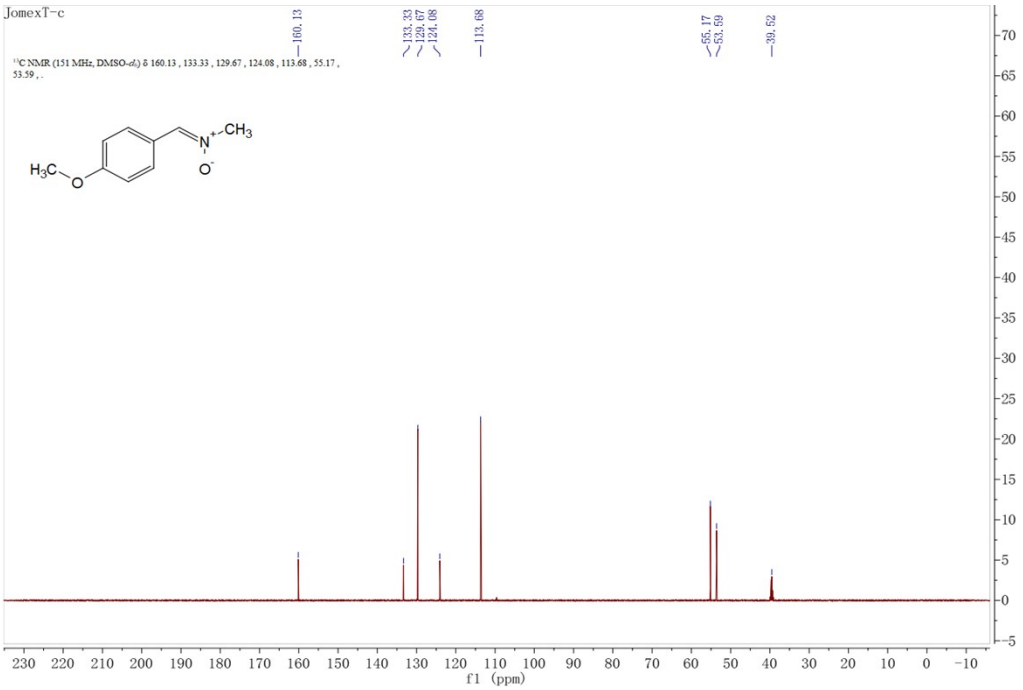

Figure S35 ^{13}C NMR of **14a**

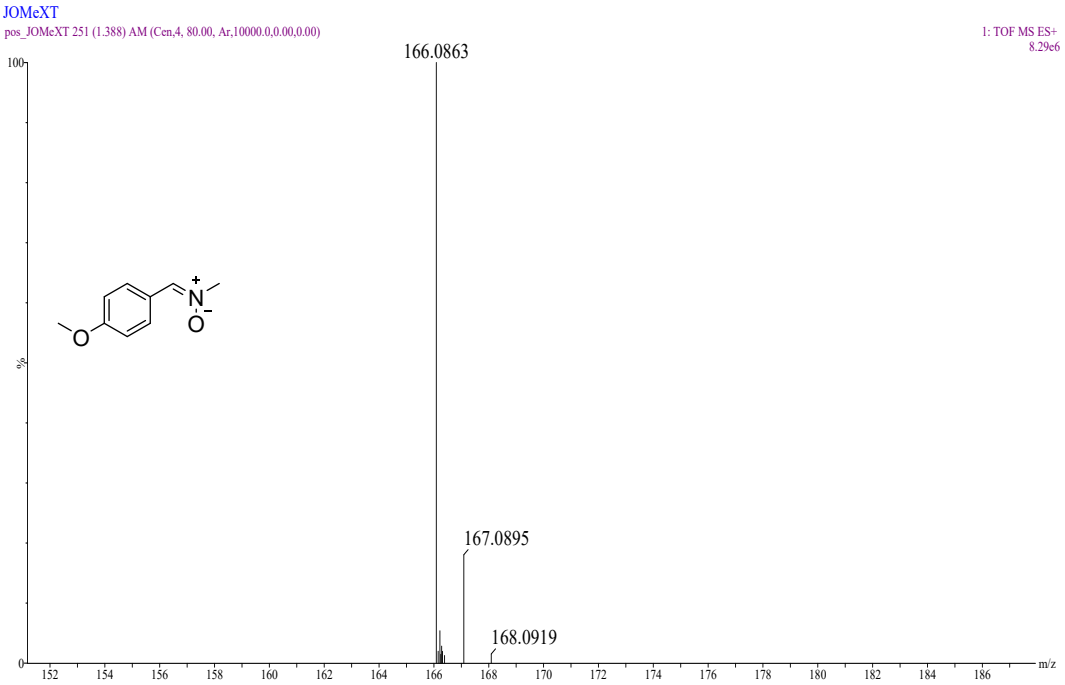

Figure S36 HRMS of **14a**

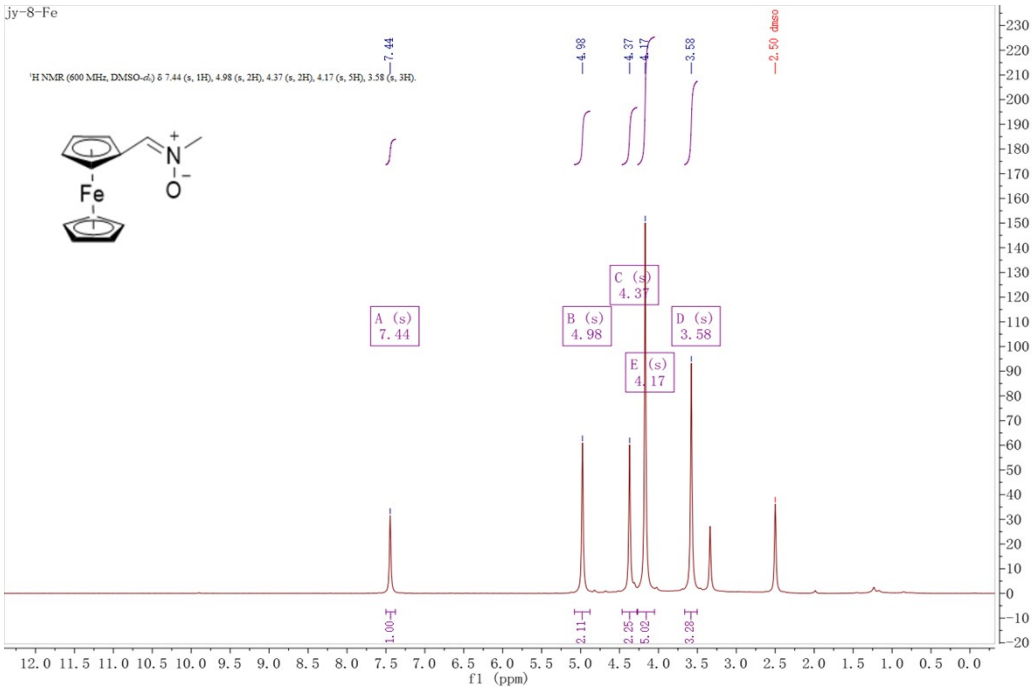

Figure S37 ^{1}H NMR of **15a**

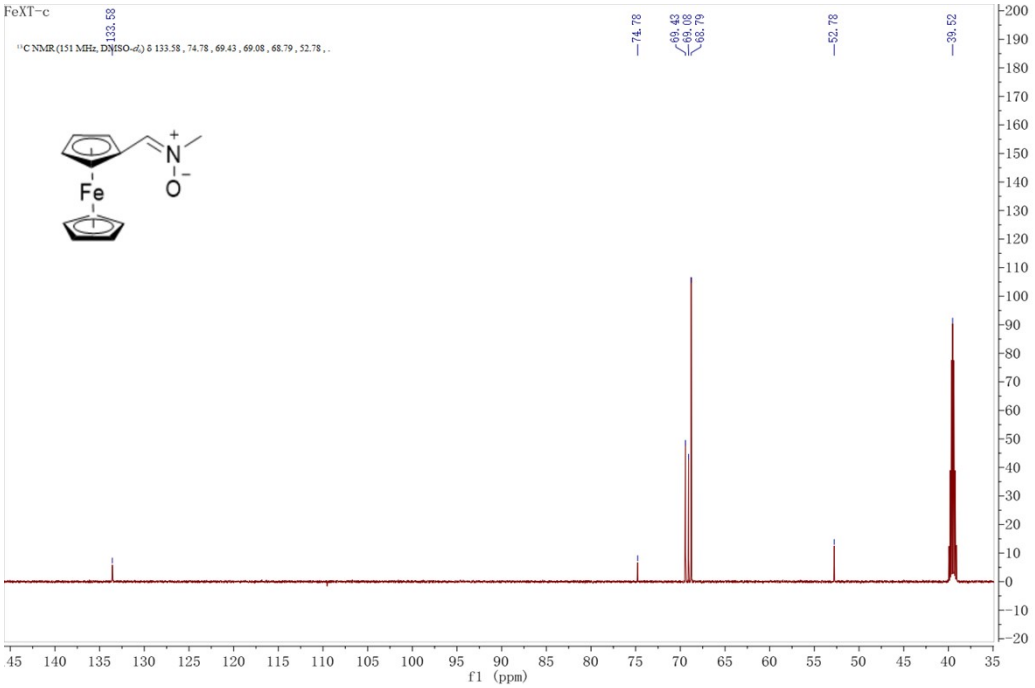

Figure S38 ^{13}C NMR of **15a**

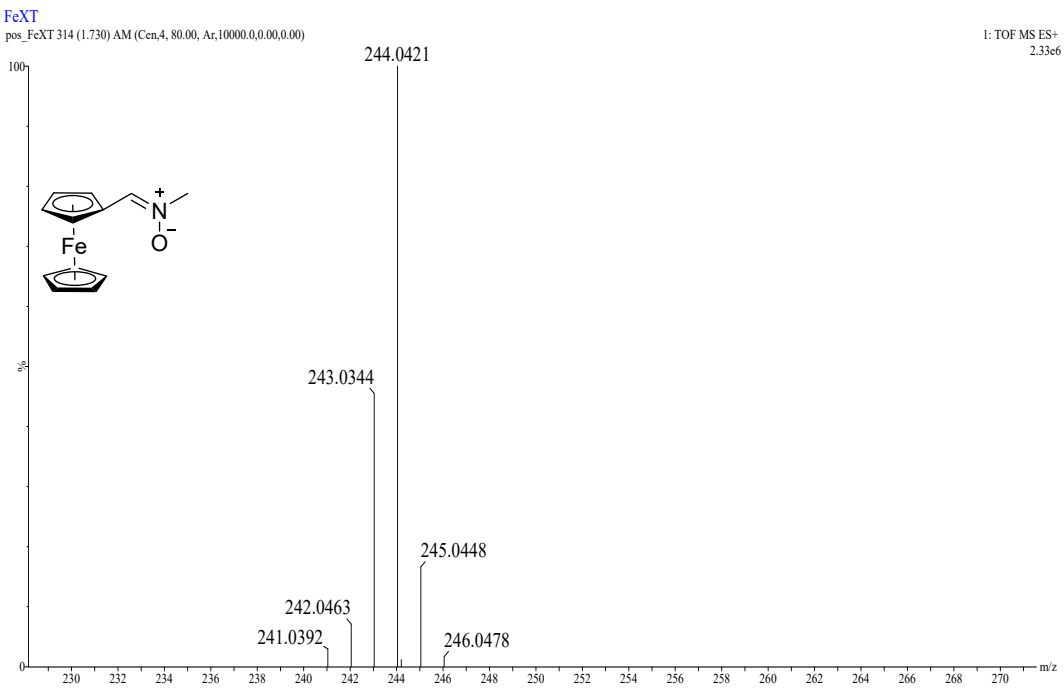

Figure S39 HRMS of **15a**

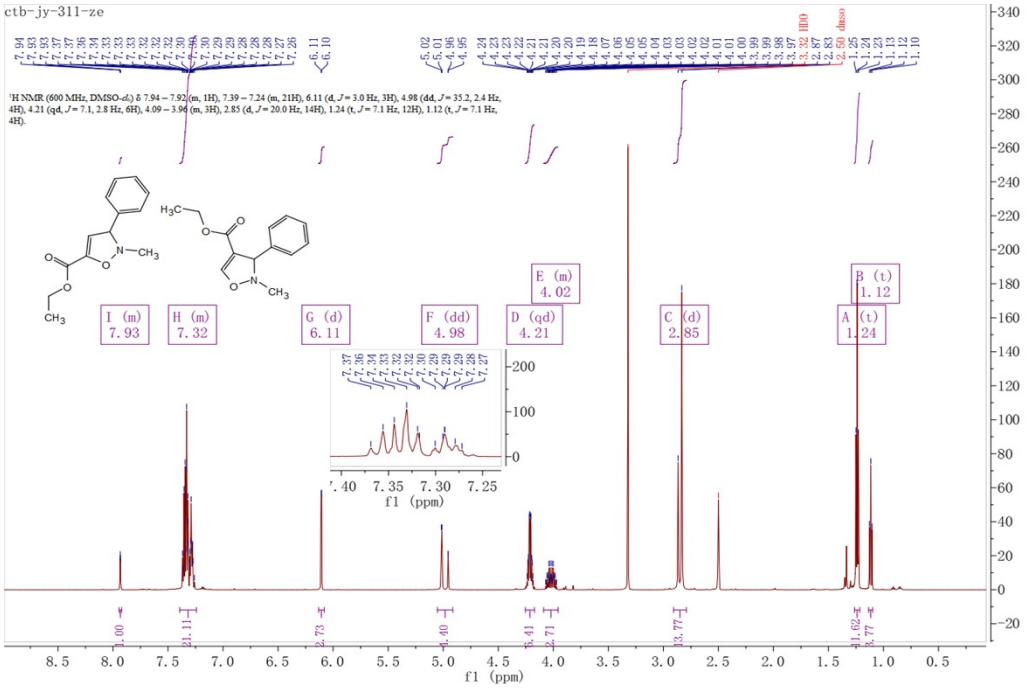

Figure S40 ^{1}H NMR of **1c** and **1c'**

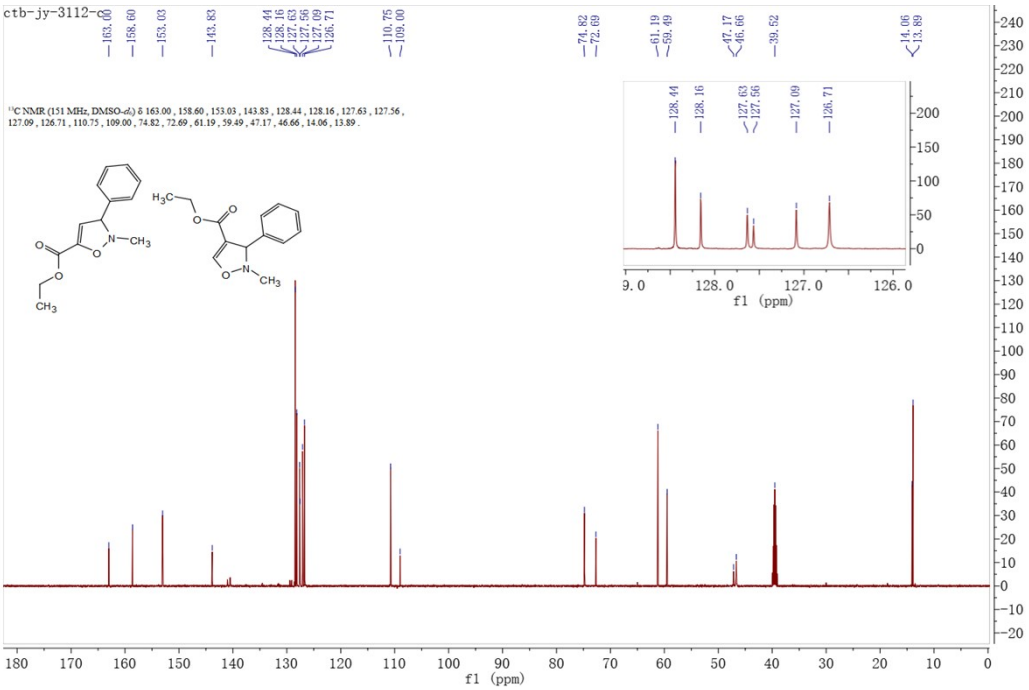

Figure S41 ^{13}C NMR of **1c** and **1c'**

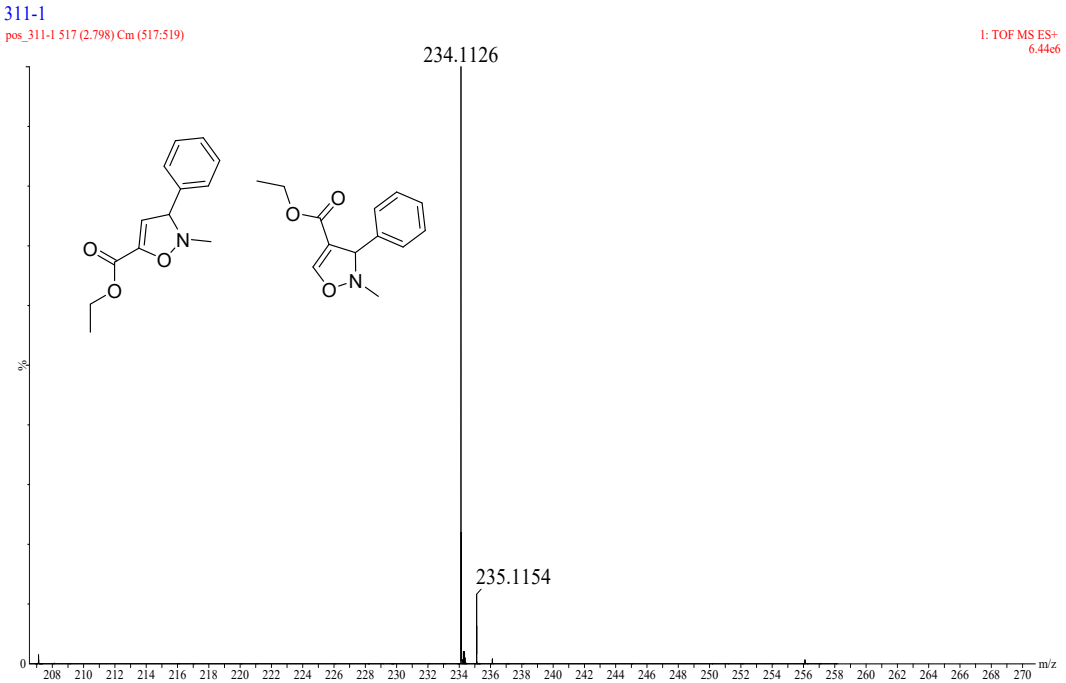

Figure S42 HRMS of **1c** and **1c'**

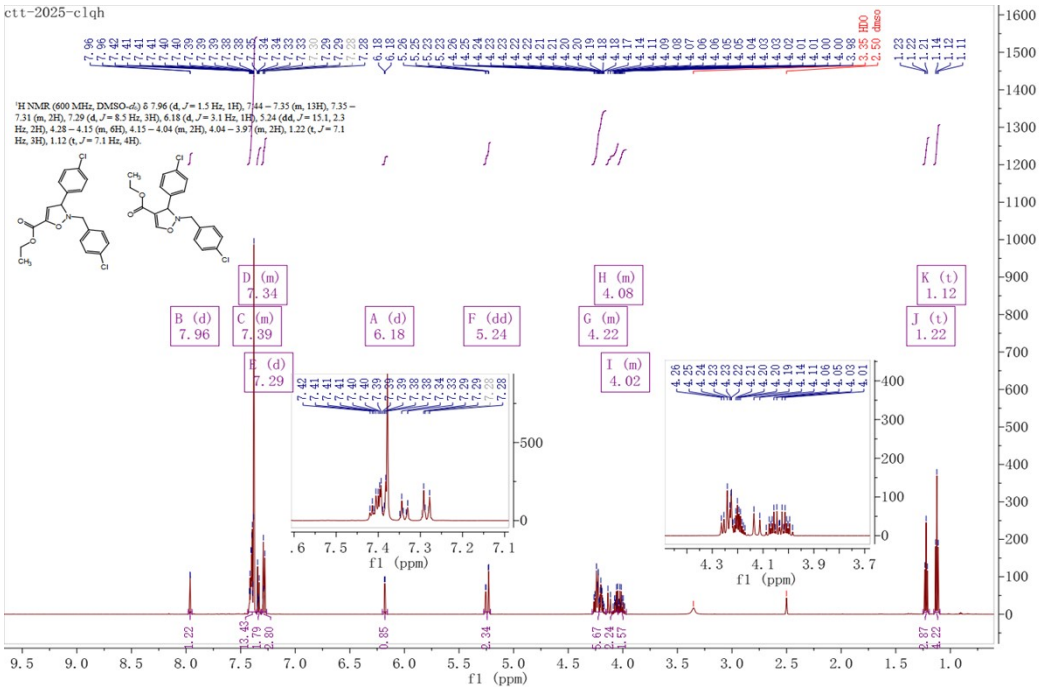

Figure S43 ^{1}H NMR of **2c** and **2c'**

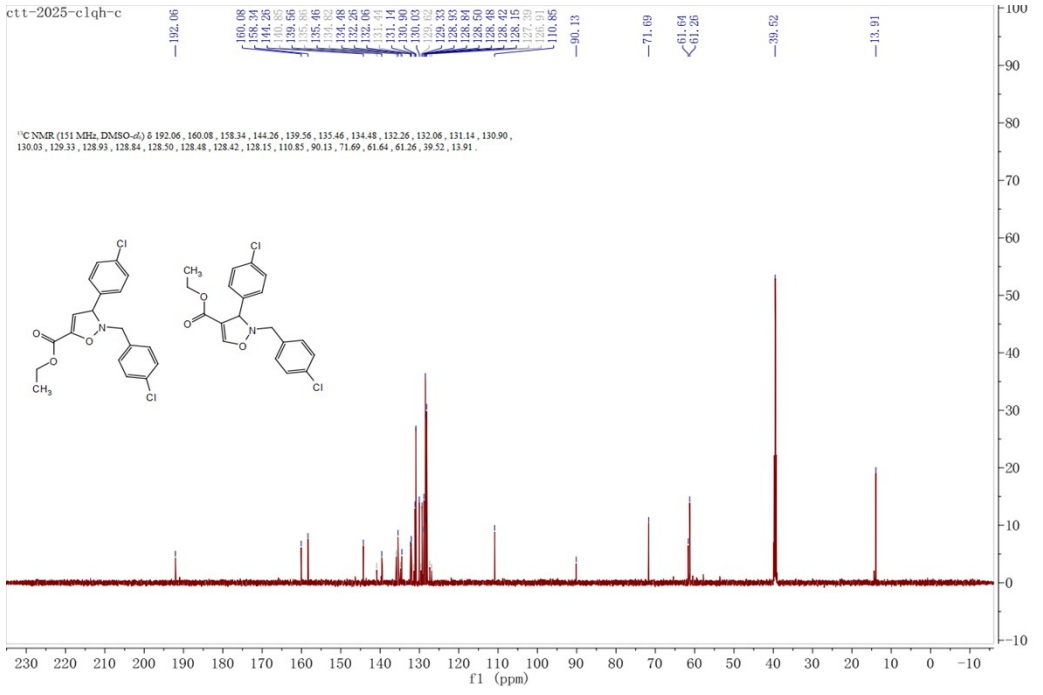

Figure S44 ^{13}C NMR of **2c** and **2c'**

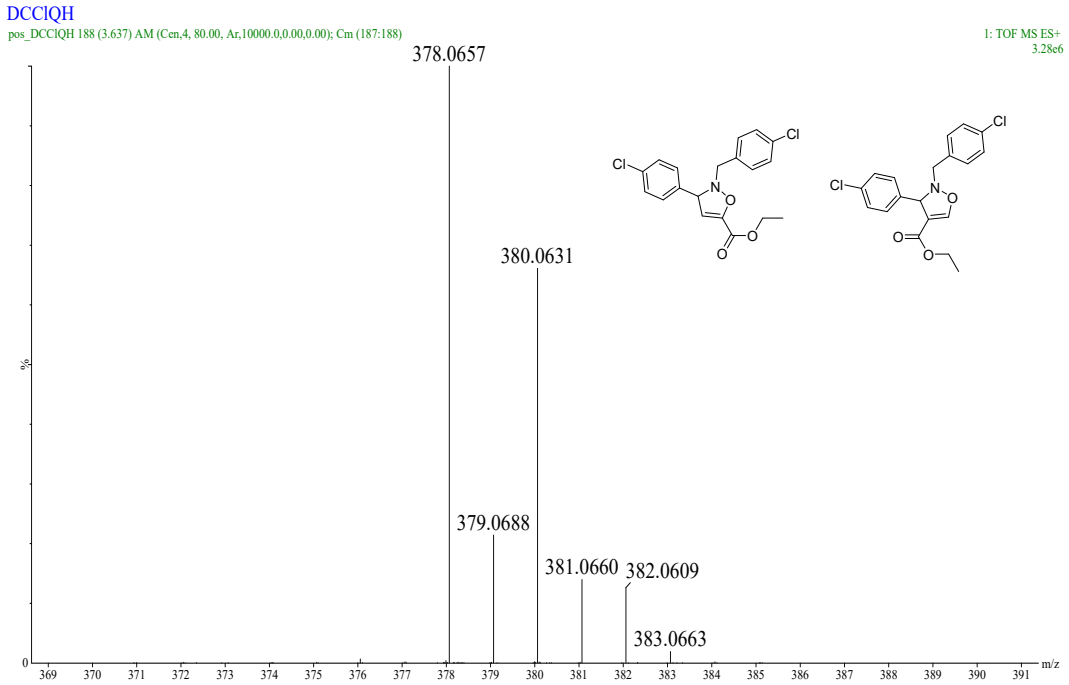

Figure S45 HRMS of **2c** and **2c'**

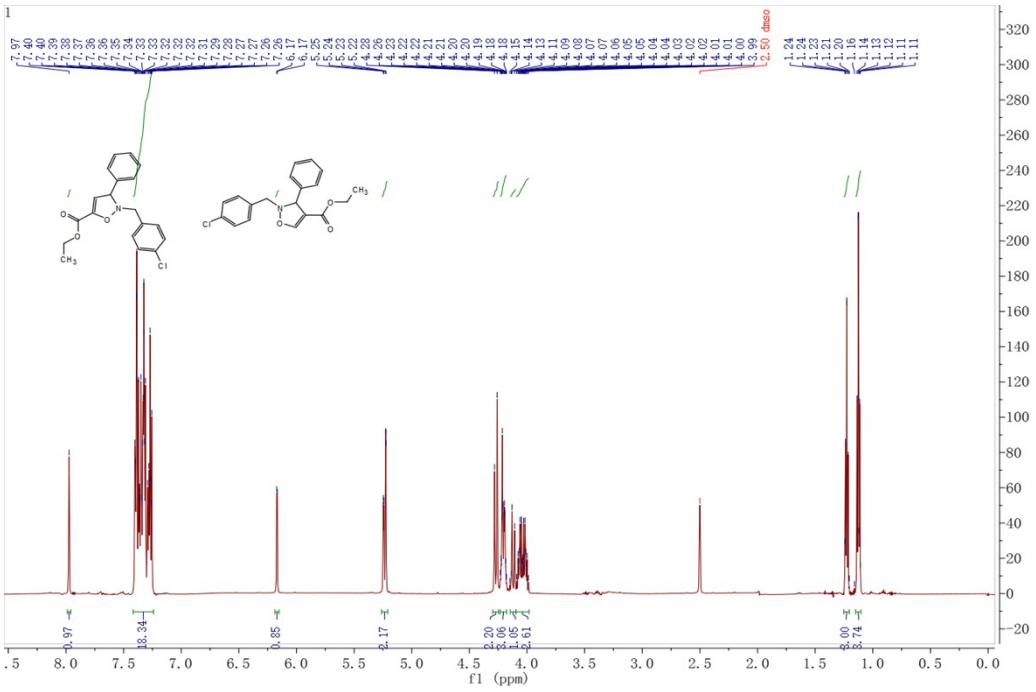

Figure S46 ^{1}H NMR of **3c** and **3c'**

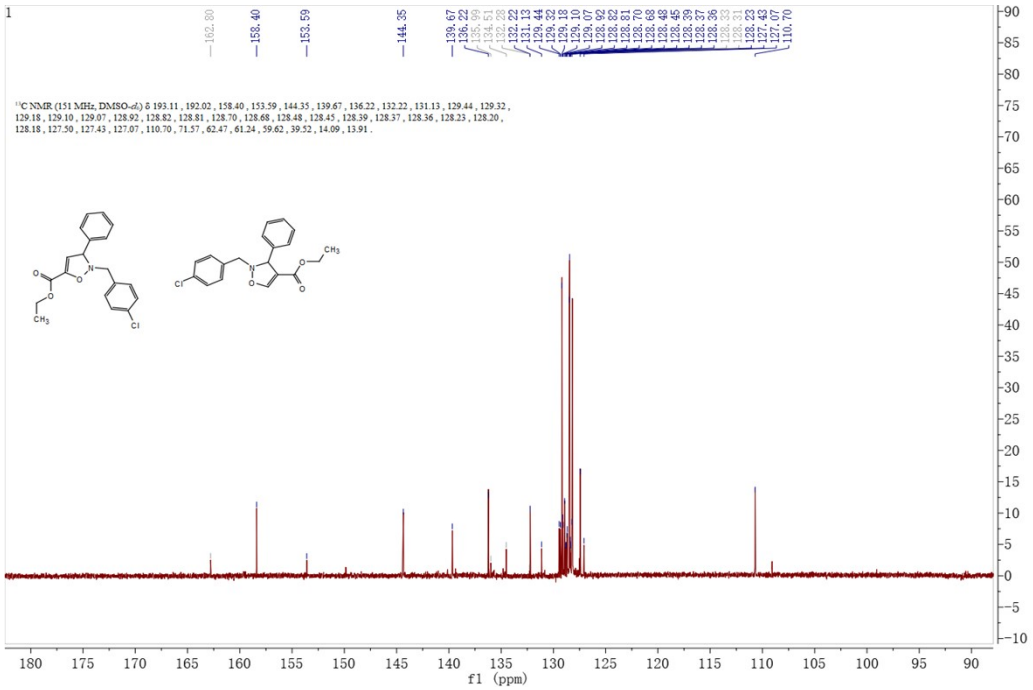

Figure S47 ^{13}C NMR of **3c** and **3c'**

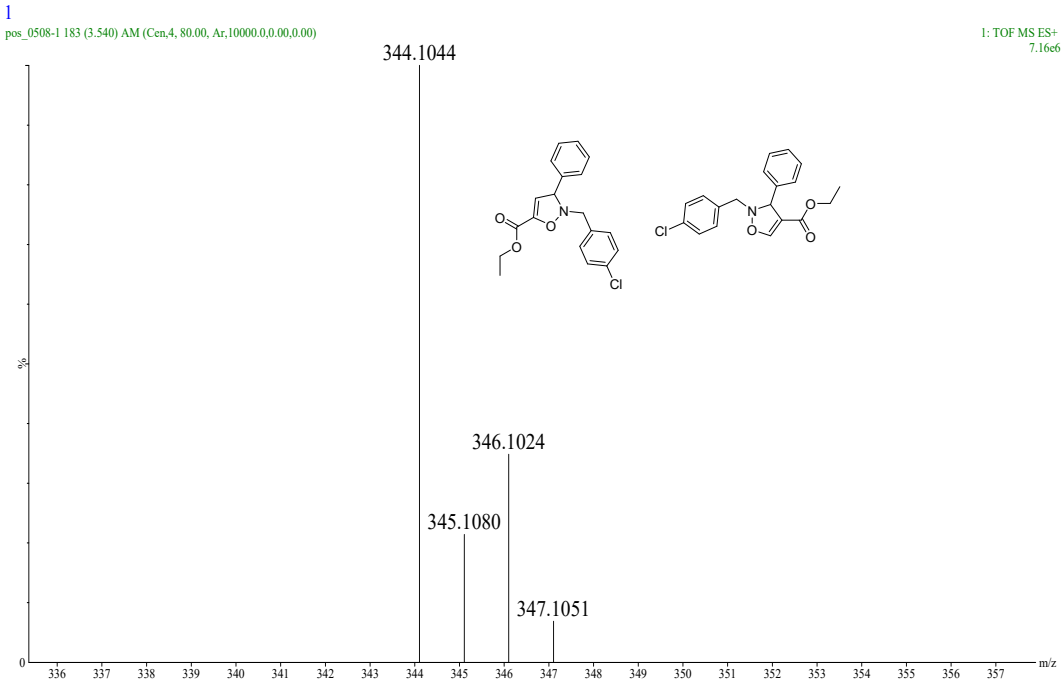

Figure S48 HRMS of **3c** and **3c'**

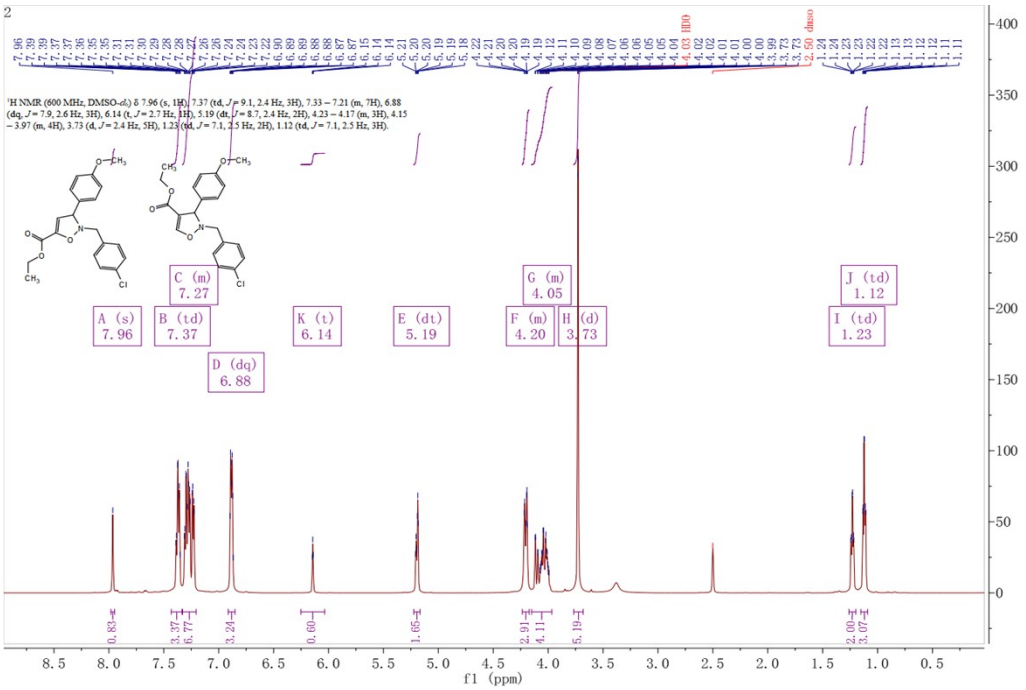

Figure S49 ^{1}H NMR of **4c** and **4c'**

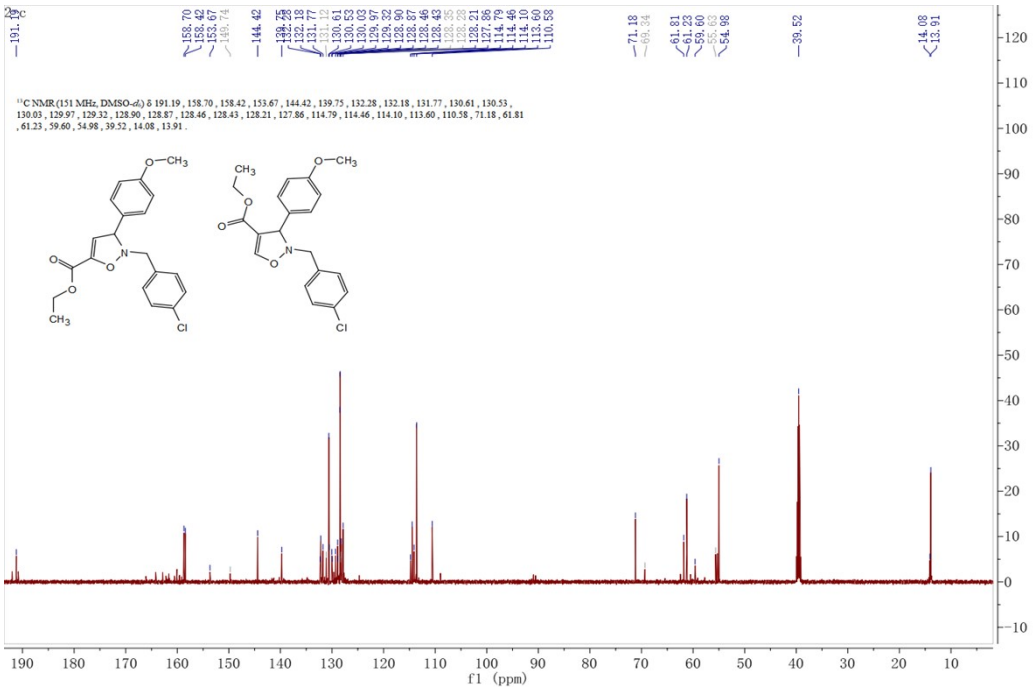

Figure S50 ^{13}C NMR of **4c** and **4c'**

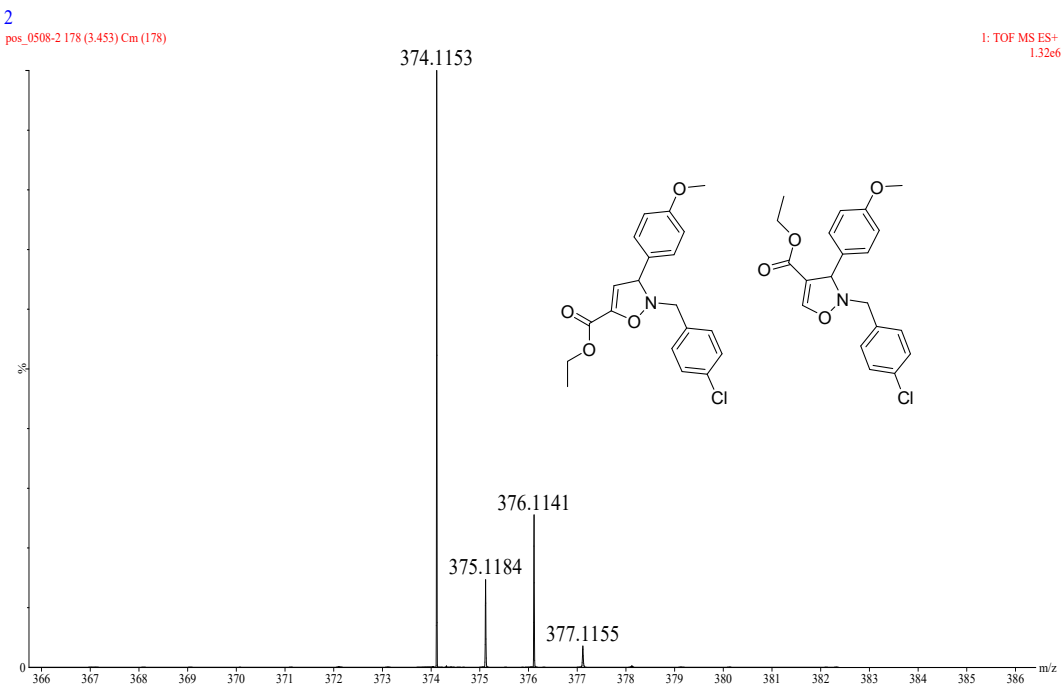

Figure S51 HRMS of **4c** and **4c'**

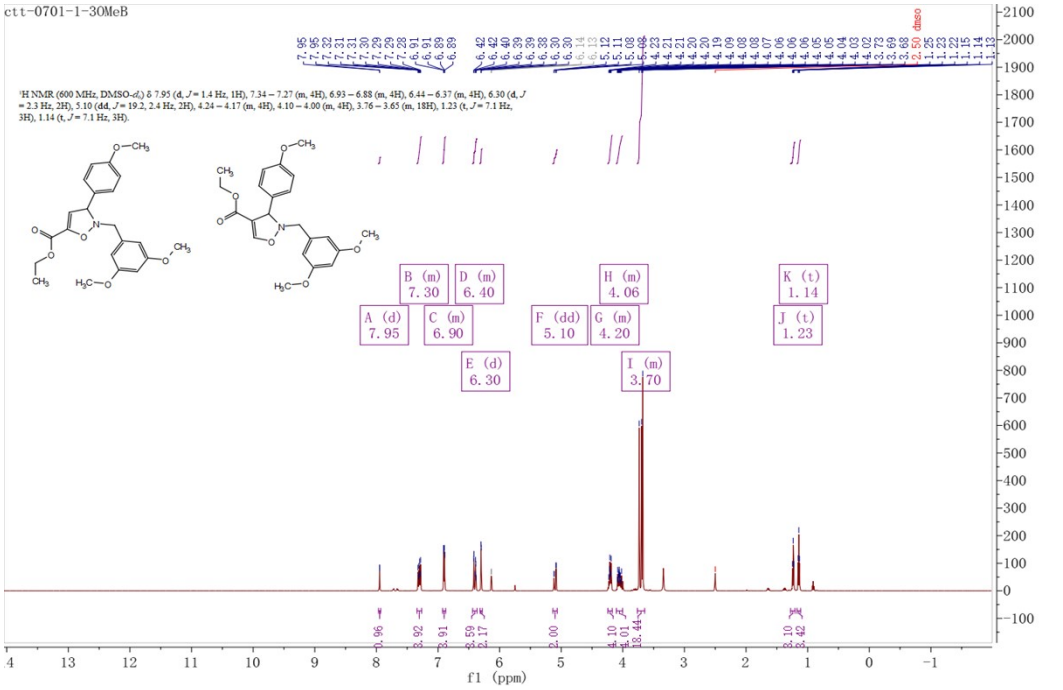

Figure S52 ^{1}H NMR of **5c** and **5c'**

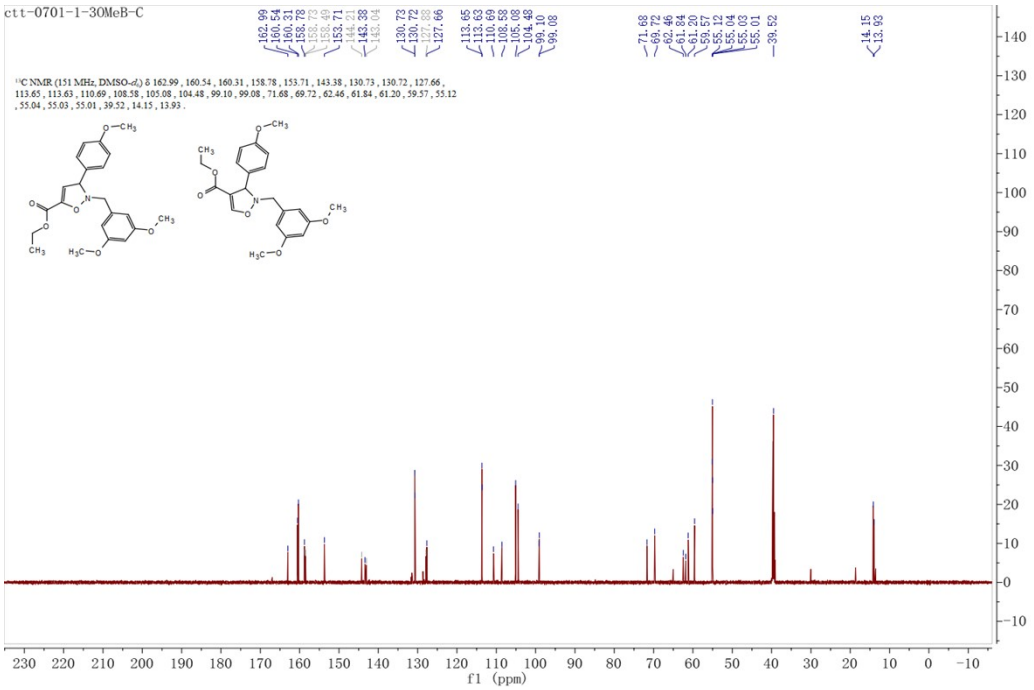

Figure S53 ^{13}C NMR of **5c** and **5c'**

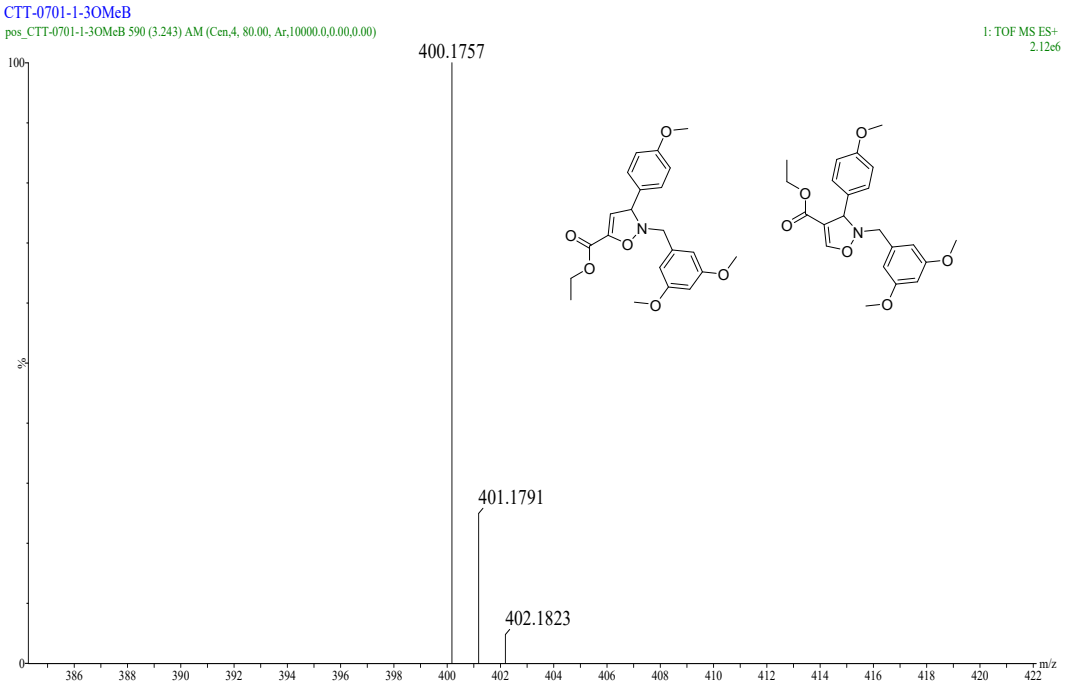

Figure S54 HRMS of **5c** and **5c'**

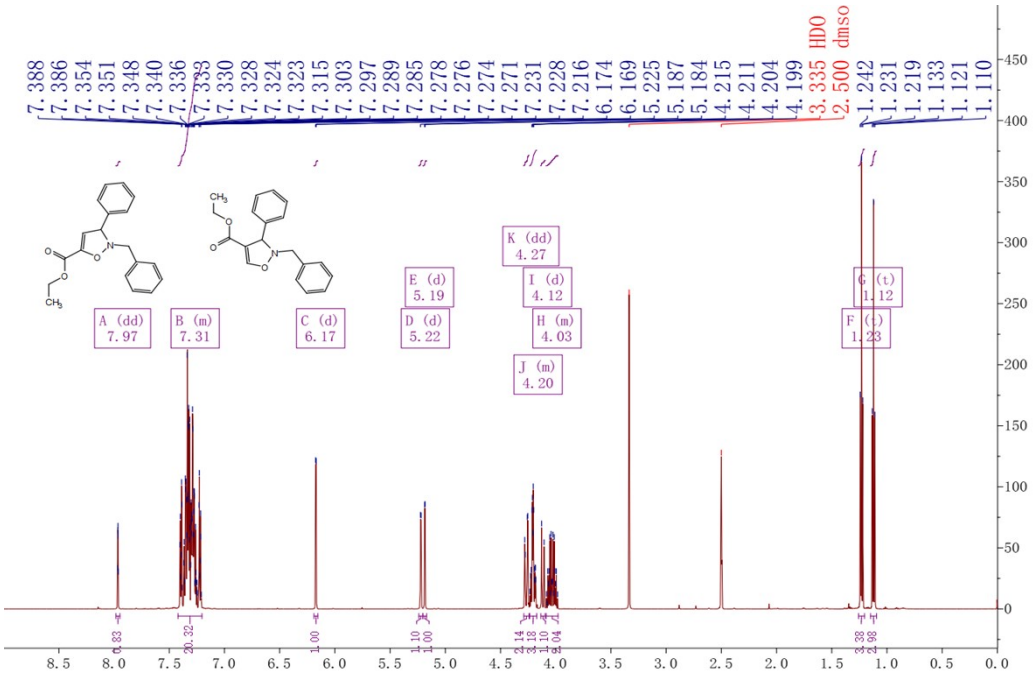

Figure S55 ^{1}H NMR of **6c** and **6c'**

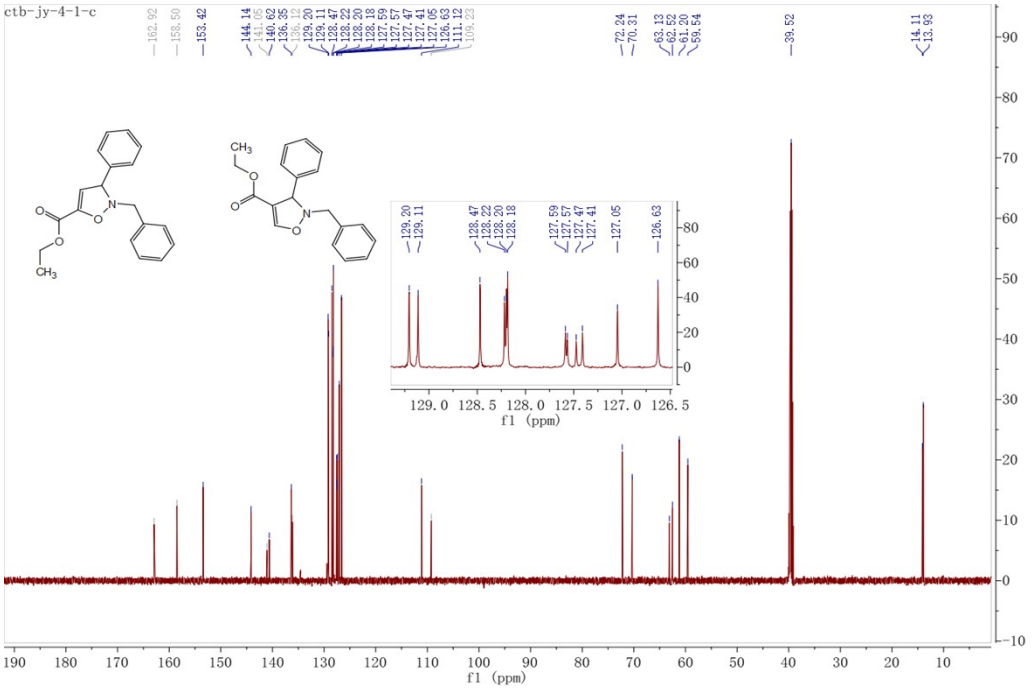

Figure S56 ^{13}C NMR of **6c** and **6c'**

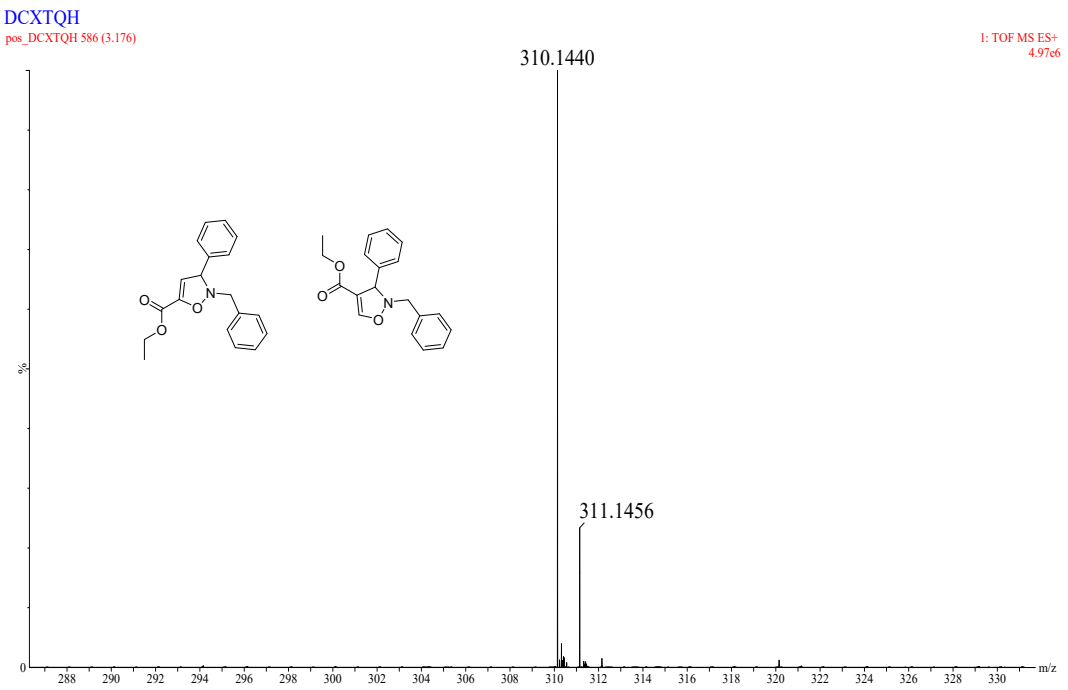

Figure S57 HRMS of **6c** and **6c'**

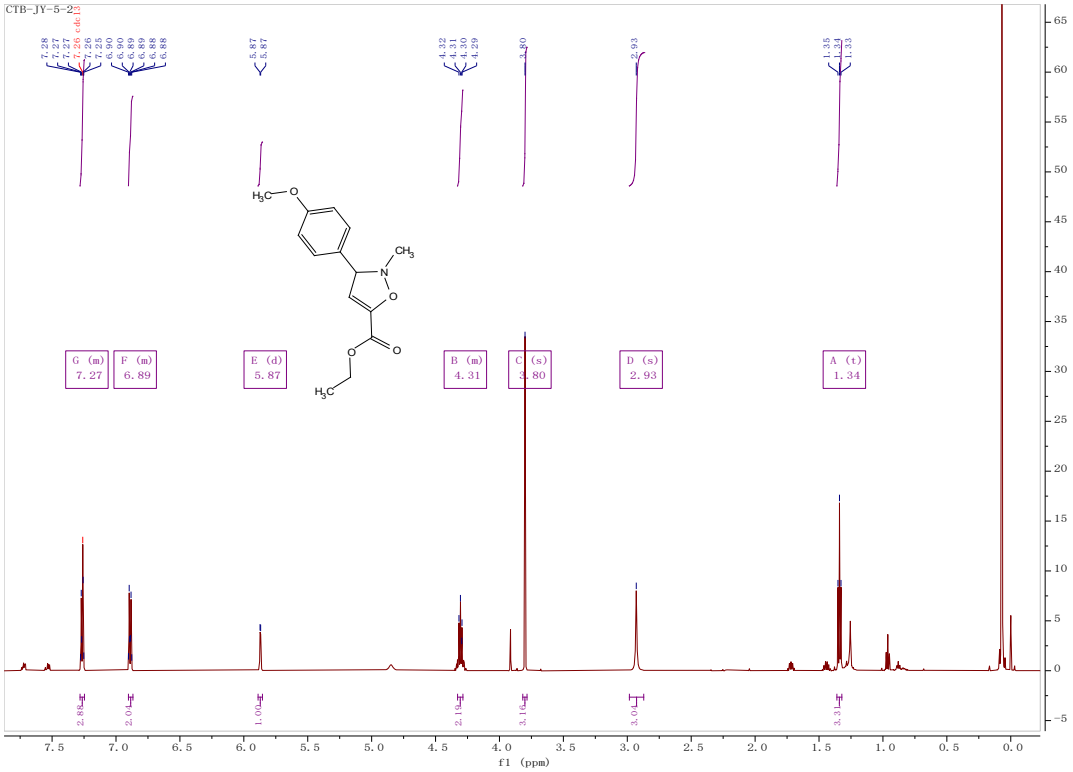

Figure S58 ^{1}H NMR of **7c**

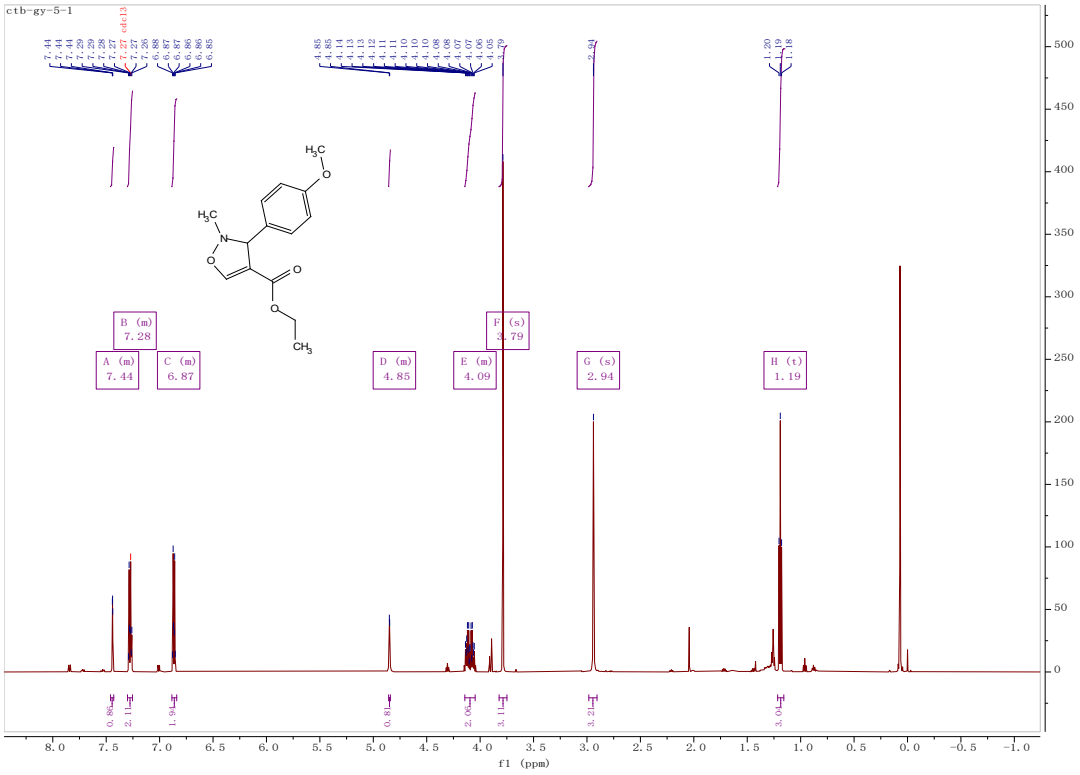

Figure S59 ^{1}H NMR of **7c'**

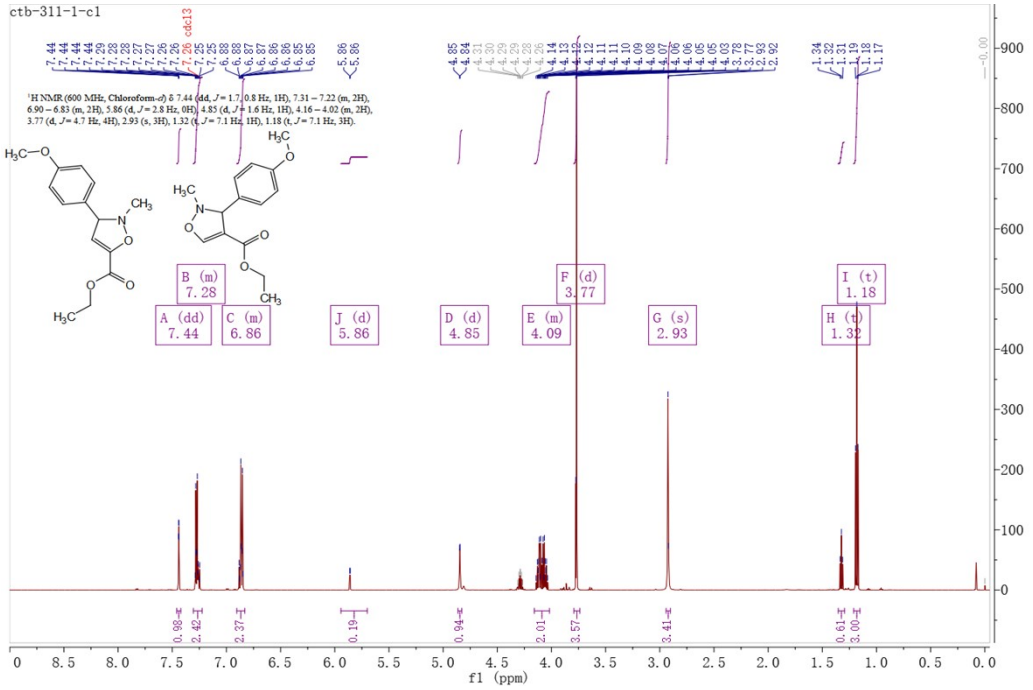

Figure S60 ^{1}H NMR of **7c** and **7c'**

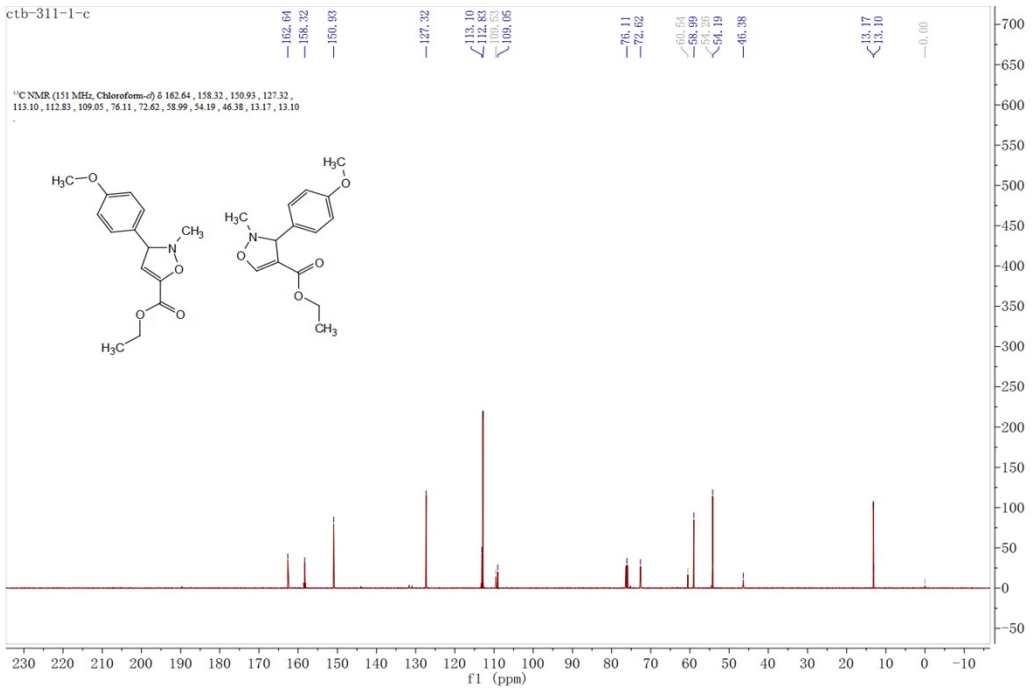

Figure S61 ^{13}C NMR of **7c** and **7c'**

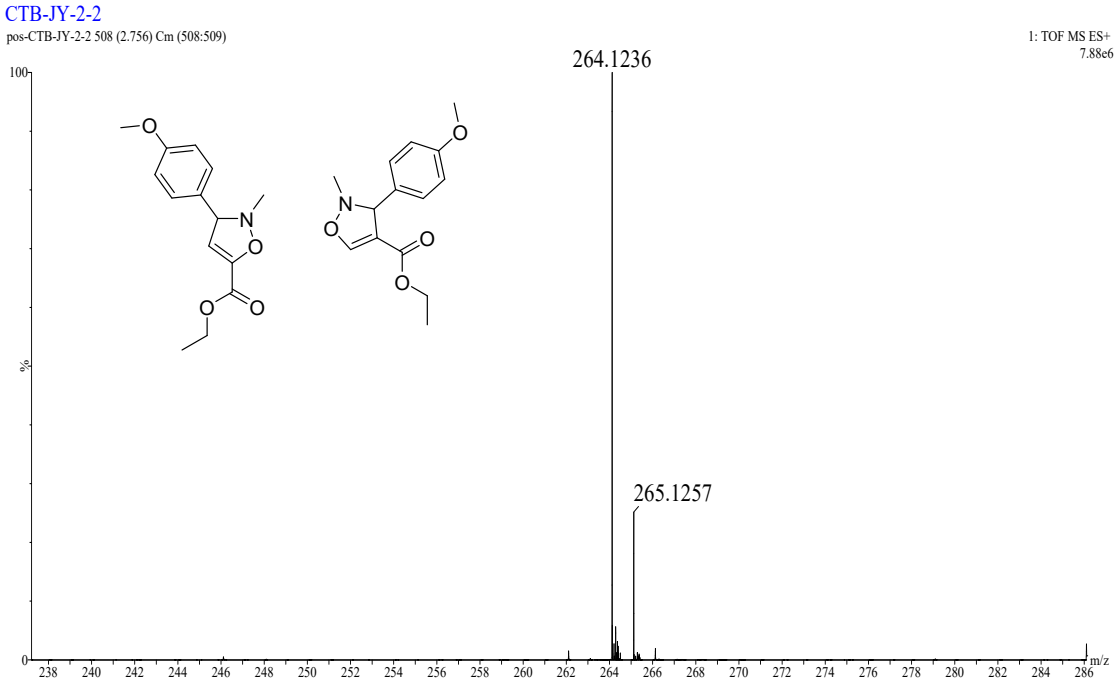

Figure S62 HRMS of **7c** and **7c'**

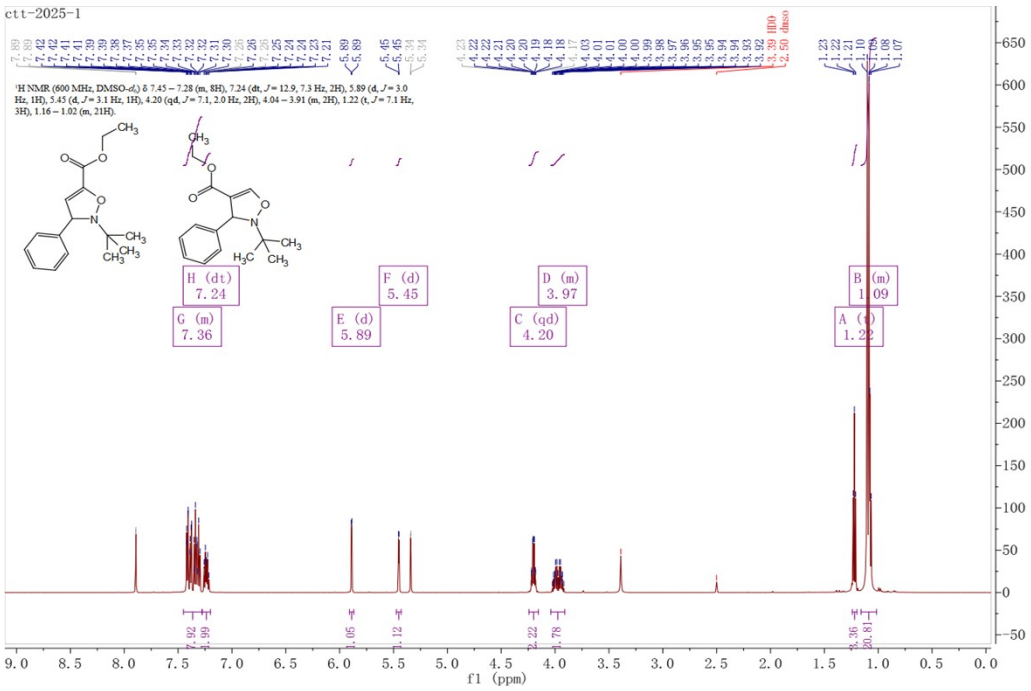

Figure S63 ^{1}H NMR of **8c** and **8c'**

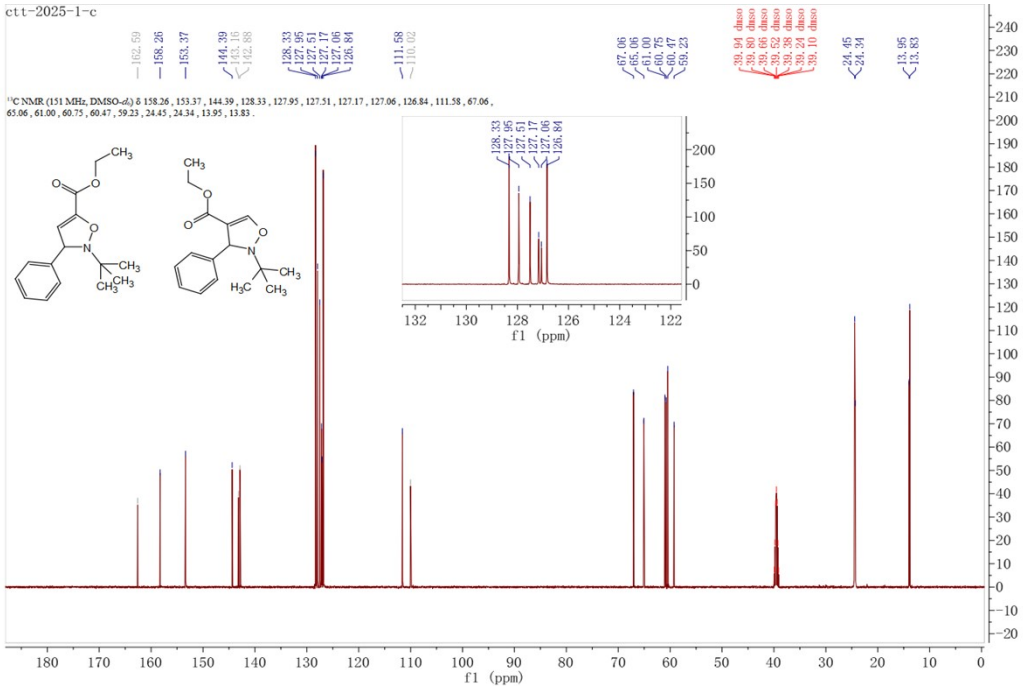

Figure S64 ^{13}C NMR of **8c** and **8c'**

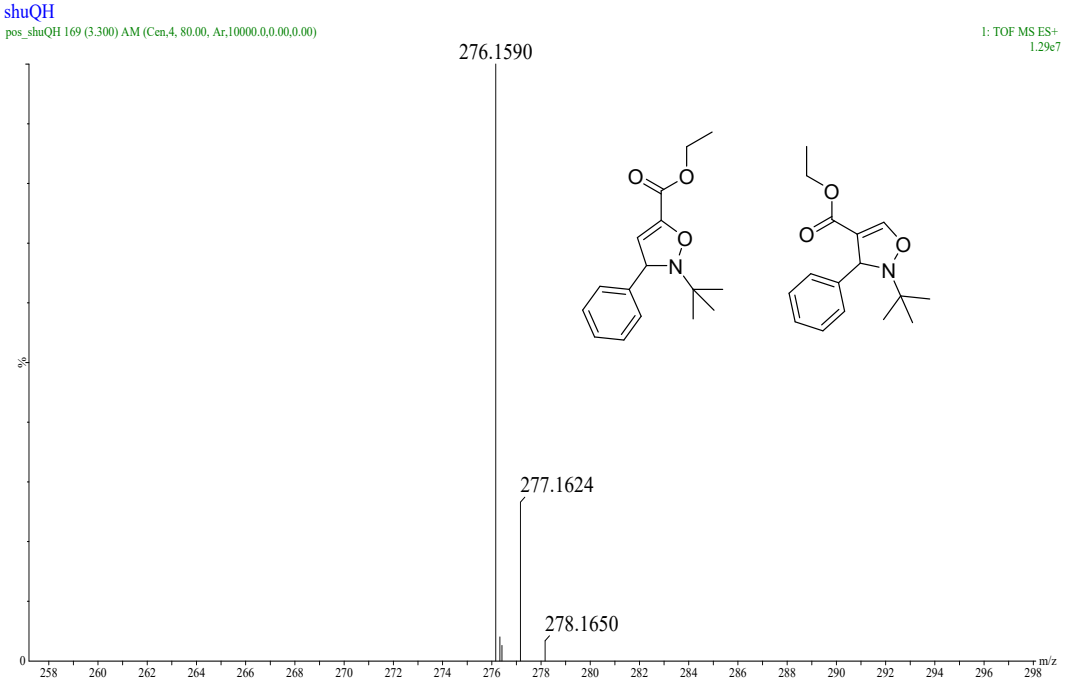

Figure S65 HRMS of **8c** and **8c'**

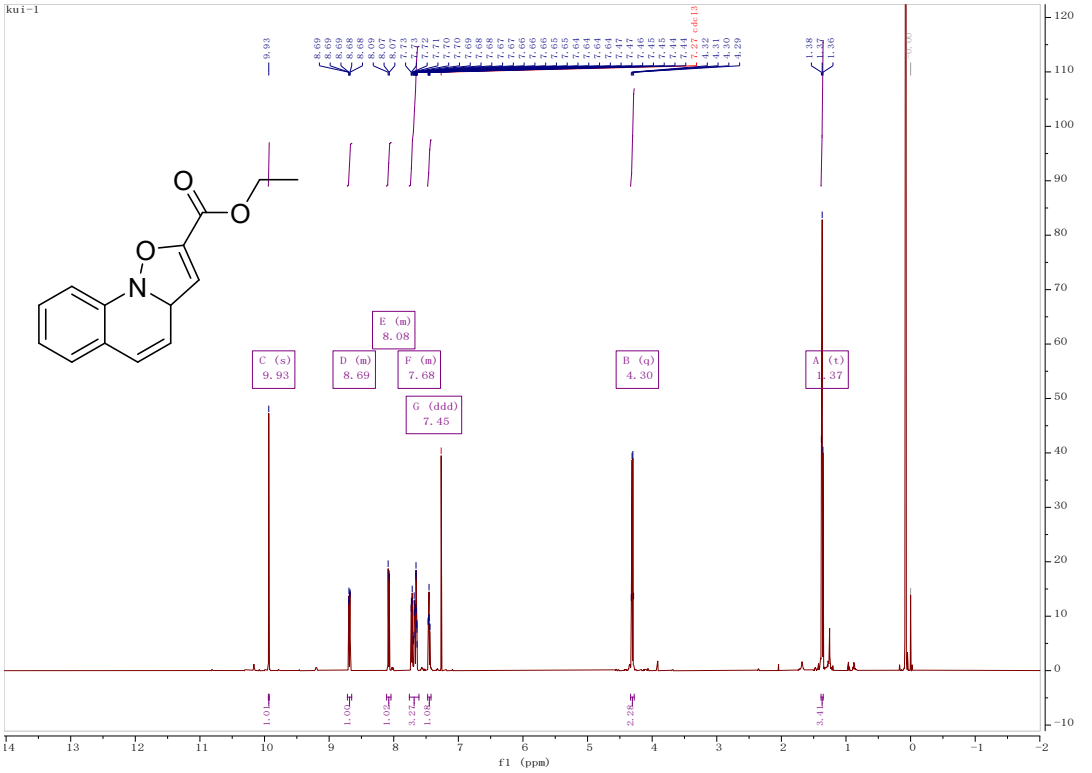

Figure S66 ^{1}H NMR of **9c**

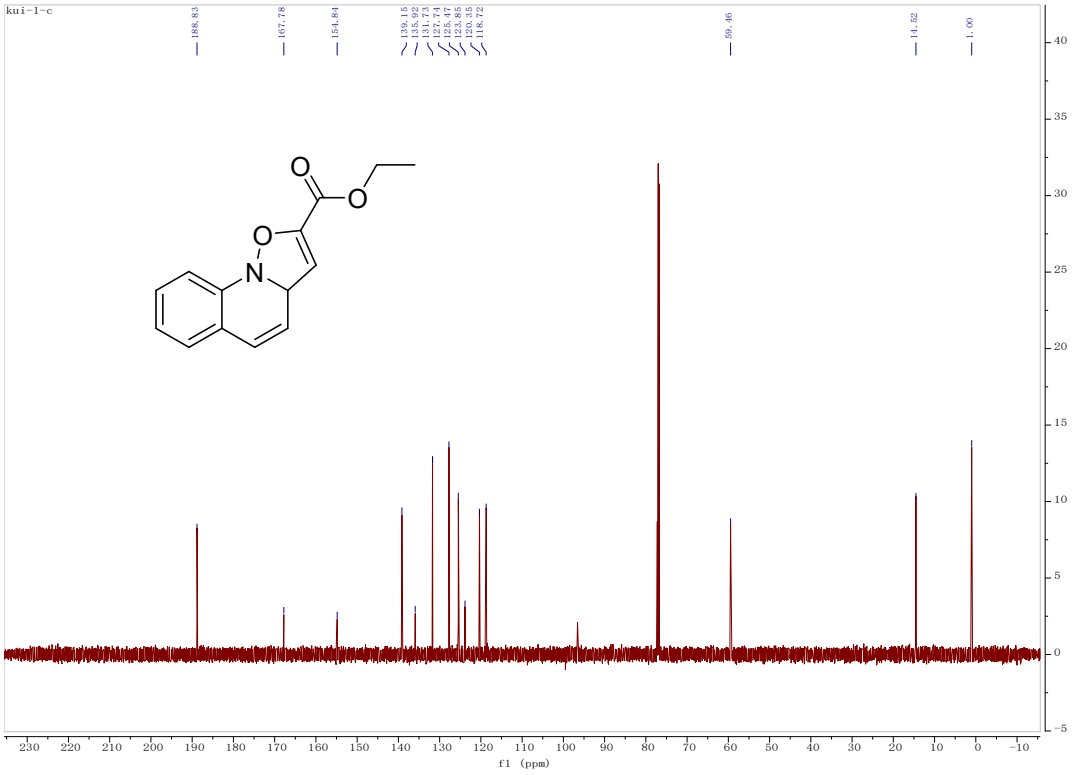

Figure S67 ^{13}C NMR of **9c**

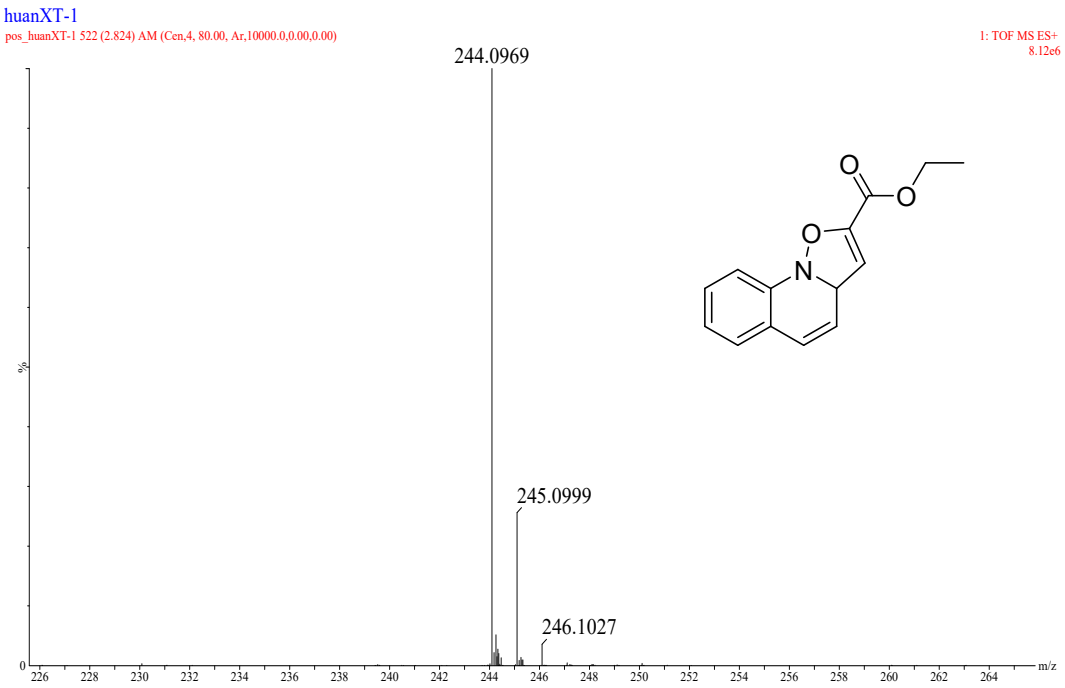

Figure S68 HRMS of **9c**

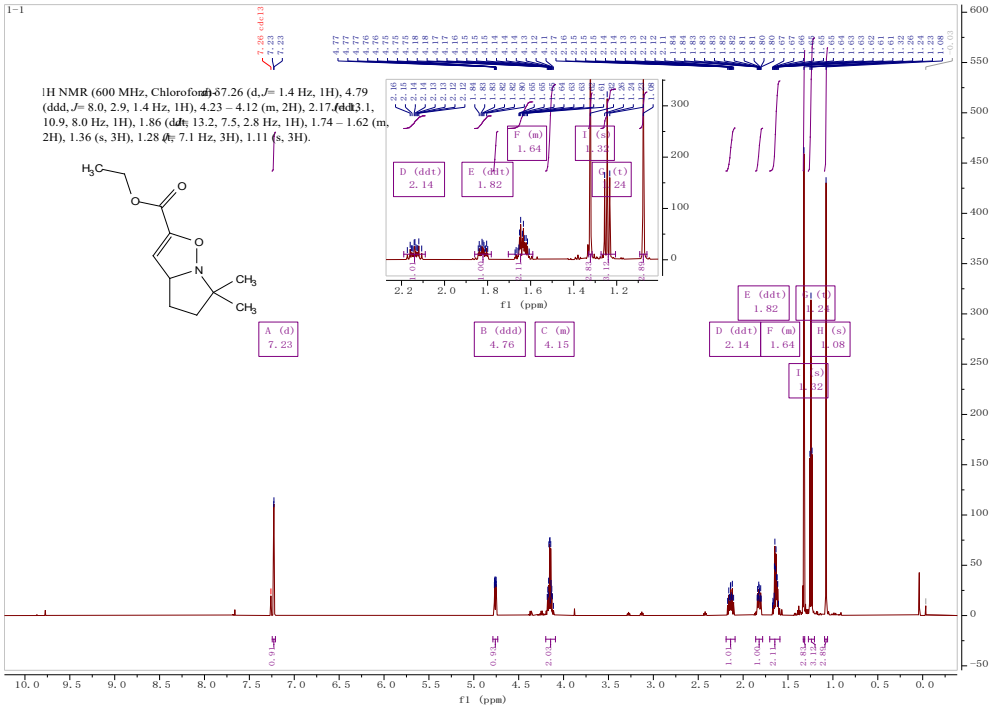

Figure S69 ^{1}H NMR of **10c**

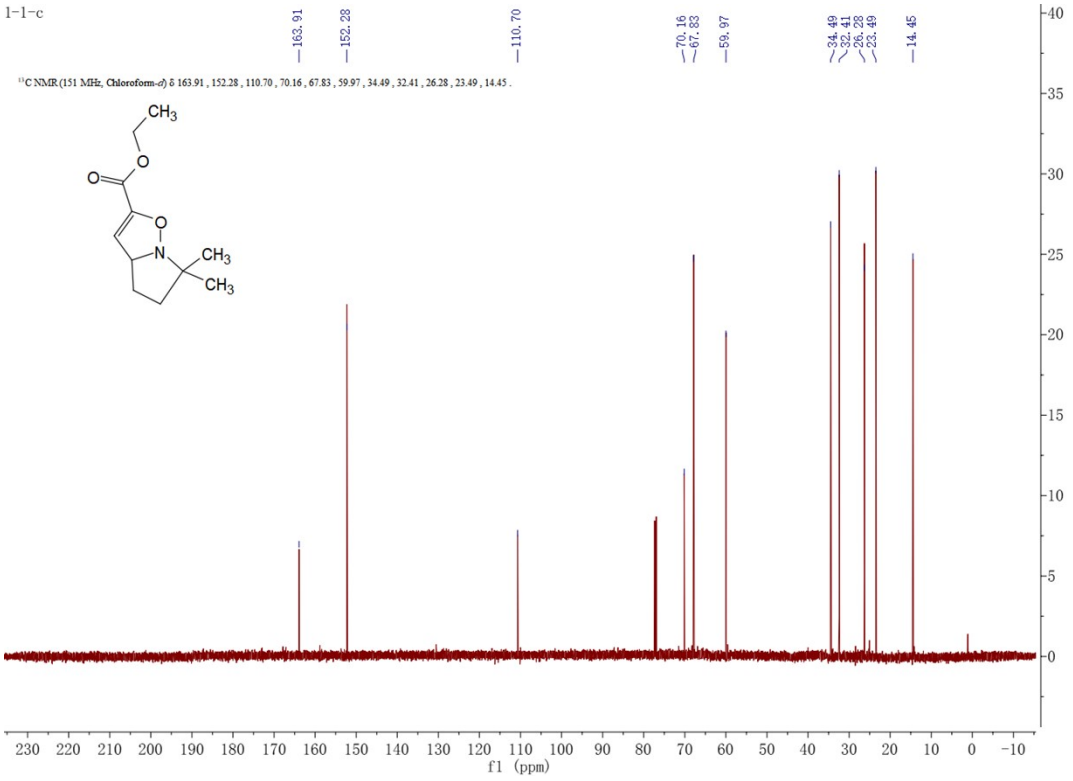

Figure S70 ^{13}C NMR of **10c**

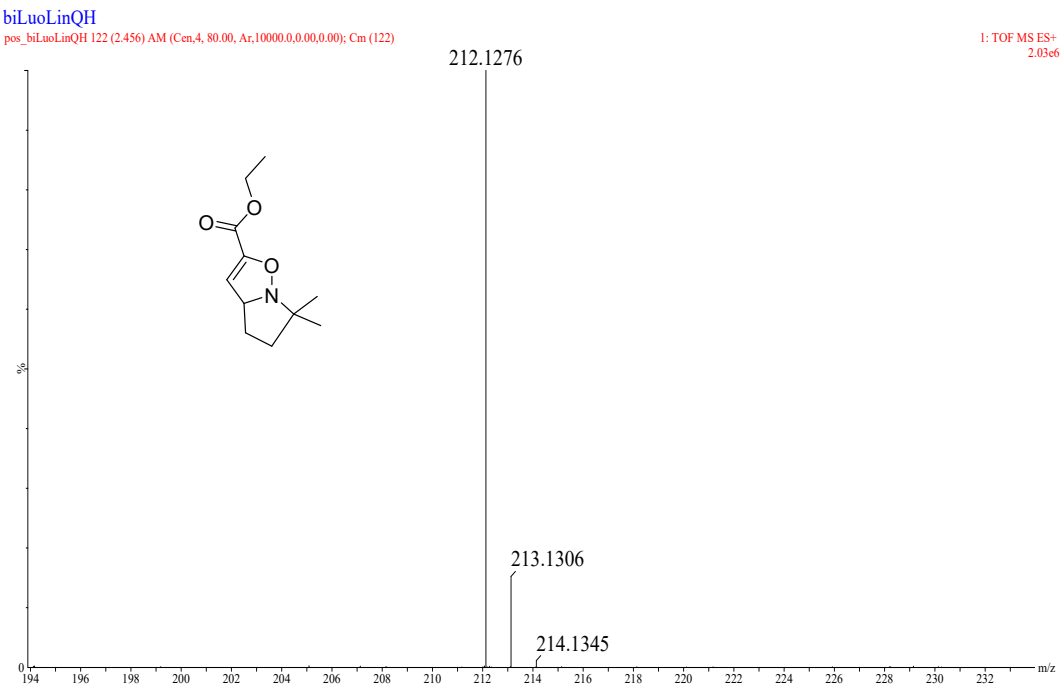

Figure S71 HRMS of **10c**

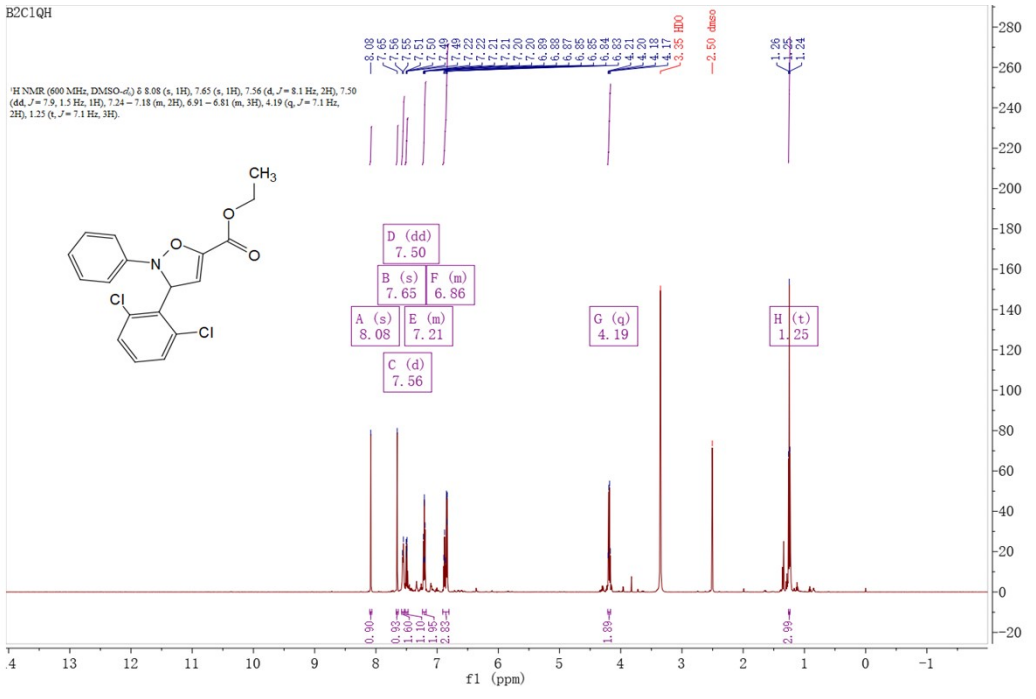

Figure S72 ^{1}H NMR of **11c**

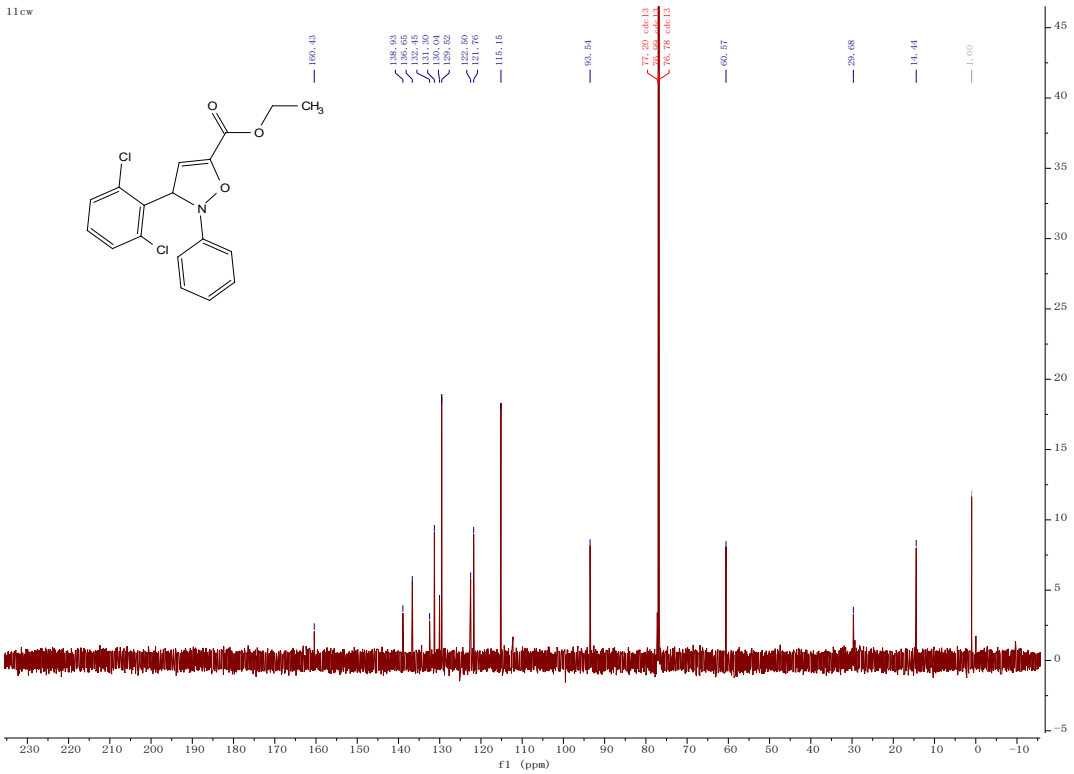

Figure S 73 ^{13}C NMR of **11c**

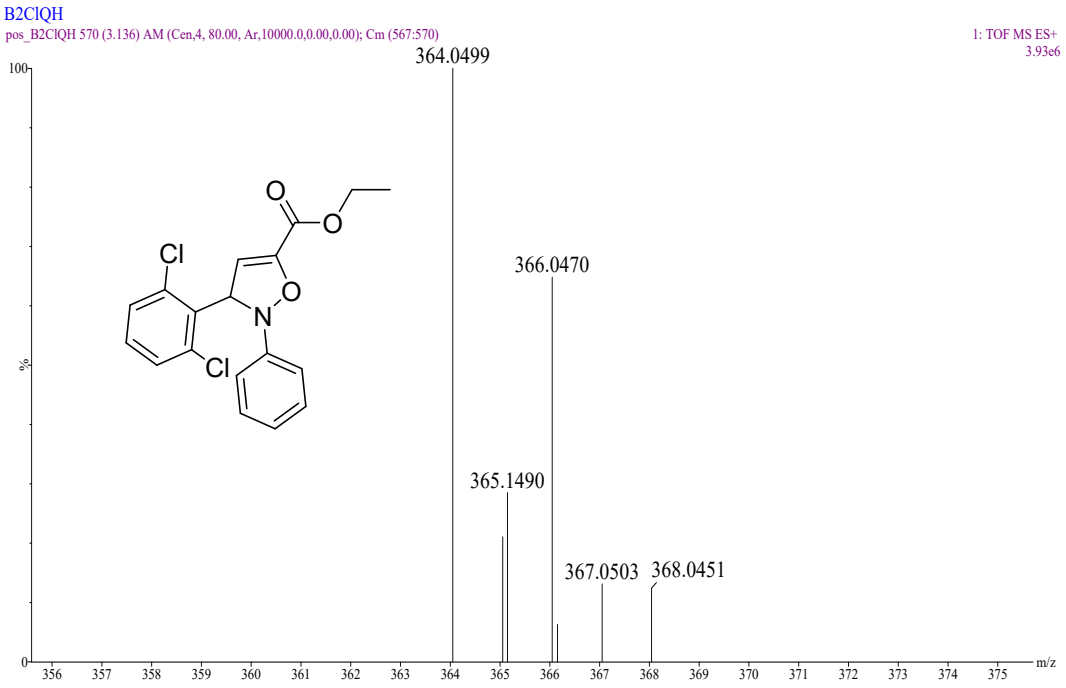

Figure S74 HRMS of **11c**

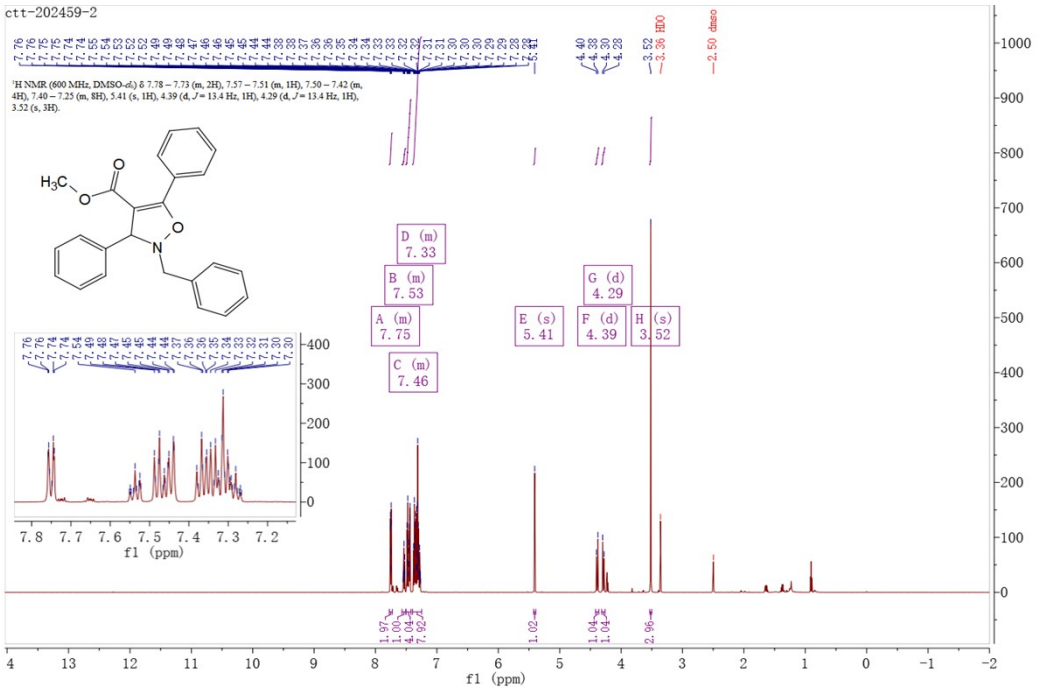

Figure S75 ^{1}H NMR of **12c**

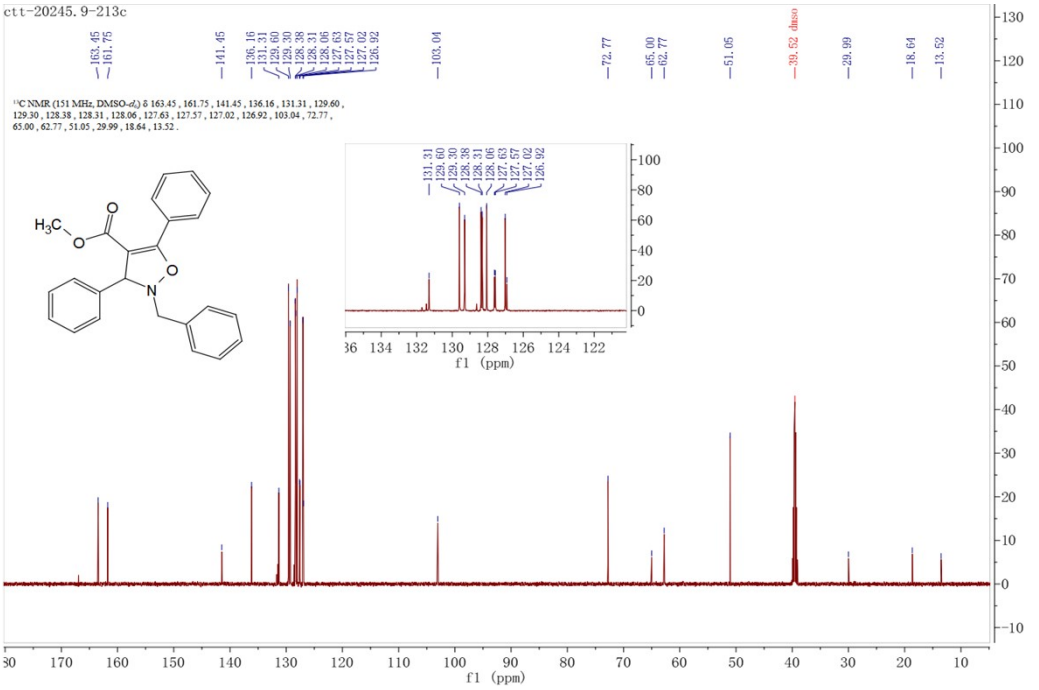

Figure S76 ^{13}C NMR of **12c**

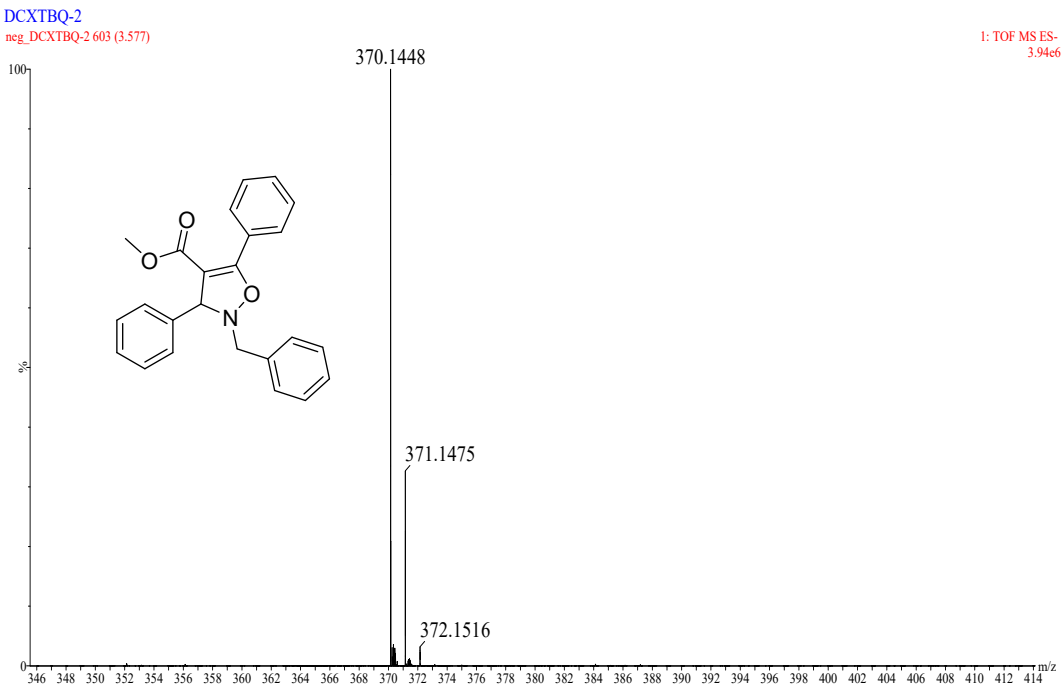

Figure S77 HRMS of **12c**

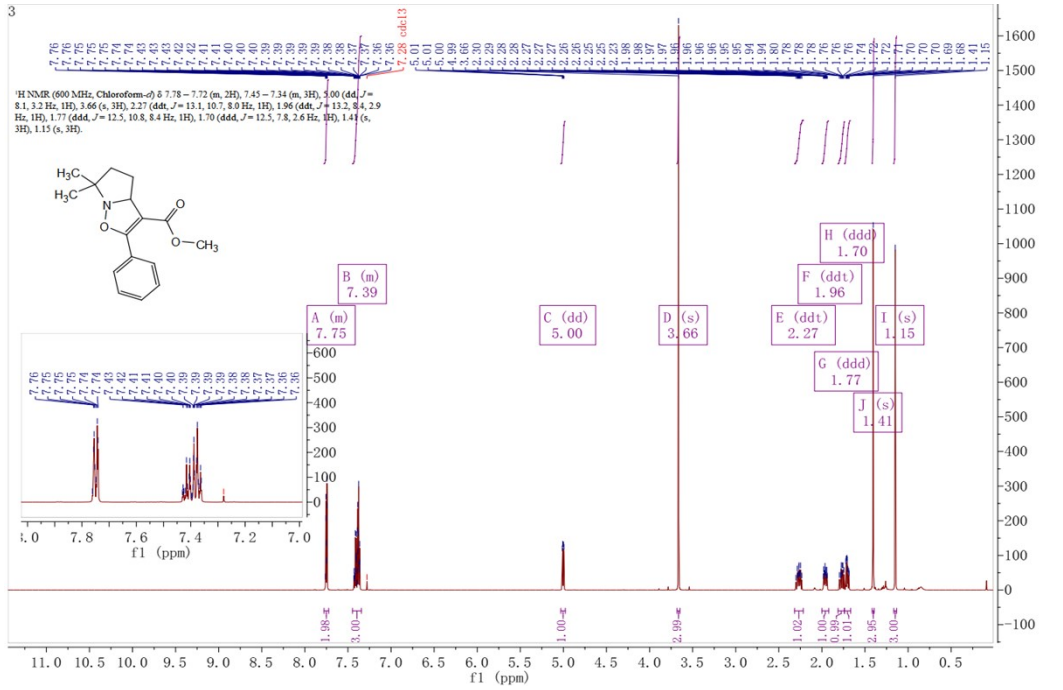

Figure S78 ^{1}H NMR of **13c**

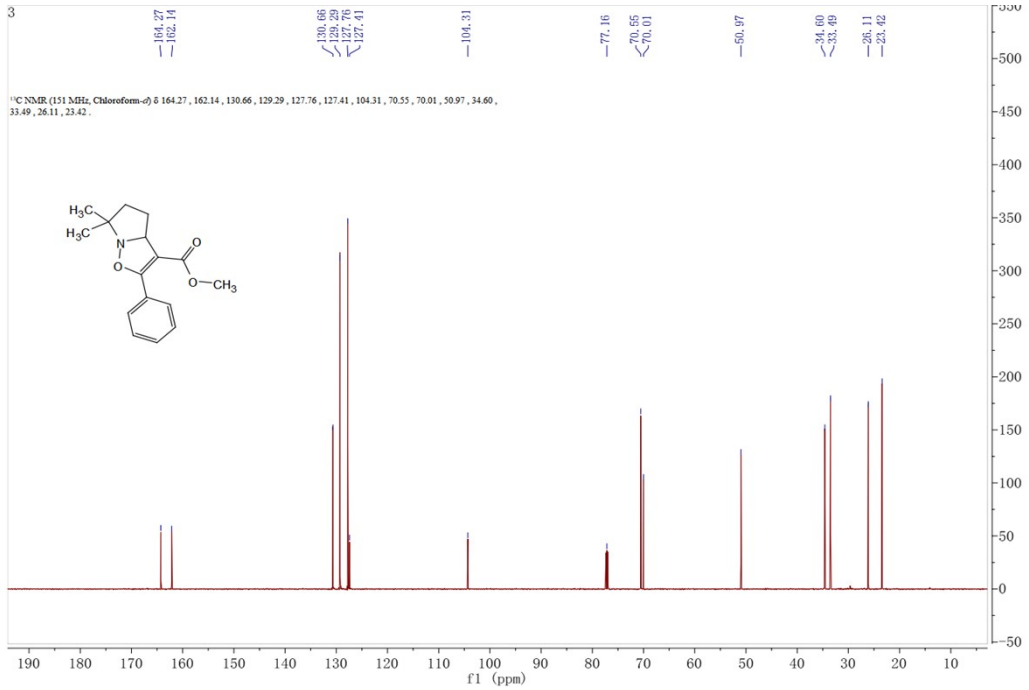

Figure S79 ^{13}C NMR of **13c**

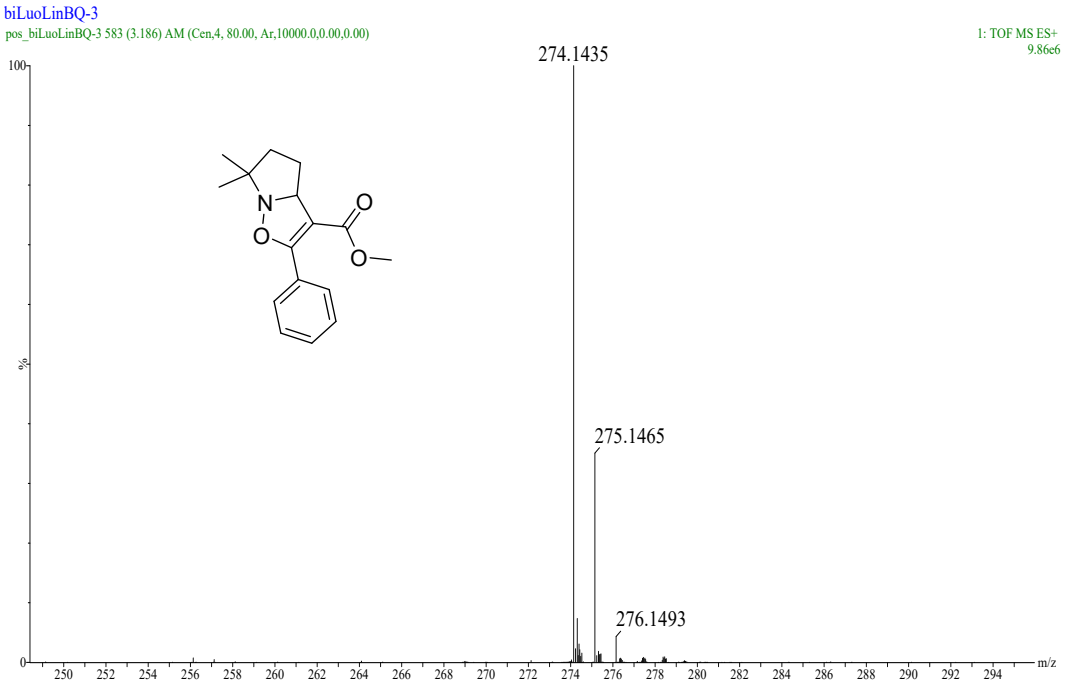

Figure S80 HRMS of **13c**

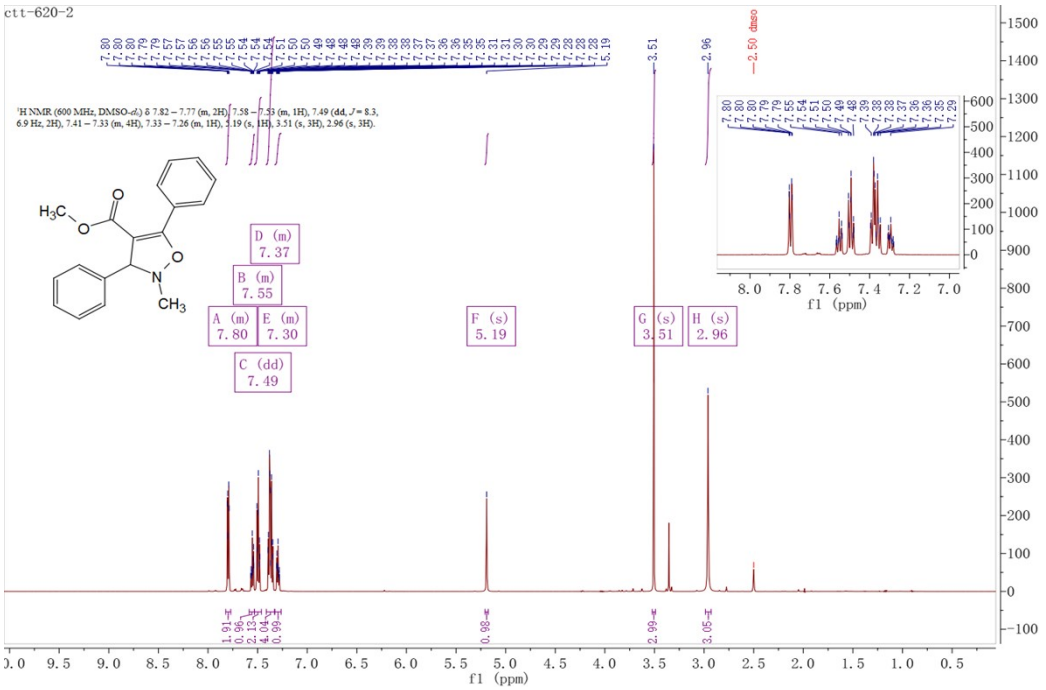

Figure S81 ^{1}H NMR of **14c**

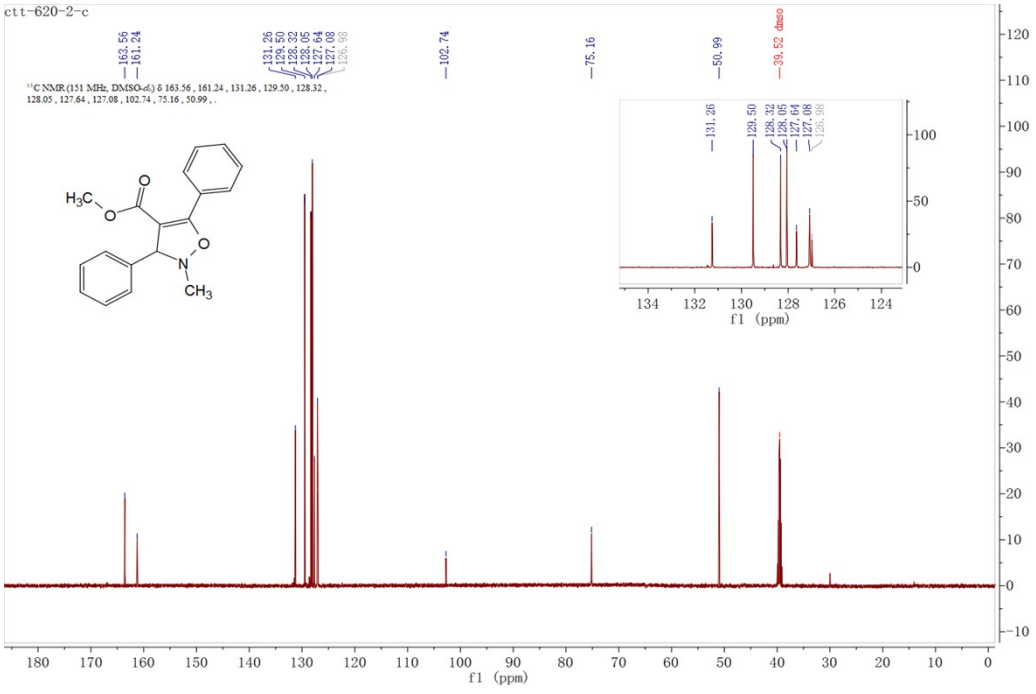

Figure S82 ^{13}C NMR of **14c**

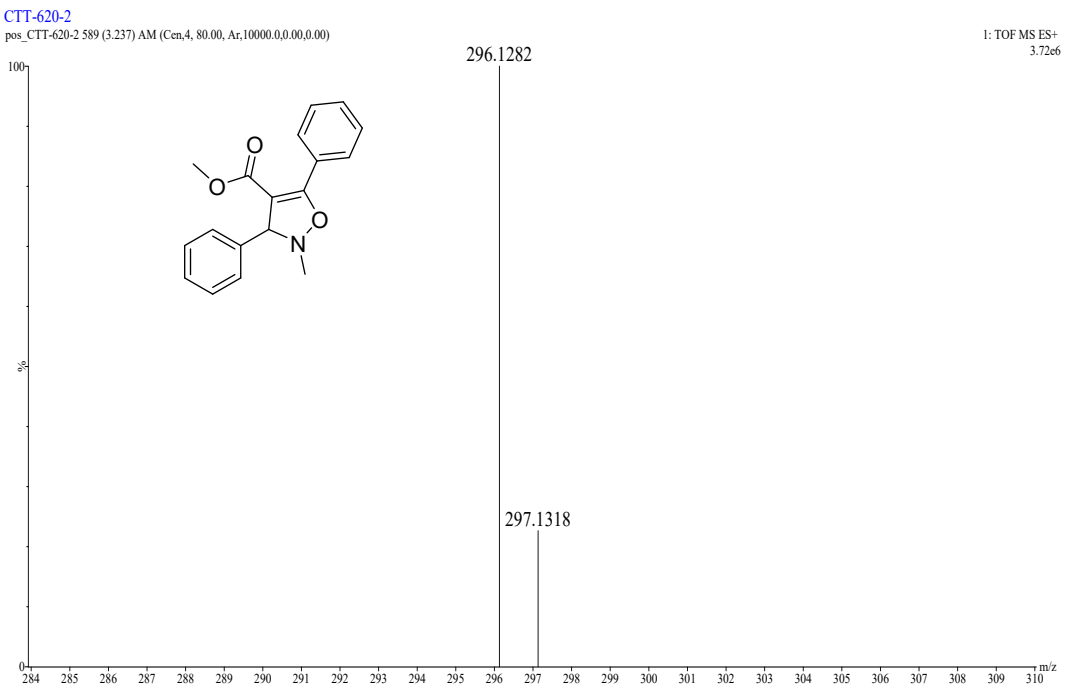

Figure S83 HRMS of **14c**

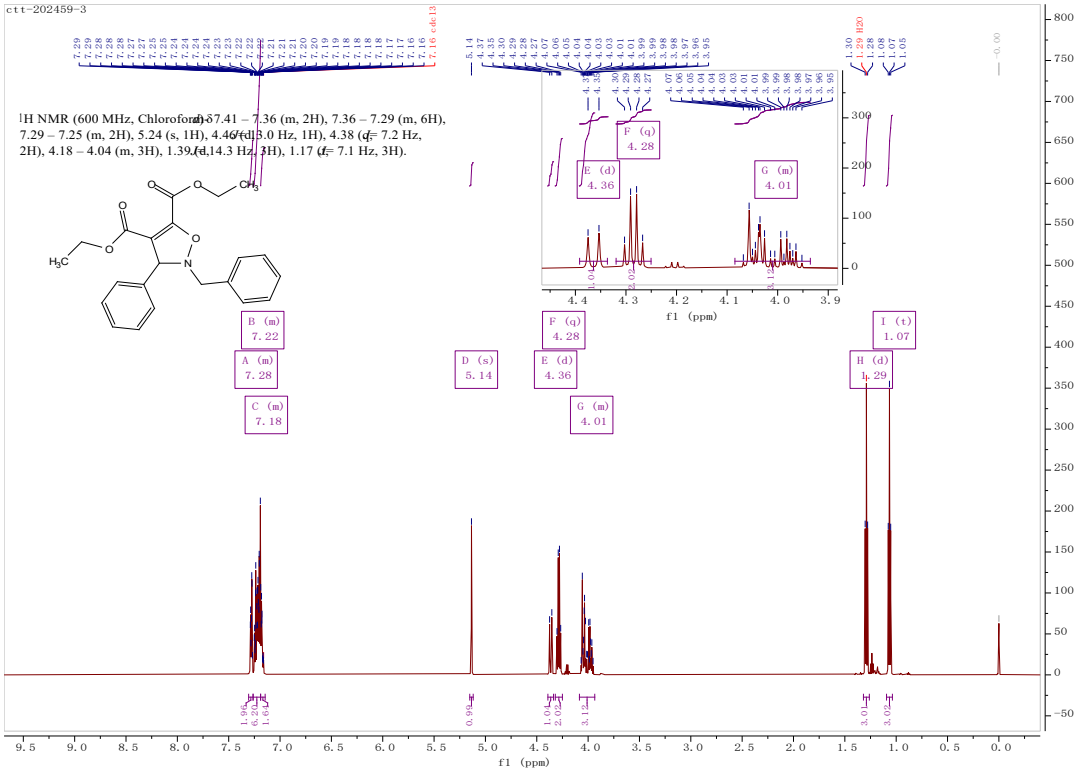

Figure S84 ¹H NMR of **15c**

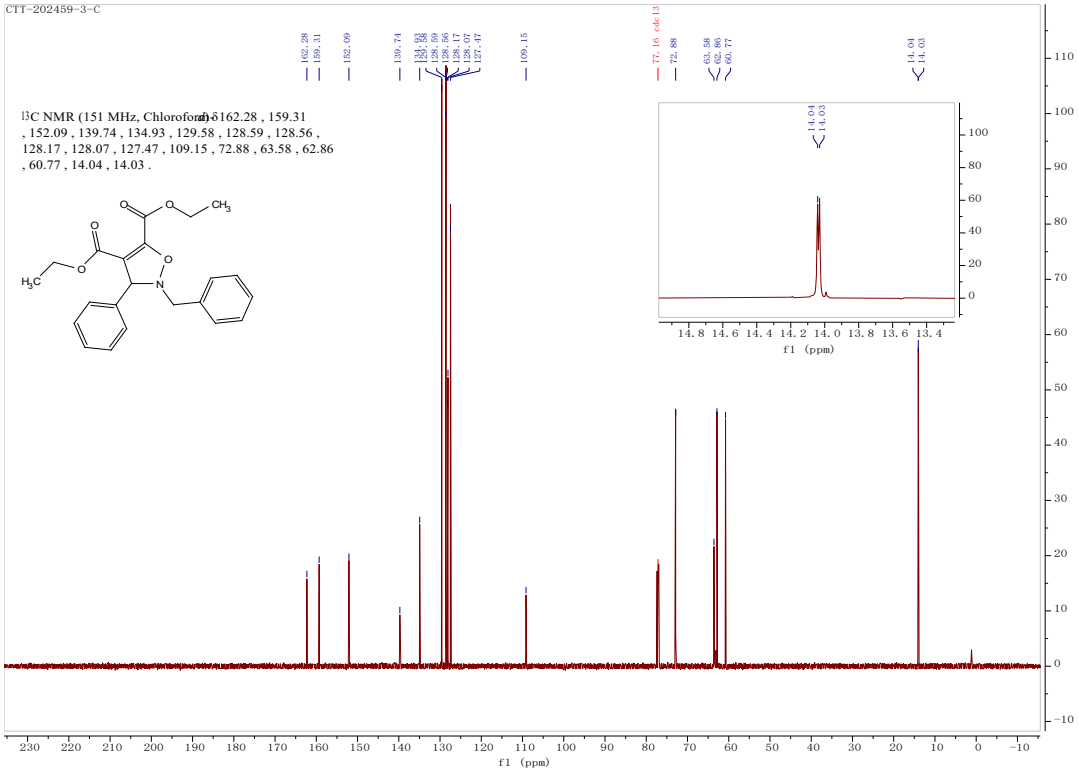

Figure S85 ^{13}C NMR of **15c**

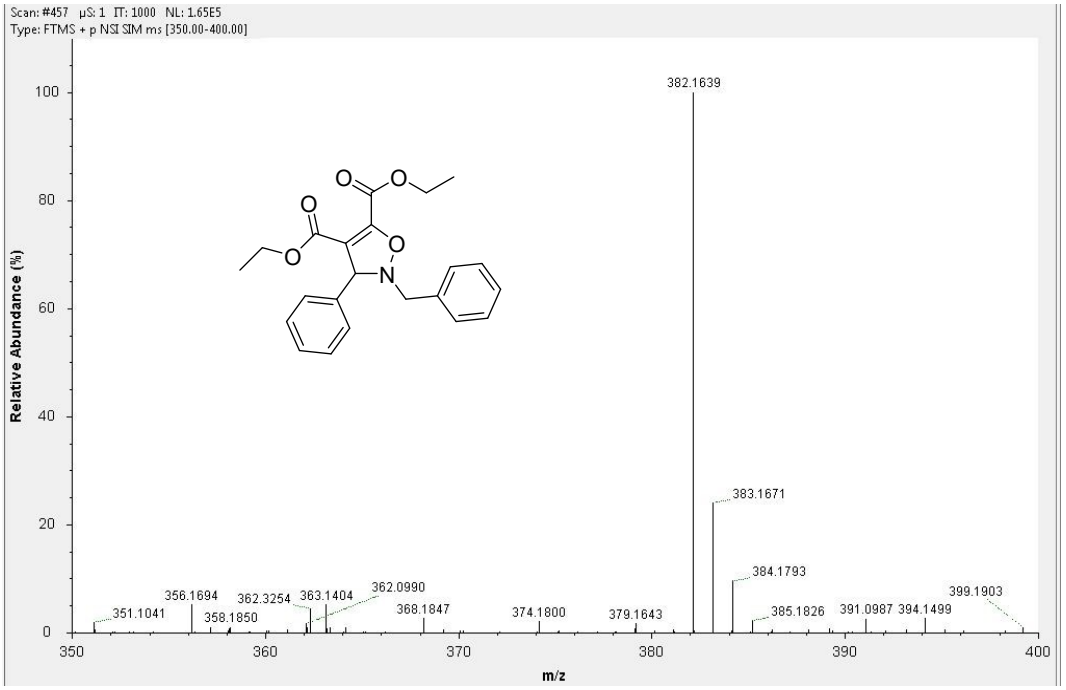

Figure S86 HRMS of **15c**

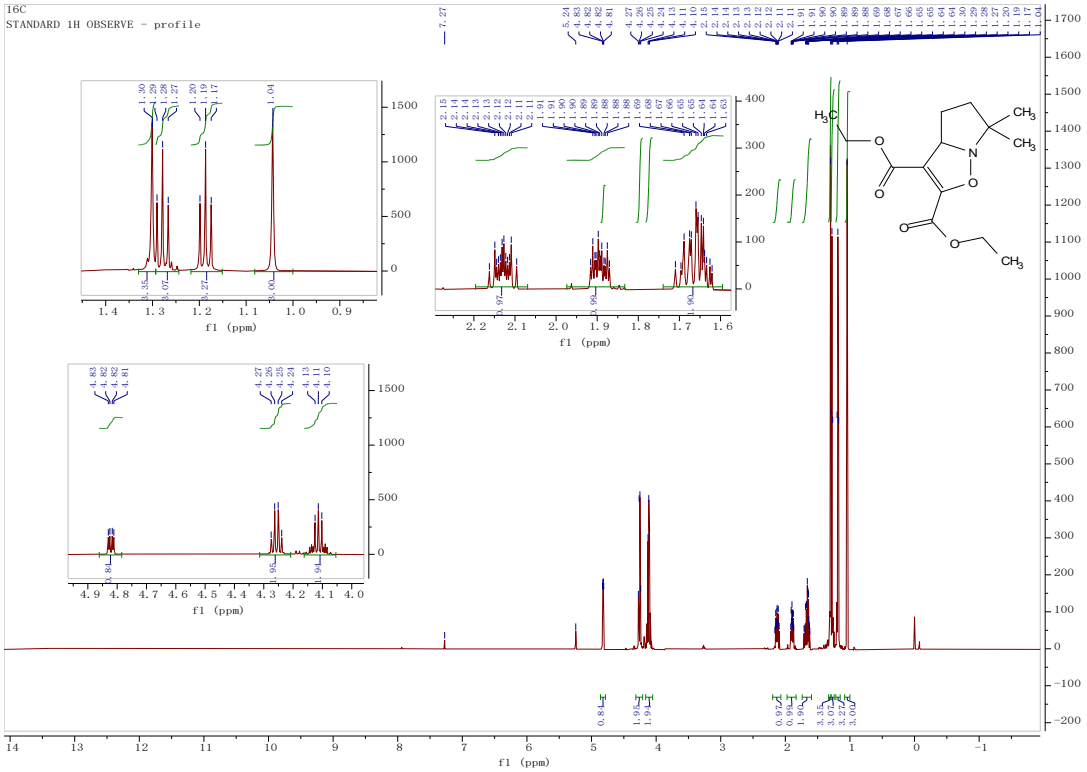

Figure S87 ^{1}H NMR of **16c**

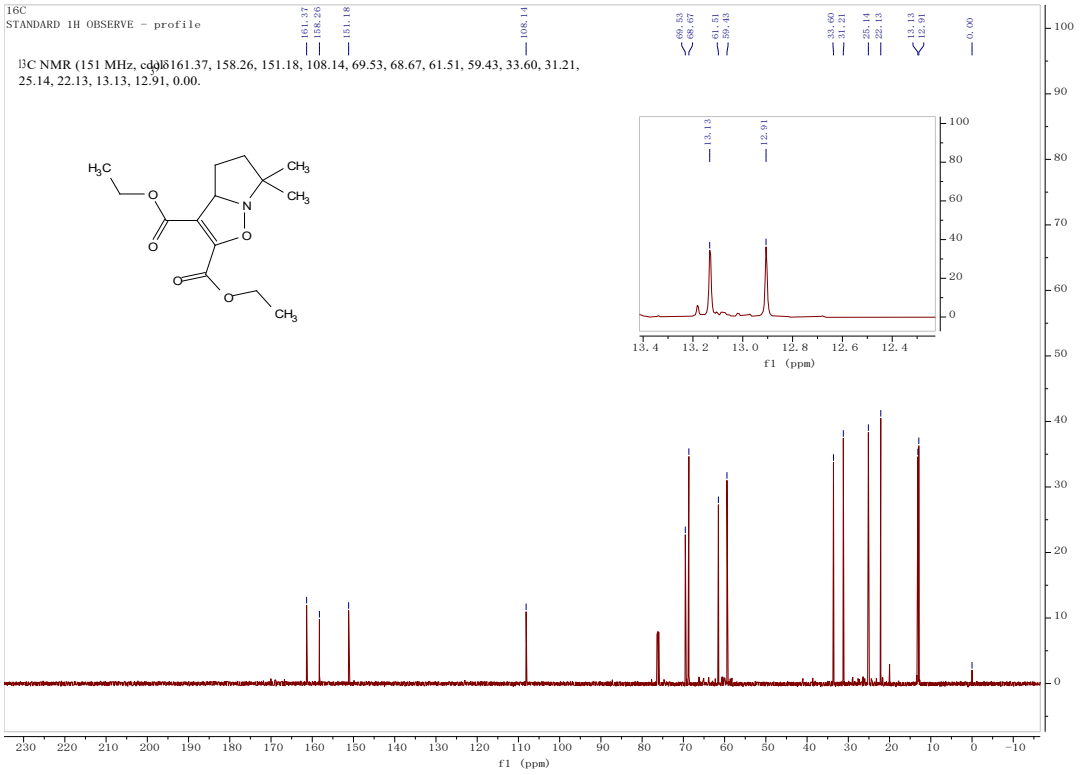

Figure S88 ^{13}C NMR of **16c**

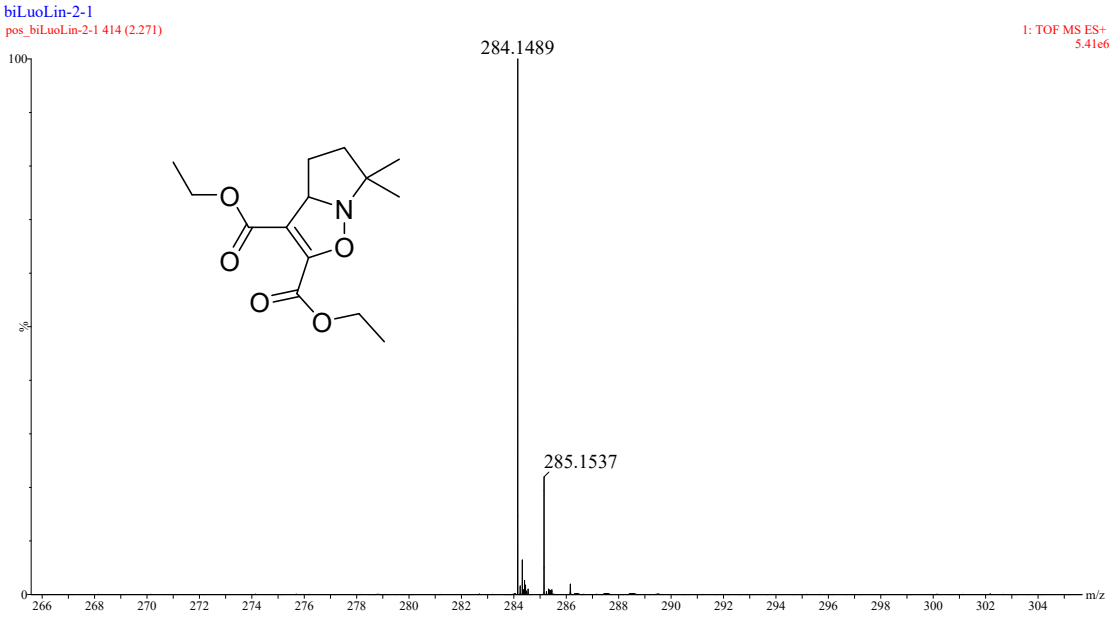

Figure S89 HRMS of **16c**

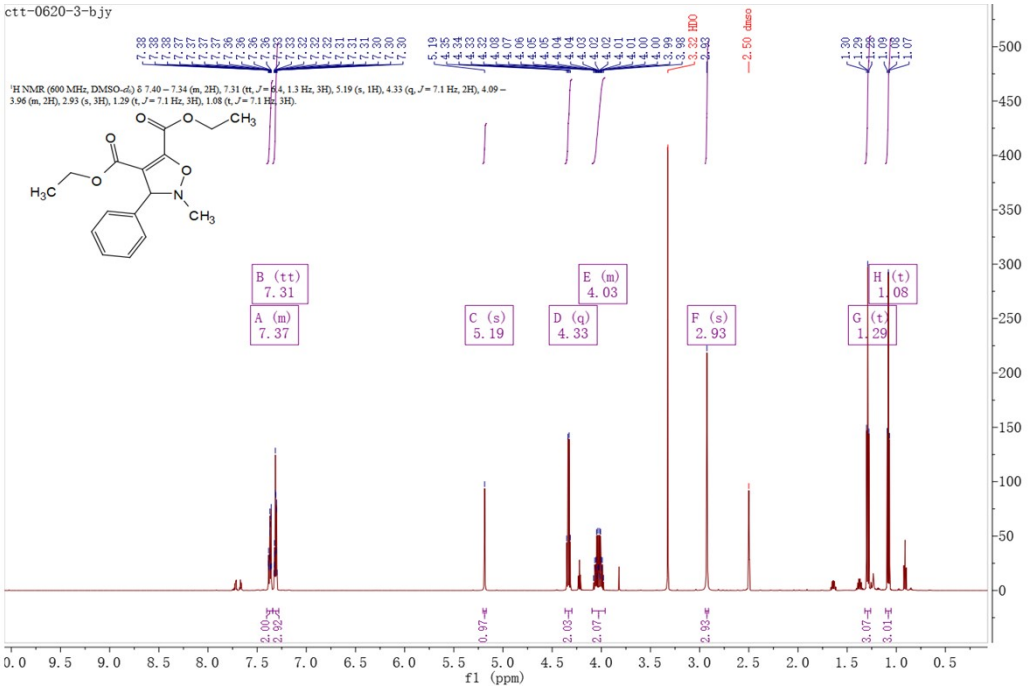

Figure S90 ^{1}H NMR of **17c**

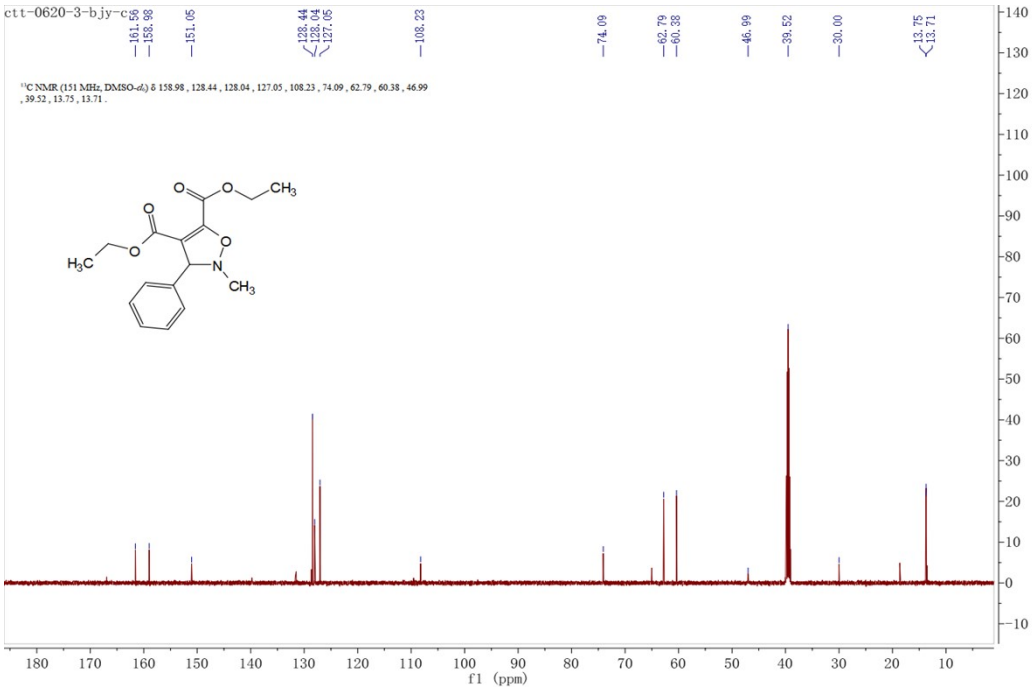

Figure S91 ^{13}C NMR of **17c**

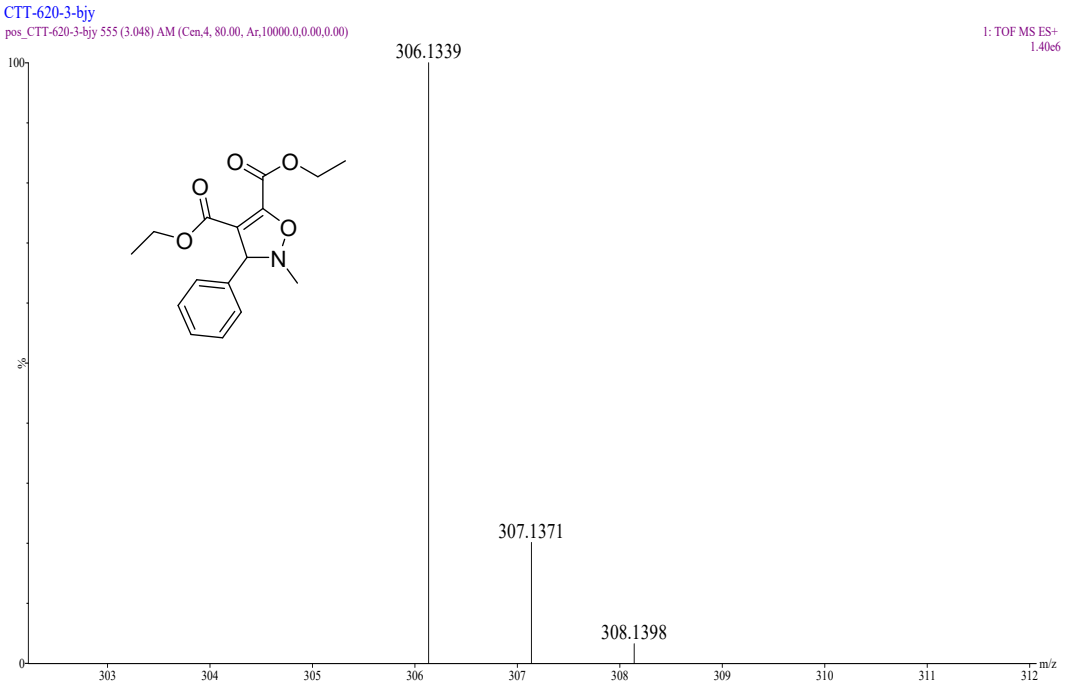

Figure S92 HRMS of **17c**

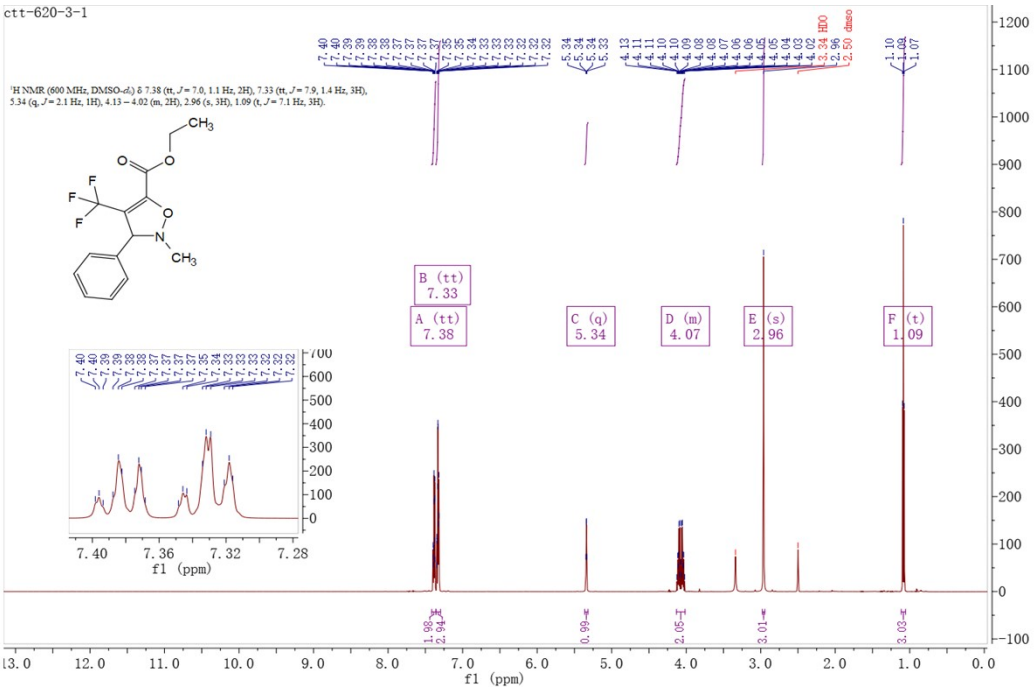

Figure S93 ^{1}H NMR of **18c**

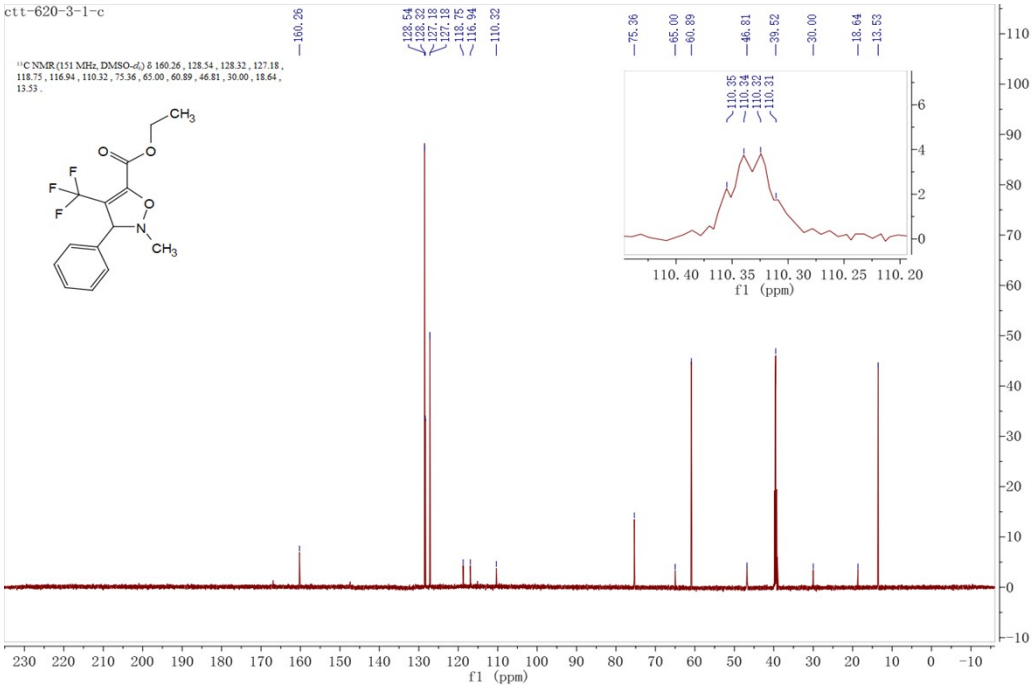

Figure S94 ^{13}C NMR of **18c**

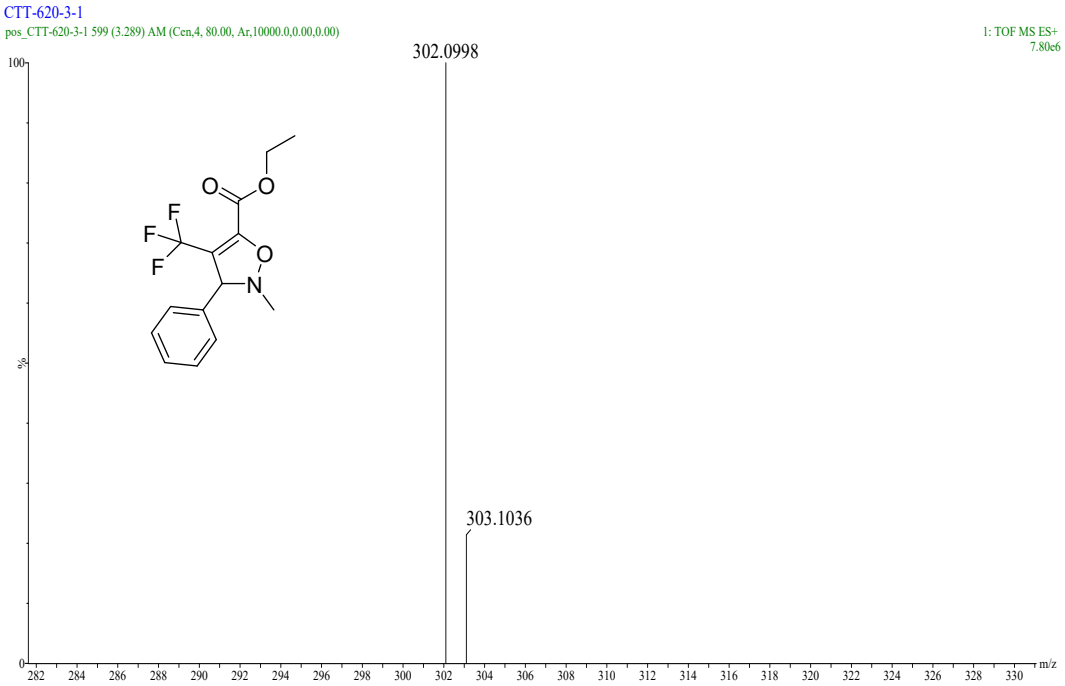

Figure S95 HRMS of **18c**

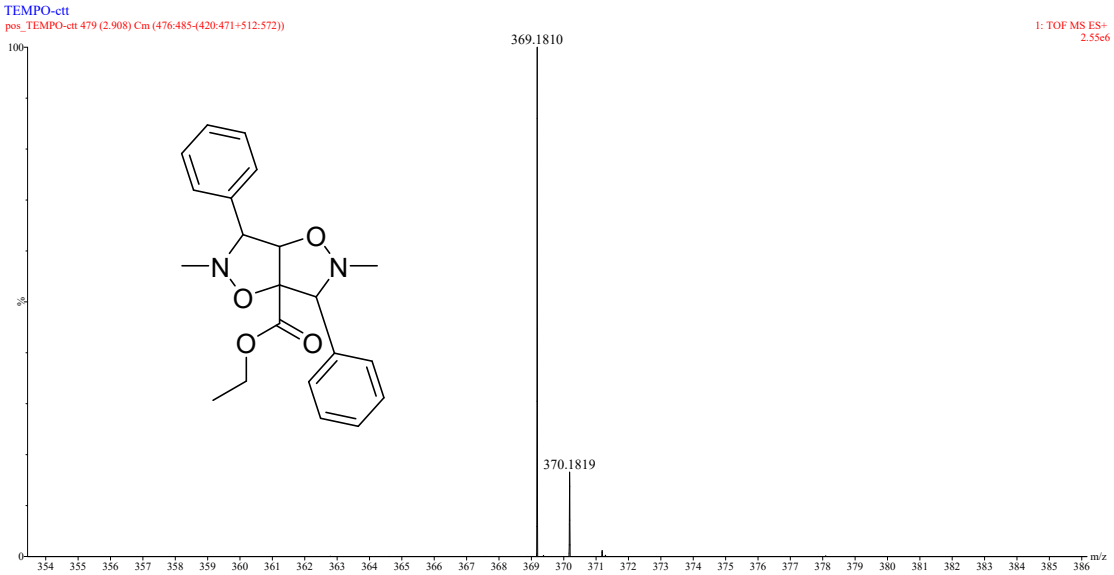

Figure S96 HRMS of **1f**